POLISH ACADEMY OF SCIENCES – WROCŁAW BRANCH
WROCŁAW UNIVERSITY OF TECHNOLOGY

ARCHIVES OF CIVIL AND MECHANICAL ENGINEERING

Quarterly
Vol. X, No. 3

WROCŁAW 2010

EDITOR IN CHIEF

ZBIGNIEW GRONOSTAJSKI

EDITORIAL LAYOUT AND PROOF-READING

WIOLETTA GÓRALCZYK

TYPESETTING

SEBASTIAN ŁAWRUSEWICZ

SECRETARY

WIOLETTA GÓRALCZYK

Publisher: Committee of Civil and Mechanical Engineering
of Polish Academy of Sciences – Wrocław Branch,
Faculty of Civil Engineering and Faculty of Mechanical Engineering
of Wrocław University of Technology

OFICYNA WYDAWNICZA POLITECHNIKI WROCŁAWSKIEJ
Wybrzeże Wyspiańskiego 27, 50-370 Wrocław
http://www.oficyna.pwr.wroc.pl
e-mail: oficwyd@pwr.wroc.pl

ISSN 1644-9665

Drukarnia Oficyny Wydawniczej Politechniki Wrocławskiej. Zam. nr 830/2010.

Contents

Spis treści

ARCHIVES OF CIVIL AND MECHANICAL ENGINEERING

Vol. X 2010 No. 3

State-of-the-art non-destructive methods for diagnostic testing of building structures – anticipated development trends

J. HOŁA, K. SCHABOWICZ
Wrocław University of Technology, Wybrzeże Wyspiańskiego 27, 50-370 Wrocław, Poland.

The paper presents a survey of state-of-the-art non-destructive diagnostic techniques of testing building structures and examples of their applications. Much attention is devoted to acoustic techniques since they have been greatly developed in recent years and there is a clear trend towards acquiring information on a tested element or structure from acoustic signals processed by proper software using complex data analysis algorithms. Another trend in the development of non-destructive techniques is towards assessing characteristics other than strength in elements or structures, particularly the ones made of concrete or reinforced concrete. The paper focuses on techniques suitable for: detecting defects invisible on the surface, estimating the depth of cracks, determining the dimensions of elements accessible from one side only and 2D and 3D imaging of reinforcement distribution in such elements. Finally, directions of further development in this field are indicated.

Keywords: *non-destructive methods, building structures, diagnostic testing*

1. Introduction

The methods used in the diagnostic testing of building structures are divided into destructive, semi-destructive and non-destructive methods. Destructive tests can be applied to samples and natural-scale structural elements. Both are destroyed in the tests. For this reason only a few representative natural-scale elements are subjected to such tests. Semi-destructive tests are also applied to samples and natural-scale elements and structures and they involve a small (usually superficial) intrusion into the structure of the material, resulting in local loss of service properties and requiring repair. There is no such intrusion in the case of non-destructive tests which are applied to mainly natural-scale elements and structures. Moreover, non-destructive tests can be applied to the same elements and structures many times and at different times whereby such methods are suitable for the diagnostic testing of building structures during both their erection and the many years of their service life [3, 9].

Figure 1 shows a classification of non-destructive methods suitable for the diagnostic testing of building structures. The classification is based on [1, 4–5, 8–9].

This paper presents state-of-the-art non-destructive methods for the diagnostic testing of building structures and examples of their application. Much space is devoted to acoustic methods. The latter are being intensively developed and there is a distinct

trend to acquire unequivocal information about the tested element or structure not on the basis of raw acoustic signals registered by the testing equipment, but on the basis of signals processed by appropriate software using complex mathematical algorithms, artificial intelligence or wavelet transformations [2, 10, 13, 16, 18]. Such software is part of the offered measuring sets. The paper also presents the anticipated development trends.

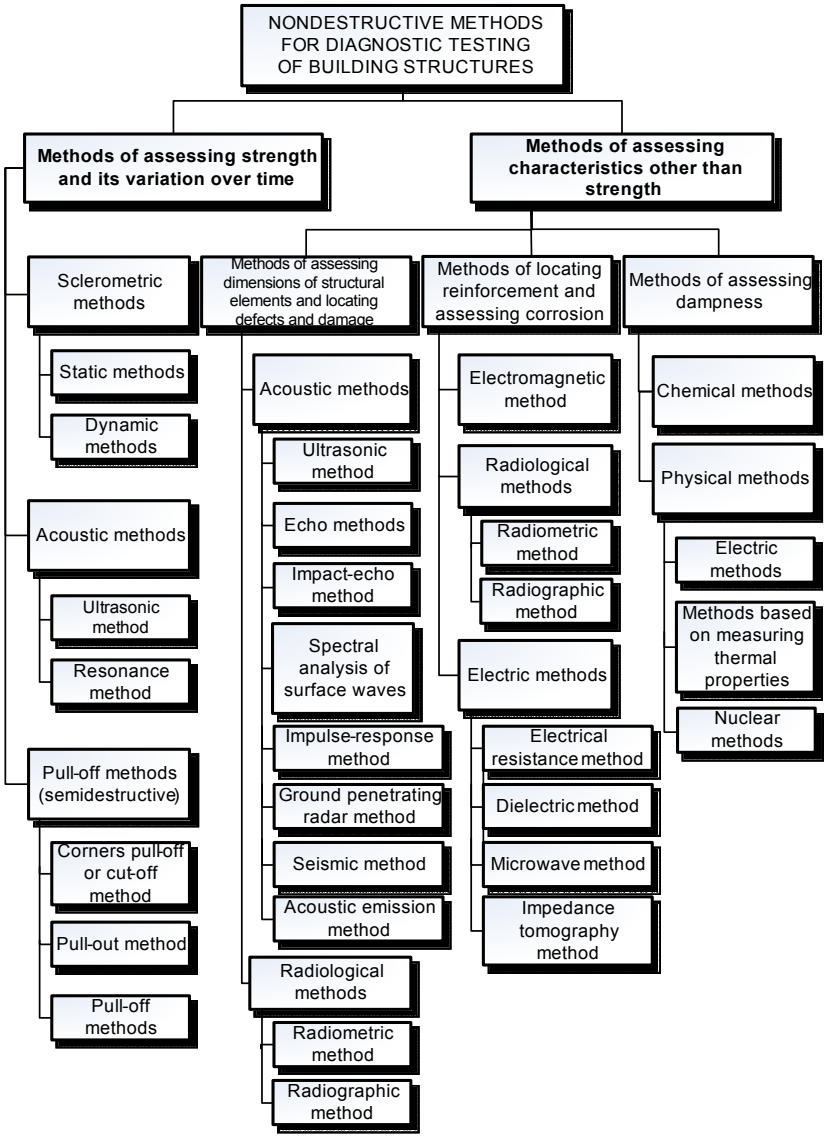

Fig. 1. Non-destructive methods for diagnostic testing of building structures

2. Survey of state-of-the-art methods

The main aim of the currently developed non-destructive methods is to enable the assessment of other characteristics than strength in structural elements and structures, particularly the ones made of concrete or reinforced concrete. The R&D work focuses on: the detection of defects invisible on the surface of structural elements, the assessment of the depth of cracks, the determination of the dimensions of elements accessible from one side and the flat or 3D imaging of the reinforcement in such elements. Table 1 presents six state-of-the-art methods selected by the authors, suitable for the diagnostic testing of building structures. Subsequently, the methods are described in detail.

Table 1. Selected state-of-the-art methods of non-destructive testing of building structures

No.	Method	Group of methods	Measured physical quantity	Application
1	Parallel seismic	Acoustic	Acoustic wave pass-through time	Testing of concrete, reinforced concrete and steel foundation piles, contiguous piles and sheet piling
2	Impulse response	Acoustic	Vibration frequency	Testing of concrete, reinforced concrete foundation piles, slabs and floor toppings
3	Impact – echo	Acoustic	Vibration frequency	Testing of concrete and reinforced concrete foundation slabs, floors, flooring slabs, columns, beams, post-tensioned concrete girders, sewers, etc.
4	Ultrasonic tomography	Acoustic	Ultrasonic wave velocity	Testing of concrete and reinforced concrete flooring slabs, foundation slabs, floor toppings, columns, beams, etc.
5	Ground penetrating radar	Electro-magnetic	Magnetic flux	Testing of soil subbase, concrete and reinforced concrete flooring slabs, foundation slabs, floor toppings, columns, beams, etc.
6	Impedance tomography	Electrical	Electric potential	Testing of masonry walls, pillars, columns

2.1. Parallel seismic method

The *parallel seismic method* belongs to low-energy seismic methods. It is useful for testing concrete and reinforced concrete, precast or cast-on-site foundation piles as regards their length and the continuity of their cross section along the length [11, 19, 27–28]. It is also useful for determining the length of steel and reinforced concrete sheet pilings and contiguous piles. This method involves boring a hole (deeper than the element's design length) along the investigated element. A hydrophone (operating frequency of about 40 kHz) is placed in this hole. The hydrophone can move in the hole along the pile. The pile's head or cap is struck with a calibrated hammer and after each strike the time it takes the acoustic wave to pass from the investigated element to

the hydrophone is recorded. Dedicated software installed on a laptop (part of the measuring set) is used to process the registered signals in order to determine the acoustic wave passage time. A marked increase (sharp peak) in acoustic wave passage time registered along the length of the investigated element may indicate the element's length or a discontinuity in its cross section.

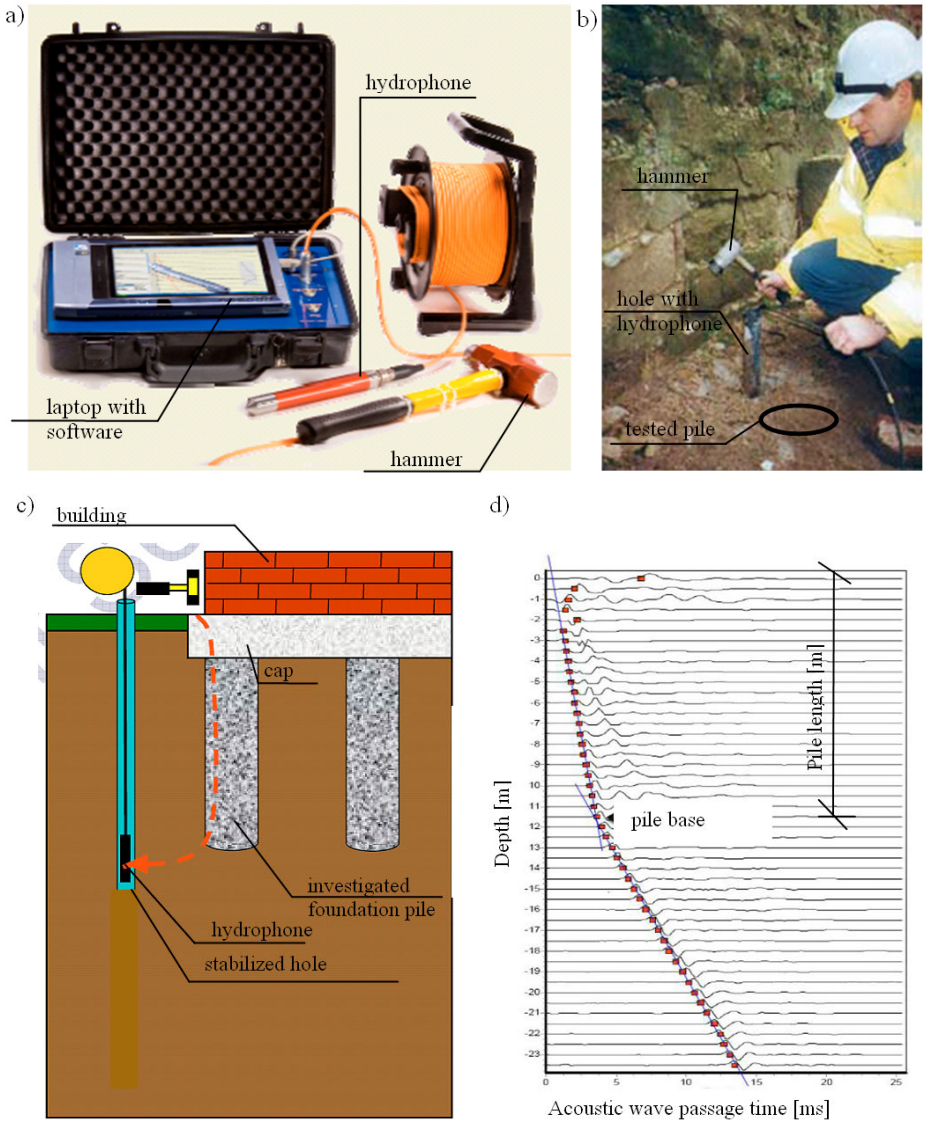

Fig. 2. Idea of *parallel seismic method*: a) measuring set, b) typical test procedure c) test diagram, d) registered acoustic wave passage time [27–28]

Figure 2 shows a measuring set used in the *parallel seismic method*, a diagram illustrating the testing of a pile under a building and typical test results from which one can determine the actual length of the tested element.

The method's advantages are: the simple way of testing of both single piles and capped sets of piles. The drawback is the necessity of boring a hole in the ground along the side of the investigated element, which is not always possible.

2.2. Impulse response method

The *impulse response method* is useful for: detecting voids under concrete and reinforced concrete slabs laid on the ground (e.g. under a foundation slab or an industrial floor), detecting the lack of interfacial cohesion (delaminations) in multilayer systems, locating defective areas and inhomogeneities (honeycombing) in concrete elements and checking the length and continuity of piles.

The idea of the *impulse response method* is shown in Figure 3. The measuring set includes: a hammer, a geophone and an amplifier with a laptop.

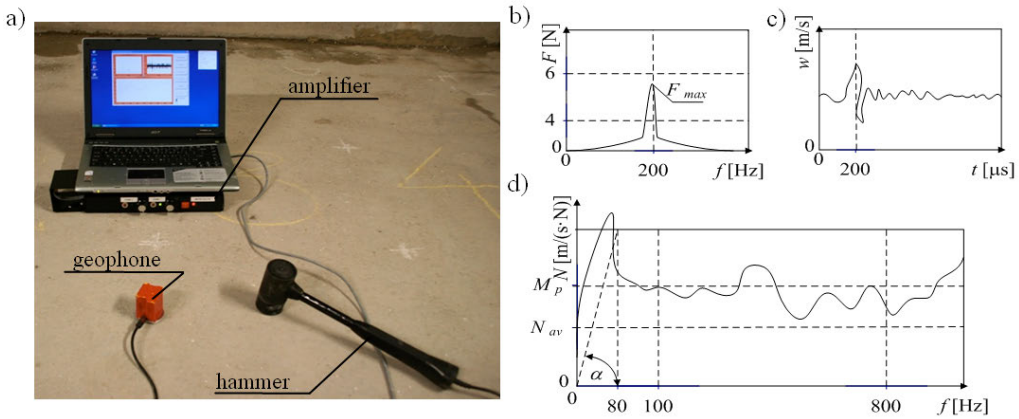

Fig. 3. Idea of *impulse response method*: a) measuring set, b) typical trace of elastic wave F generated by hammer, c) typical trace of elastic wave velocity w registered by geophone, d) typical diagram of mobility N_{av} versus frequency

In the *impulse response method* an elastic wave is induced in the tested element by striking its surface with the calibrated rubber-ended hammer in previously selected measuring points [6–8, 12, 14]. The signal of the elastic wave propagating in the element is registered by the geophone and simultaneously amplified by the amplifier (with a maximum frequency of 1000 Hz). The registered signals are processed by dedicated software installed on the laptop being part of the measuring set. As a result, maps of five characteristic parameters: average mobility N_{av}, stiffness K_d, mobility

slope M_p, mobility times mobility slope $N_{av} \times M_p$ and voids index v are obtained for the investigated surface.

Figure 4 shows typical maps of average mobility obtained by the impulse response method. The results in Figure 4a are for a concrete floor topping. The defective area (with a delamination at the topping/foundation slab interface) is demarcated by an ellipse. Figure 4b shows typical test results for a foundation slab which cracked near column 5.

The method's advantages are: the simple way of testing (no need for any device to couple the geophone with the base) and the fact that the method can be readily used to test large concrete and reinforced concrete slabs. Its drawback is the rather low defect location precision and the complicated interpretation of the results.

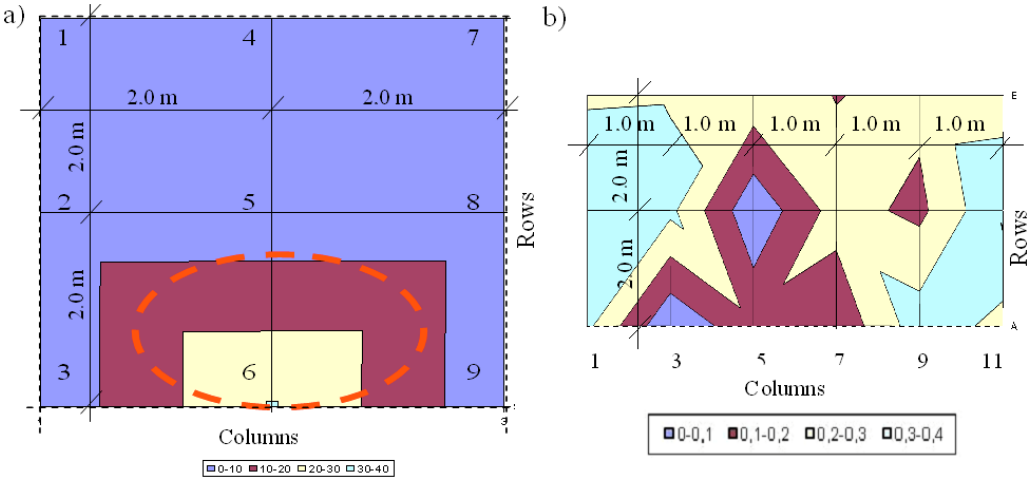

Fig. 4. Typical maps of one characteristic parameter on surface of tested element, obtained by *impulse response method*: a) map of average mobility N_{av} for floor topping, b) map of average mobility N_{av} for foundation slab

2.3. Impact-echo method

The *impact-echo* method is suitable for determining the thickness of concrete and reinforced concrete slabs accessible from one side, detecting defects (delamination, debonding, local flaws, cracks, etc.) in such slabs and floor toppings. The method is particularly suitable for checking the interlayer adhesion in floor toppings, checking the adhesion of repair layers to the base in various concrete and reinforced concrete elements, determining the depth of cracks, checking the filling of tendons with cement grout in post-tensioned concrete girders and the diagnostic testing of sewer mains [14, 17, 20, 24]. The *impact-echo method* consists in exciting an elastic wave in the tested element by striking its surface with an exciter in the form of a steel ball.

The frequency of the generated vibrations depends on the ball's diameter and it ranges from 10 kHz to 150 kHz. A dedicated software is used to record (in the amplitude-time system) the image of the elastic wave propagating in the tested element and then to convert it into an amplitude-frequency spectrum by means of the fast Fourier transform or artificial neural networks. The spectrum is subject to further analysis.

The idea of the *impact-echo method* and the measuring set (consisting of measuring probes with exciters in the form of a set of steel balls with different diameters, and a laptop) are shown in Figure 5.

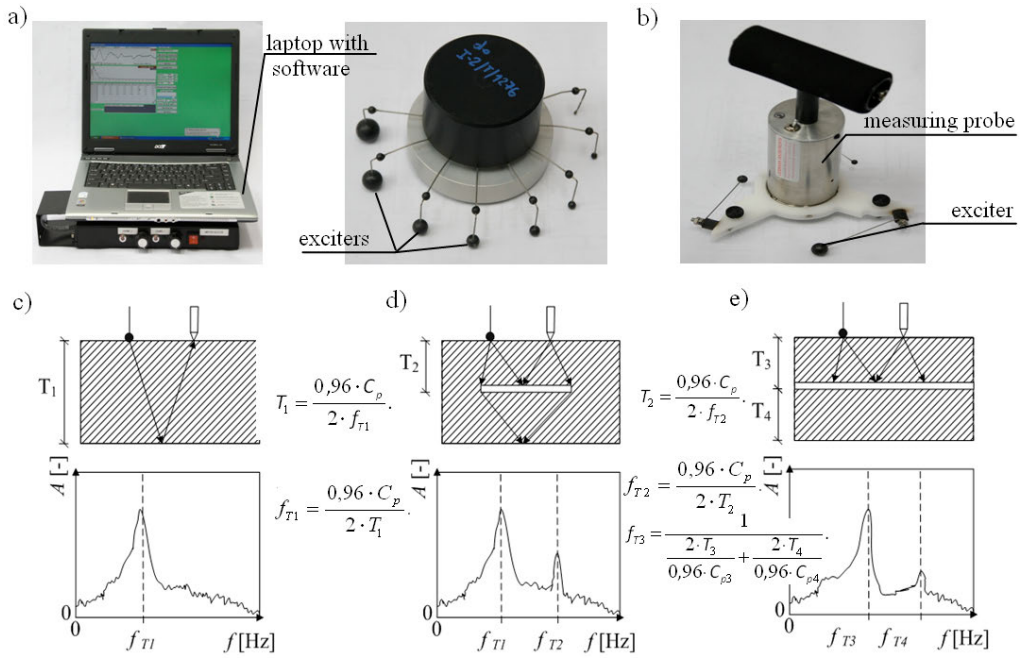

Fig. 5. Idea of *impact-echo method*: a) measuring set, b) exciters and measuring probe, c) typical amplitude-frequency spectrum obtained when measuring thickness of concrete slab or floor topping, d) typical amplitude-frequency spectrum obtained for defect in slab or floor topping, e) typical amplitude-frequency spectrum for interlayer delamination in slab or floor topping

Exemplary test results obtained by this method are shown in Figure 6.

The method's advantage is the simple way of testing without a need for any device to couple the measuring probe with the base. The drawbacks are: the laboriousness of the tests due to the close spacing of the measuring points, no possibility of determining the dimensions of defects (e.g. cracks) filled with water and difficulties in the interpretation of the results.

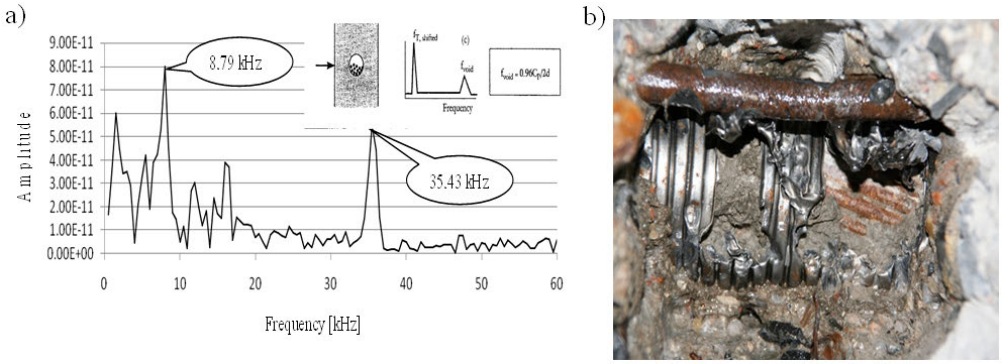

Fig. 6. Exemplary elastic wave amplitude-frequency spectrum registered by *impact-echo apparatus* in post-tensioned concrete bridge girder: a) registered signal indicating missing cement grout tendon filling, b) exposure confirming lack of filling

2.4. Ultrasonic tomography method

The ultrasonic tomography method is particularly suitable for testing concrete and reinforced concrete elements accessible from one side in order to determine their thickness and detect cracks, intrusions, voids and places which may be empty or filled with a liquid or a material having a different density and different physical and mechanical properties than the surrounding concrete [21–22]. The method consists in exciting an elastic wave in the tested element. The exciter is a multi-probe antenna incorporating a few tens of independent ultrasonic probes. The probes generate ultrasonic pulses with a frequency of 50 kHz.

Figure 7 shows an ultrasonic tomography incorporating a special multi-probe ultrasonic antenna with computer and dedicated software enabling the recording of the images.

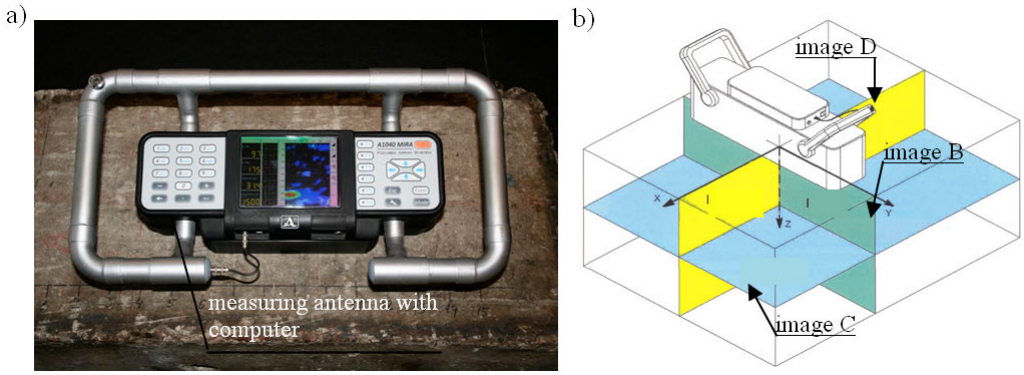

Fig. 7. Ultrasonic tomograph: a) measuring set, b) measuring antenna in coordinate system and possible images

Typical images obtained by means of the ultrasonic tomography are shown in Figure 8. The images show the results of investigations aimed at determining the thickness of a foundation slab accessible from one side. The arrows in figure 8b indicate the shape and the actual thickness of the tested slab. In its middle zone the slab's design thickness of 0.80 m was reduced to 0.40 m during construction [21].

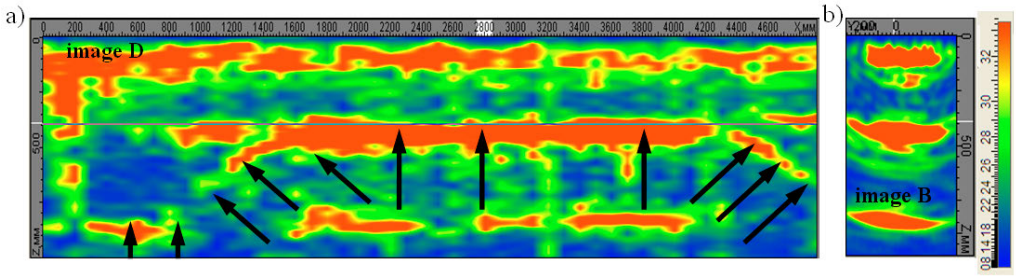

Fig. 8. Exemplary images for foundation slab: image D (arrows indicate shape and thickness of slab), b) image B

The advantage of this method is that no device is needed to couple the surface of the tested element with the ultrasonic probes (dry point contact is used). Another advantage is that the test is fast whereby in a relatively short time one can test large elements, structures and surfaces. The drawback is the difficult interpretation of the results, partly due to the testing personnel's poor experience and to the fact that the minimum dimension (width) of the tested element should be 500 mm.

2.5. Ground penetrating radar method

The *ground penetrating radar (GPR) method* is used to determine or detect: thickness, delaminations, large voids, extensive defects and reinforcement bars in concrete and reinforced concrete elements accessible from one side. Literature reports suggest that it is also useful for assessing concrete dampness [5, 9–10, 26].

According to table 1 this method belongs to electromagnetic methods. The testing probes, depending on the purpose of the GPR, generate electromagnetic waves with a frequency of 0.1–2.5 GHz. The transmitting-receiving probe (antenna) is equipped with wheels whereby it can travel on the surface of the tested element. It is connected by a transmission cable or via a radio link with a data recorder.

A typical GPR set is shown in Figure 9. It includes a control unit in the form of a special transmitting-receiving probe, a data recorder, a distance measuring device and a measuring pad.

Figure 9b shows an exemplary GPR image showing the distribution of reinforcement in a model reinforced concrete element.

The advantage of the method is that elements with large surfaces can be quickly tested in order to locate reinforcement. Its drawback is the rather low accuracy with which

the reinforcement diameter and the thickness of the reinforcement cover are determined.

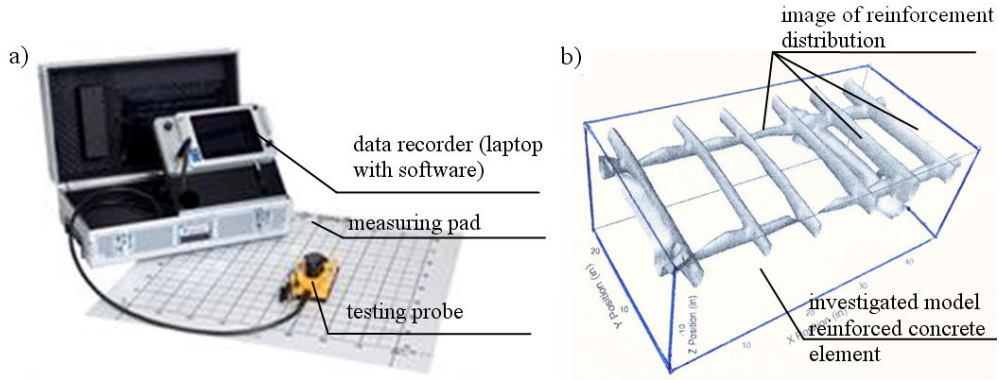

Fig. 9. GPR set (a) and its exemplary image showing reinforcement distribution in model reinforced concrete element (b) [9, 26]

2.6. Electrical impedance tomography

The *electrical impedance tomography* (EIT) is suitable for determining dampness distribution in brick walls affected by rising damp [15, 23].

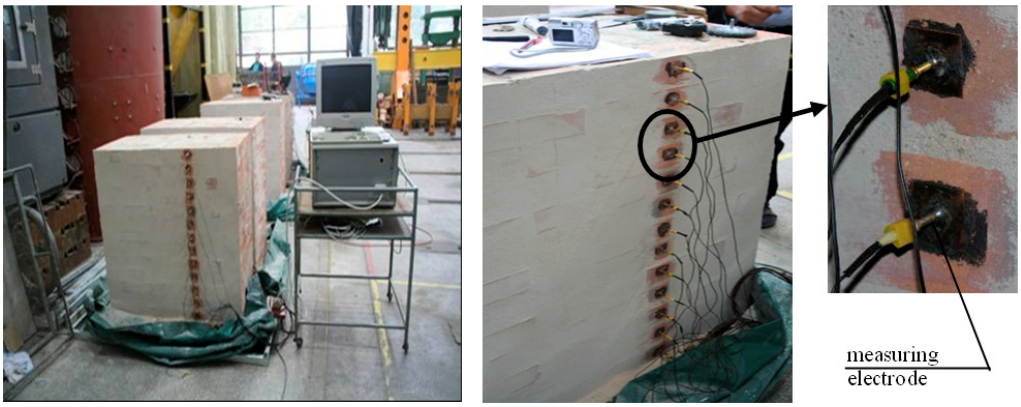

Fig. 10. Test rig with measuring set for electrical impedance tomography

The method belongs to the group of electric methods and its aim is to obtain a 3D image of dampness distribution in a brick wall through measurements of its electrical properties. A picture of electrical conductivity distribution inside an investigated object is produced on the basis of measurements of electric potential distribution on its surface. The distribution of conductivity is determined through repeated measurements

(for different configurations of the excitation probes) of potentials on the surface of the masonry. The main difficulty in this method consists in experimentally determining the dependence between conductivity distribution and dampness for the particular internal structure of the investigated element. The distribution of electric potentials on the surface of an object depends on the distribution of conductivity inside the object. Surface potential measurements are performed at different projection angles whereby enough information is acquired to determine the distribution of conductivity inside the masonry.

Figure 10 shows a measuring set (impedance tomography) built for this purpose. Exemplary results obtained for a damp brick wall are shown in Figure 11.

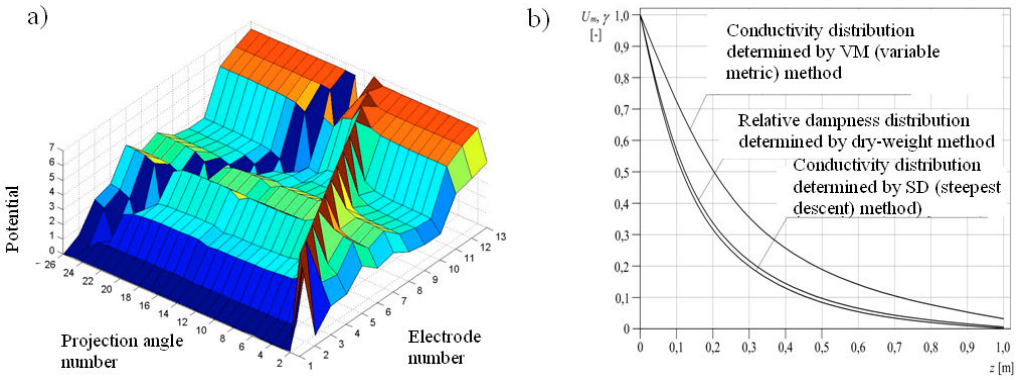

Fig. 11. Exemplary potential distribution results for damp brick wall (a) and comparison of relative distributions of dampness and conductivity along height of investigated masonry

The method allows one to determine the distribution of dampness within a brick wall. Its drawback is that currently no proper mass-produced equipment is available.

3. Anticipated development trends

The development of non-destructive methods for the diagnostic testing of building structures aims at simplifying measurements through their automation. Currently more or less successful attempts are made to develop various scanner designs for this purpose. Such scanners are designed specifically for a particular test method, e.g. the *impact-echo method* or the *GPR method*. Attempts are also made to develop robots combining two or even three test methods. This stimulates search for more advanced information tools for the analysis and interpretation of results obtained simultaneously by several non-destructive test methods.

Figure 12a shows a scanner making it possible to automate the testing of concrete bridge girders by the *impact-echo method*. Figure 12b shows robots equipped with devices for testing large flat elements.

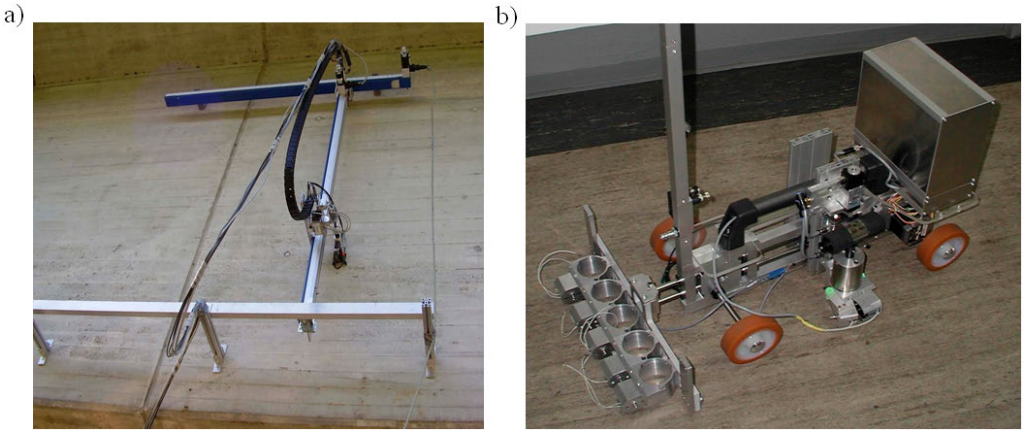

Fig. 12. Examples of: a) scanner for testing vertical surfaces of concrete bridge girders, b) robot for non-destructive testing of large flat concrete elements [25]

It is expected that researchers and designers will intensify their efforts aimed at developing testing equipment allowing one to gain (similarly as in medicine) an accurate picture of the inside of concrete, reinforced concrete and masonry building elements or structures. Undoubtedly, this will lead to more precise location of various defects and more efficient control of the execution of building elements and structures. Moreover, it seems that the wired equipment used today will be replaced by wireless systems in the nearest future.

4. Conclusions

On the basis of the literature on the subject and their own research the authors have come to the conclusion that the current trend in the development of new non-destructive methods for the diagnostic testing of building structures is mainly towards detection of flaws and defects in concrete elements and structures and that acoustic methods predominate in this field.

Similarly as in medicine, the trend is towards designing test equipment allowing one to gain a picture of the inside of the tested element. Increasingly more often the offered apparatus is equipped with software based on sophisticated mathematical algorithms and artificial intelligence, which makes advanced analysis of the test results possible.

Attempts are made to develop scanners and robots not only in order to simplify and automate repeatable tests performed on large structural elements and building structures, but also to use two or three test methods simultaneously.

References

[1] American Concrete Institute Report ACI 228.2R-98. Nondestructive test methods for evaluation of concrete in structures, ACI. Farmington Hills, Michigan, 1998.

[2] Beutel R., Reinhardt H., Grosse C., Glaubitt A., Krause M., Maierhofer C., Algernon D., Wiggenhauser H., Schickert M.: *Comparive performance tests and validation of NDT methods for concrete testing*, Journal of Nondestructive Evaluation, Vol. 27, No. 1–3, 2008.

[3] Brunarski L., Runkiewicz L.: *Fundamentals and examples of the use of nondestructive methods in the testing of concrete structures* (in Polish), Institute of Construction Engineering, Warsaw, 1983.

[4] Bungey J., Millard S., Gratham M.: *Testing of concrete in structures*, Taylor & Francis, London and New York, 2006.

[5] Carino N.J.: *Nondestructive test methods*, Concrete Construction Engineering Handbook, CRC Press, 1999.

[6] Davis A.G., Hertlein B.H., Lim M.K., Michols K.: *Impact-echo and impulse response stress wave methods: advantages and limitations for the evaluation of highway pavement concrete overlays*, Proc. Conference on Nondestructive Evaluation of Bridges and Highways, 1996.

[7] Davis A.G., Hertlein B.H.: *Nondestructive testing of concrete pavement slabs and floors with the transient dynamic response method*, Proc Int. Conf Struct. Faults Repair, London, 1987.

[8] Davis A.G.: *The non-destructive impulse response test in North America: 1985–2001*, NDT&E International, Vol. 36, 2003.

[9] Drobiec Ł., Jasiński R., Piekarczyk A.: *Diagnostic testing of reinforced concrete structures. Methodology, field tests, laboratory tests of concrete and steel* (in Polish), Wydawnictwo Naukowe PWN, Warsaw, Vol. 1, 2010.

[10] Garbacz A.: *Nondestructive investigations of polymer-concrete composites using stress waves – repair efficiency evaluation*, Prace naukowe: Budownictwo, Oficyna Wydawnicza Politechniki Warszawskiej, Vol. 147, 2007.

[11] Gwizdała K.: *Control of capacity and quality of foundation piles* (in Polish), Geoinżynieria i Tunelowanie, No. 1, 2004.

[12] Hertlein B.H., Davis A. G.: *Fall convention locating concrete consolidation problems using the nondestructive impulse response test*, American Concrete Institute, 1998.

[13] Hoła J., Schabowicz K.: *Methodology of neural identification of strength of concrete*, ACI Materials Journal, Vol. 102, No. 6, 2005.

[14] Hoła J., Sadowski Ł., Schabowicz K.: *Nondestructive evaluation of the concrete floor quality using impulse response method and impact-echo method*, e-Journal of Nondestructive Testing & Ultrasonics, Vol. 14, No. 3, 2009.

[15] Hoła J., Sikora J. et al..: *New tomographic method of brickwork damp identification*, Oficyna Wydawnicza Politechniki Wrocławskiej, Wrocław, 2010.

[16] Jerga J., Pokorny M.: *Damage detection of concrete by nonlinear acoustic testing methods*, Civil and Environmental Engineering, Vol. 3, No. 1, 2007.

[17] Petersen C. G., Davis A., Delahaza A.: *Impact-echo testing of steel cable ducts for injection grouting quality*, Symposium Non-Destructive Testing in Civil Engineering. NDT-CE, Berlin, 2003.

[18] Rucka M., Wilde K.: *Application of continuous wavelet transform in vibration based damage detection method for beams and plates*, Journal of Sound and Vibration, Vol. 297, 2006.
[19] Rybak J., Sadowski Ł., Schabowicz K.*: Non-destructive impulse Response S'Mash method for concrete pile testing*, e-Journal of Nondestructive Testing & Ultrasonics, Vol. 14, No. 3, 2009.
[20] Sansalone M., Streett W.B.: Impact-*echo: Nondestructive evaluation of concrete and masonry*, Bullbrier Press. Ithaca, 1997.
[21] Schabowicz K., Hoła J.: *Nondestructive elastic-wave tests of foundation slab in office building*, 13th Asia-Pacific Conference on Non-Destructive Testing, Yokohama, Japan, 2009.
[22] Schabowicz K., Hoła J., Styś D.: *Nondestructive elastic-wave tests of concrete in foundation slab*, 10th European Conference on Nondestructive Testing, Moscow, Russia, 2010.
[23] Sikora J., Wójtowicz S., Nita K., Filipowicz F., Biernat K.: *The system for impedance tomography for measuring the distribution of moisture in walls*, VII International Workshop Computational Problems of Electrical Engineering, Odessa, Ukraine, 2006.
[24] *Standard test method for measuring the P-Wave speed and the thickness of concrete plates using the impact-echo method*, American Society for Testing and Materials, 1998.
[25] Materials from webpage: www.bam.de
[26] Materials from webpage: www.malags.com
[27] Materials from webpage: www.piletest.com
[28] Materials from webpage: www.testconsult.co.uk

Najnowsze metody nieniszczące przydatne do diagnostyki konstrukcji budowlanych – przewidywane kierunki rozwoju

W artykule przedstawiono przegląd wybranych najnowszych metod nieniszczącej diagnostyki obiektów budowlanych wraz z przykładami ich zastosowań. Poświęcono sporo miejsca metodom akustycznym, ponieważ w przypadku tych metod następuje obecnie nie tylko szybki rozwój, ale i wyraźne starania w kierunku pozyskiwania informacji o badanym elemencie lub konstrukcji na podstawie sygnałów akustycznych „przetworzonych" przez odpowiednie oprogramowanie wykorzystujące złożone algorytmy analizy danych. Zwrócono uwagę na fakt, że aktualnie rozwój metod nieniszczących jest ukierunkowany na ocenę w elementach i konstrukcjach, a zwłaszcza tych wykonanych z betonu i żelbetu, innych cech niż wytrzymałość. Skupiono się w pracy przede wszystkim na metodach przydatnych do: wykrywania wad niewidocznych na powierzchni, oceny głębokości pęknięć, określenia wymiarów elementów dostępnych jednostronnie, uzyskiwania obrazu płaskiego lub przestrzennego rozmieszczenia zbrojenia w takich elementach. W końcowej części pracy zamieszczono informacje odnośnie do przewidywanych dalszych kierunków rozwoju.

ARCHIVES OF CIVIL AND MECHANICAL ENGINEERING

Vol. X 2010 No. 3

Improvement of algorithm for numerical crack modelling

G. JOVICIC, M. ZIVKOVIC, N. JOVICIC, D. MILOVANOVIC
University of Kragujevac, Faculty of Mechanical Engineering, Sestre Janjic 6, 34000 Kragujevac, Serbia.

A. SEDMAK
University of Belgrade, Faculty of Mechanical Engineering, Kraljice Marije 16, 11120 Belgrade, Serbia.

For numerical simulation of crack modelling in fracture mechanics the eXtended finite element method (Xfem) has been recently accepted as a new powerful and efficiency methodology. In the paper we present the details of implementation of the Xfem algorithm in our in-house finite elements based software. Also, in this study, we investigated the impact of the node enrichment variations on results of the developed numerical procedure. In this study, objective was to examine the properties of standard Xfem algorithm without using of Near Tip enriching functions in order to create possibilities for future application Xfem in the zone of plasticity. In order to evaluate the computational accuracy, numerical results for the Stress Intensity Factors are compared with both theoretical and conventional finite element data. Obtained numerical results have shown a good agreement with the benchmark solutions. For calculation of the Stress Intensity Factors (SIF), we used the J-Equivalent Domain Integral (J-EDI) Method. Computational geometry issues, associated with the representation of the crack and the enrichment of the finite element approximation, are discussed in detail.

Keywords: *Xfem, node enrichment variations, SIF, J-EDI method*

1. Introduction

The extended finite element method, Xfem, attempts to alleviate the computational challenges associated with mesh generation by not requiring the finite element mesh to conform to cracks, and in addition, it provides using of higher-order elements or special finite elements without significant changes in the formulation. Basis of the method proposed by Belytchko and Black [1], were presented in [2] for the two-dimensional cracks.

The essence of the Xfem lies in sub-dividing a model problem into two distinct parts: mesh generation for the geometric domain (cracks not included), and enriching the finite element approximation by additional functions that model the flaw(s) and other geometric entities. Modelling crack growth in a traditional finite element framework is cumbersome due to need for the mesh to match the geometry of the discontinuity. Many methods require remeshing of the domain at each time step. In the Xfem there is no need for the remeshing, because the mesh is not changed as the crack grows and is completely independent of the location and geometry of the crack. The enriching

functions in the standard formulation Xfem for fracture mechanics are divided into two distinct types: discontinuity functions and asymptotic crack-tip function. The discontinuities across the crack faces are modelled by Heaviside step function. While the displacement field near crack tip simulates using trigonometry functions derivates from the basic formulation of Westergaard for the displacement field in near of the crack tip. Near tip (NT) functions are defined by linear elastic crack tip displacement field, i.e., asymptotic crack tip stress field (broken line in Figure 1).

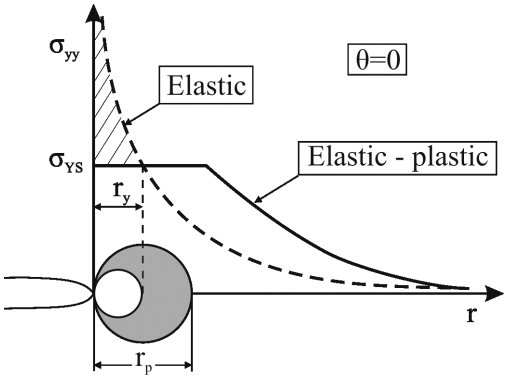

Fig. 1. Stress field near the crack

However, in the majority of materials the stress at the crack tip is not asymptotic, i.e., materials have elastic-plastic properties, and stress at the tip of crack can achieve yield stress. In that case the tip of crack is not atomically sharp-pointed but obtuse and parameter that represents the measure of crack tip obtuseness is crack tip opening displacement (CTOD). This parameter has empiric character but is also has a great practical application [3], because it is used to simulate real crack tip obtuseness which stems from the plastic deformation in the vicinity of the crack tip. For defining CTOD very often is used strip yield model that was proposed by Dugdale (Figure 2) [3]. As you can see in Figure 2 the tip is not sharp-pointed but it is obtuse with size δ – CTOD, therefore it is necessary to adjust enrichment method in the Xfem formulation to the new circumstance.

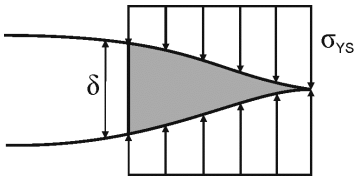

Fig. 2. Dugdale strip model of the stress around of the crack

So, Xfem is applied for crack modelling in linear elastic fracture mechanics (LEFM) [4–7]. The idea of this study is to examine the functioning of Xfem algorithm without NT functions, in order to open the application of Xfem in the zone of elastic–plasticity and plasticity. For this reason, in this study effectiveness of this algorithm is tested when eliminating the function influence and obtained numerical results for the stress intensity factors are compared with both theoretical and conventional finite element data.

2. Extended finite element method (Xfem)

In this paper, the method of discontinuous enrichment is presented in general framework. We illustrate how the two-dimensional formulation can be enriched for the crack model. The concept of incorporating local enrichment in the finite element partition of unity was introduced in Melenk and Babuska [4]. The essential feature is multiplication of the enrichment functions by nodal shape functions. The approximation for a vector-valued function $\mathbf{u}^h(\mathbf{x})$ with the partition of unity enrichment has the general form [4]:

$$\mathbf{u}^h_{\text{enr}}(\mathbf{x}) = \sum_{I=1}^{N} N_I(\mathbf{x}) \left(\sum_{\alpha=1}^{M} F_\alpha(\mathbf{x}) \mathbf{b}_{\text{I}}^\alpha \right), \tag{1}$$

where:

N_I, $I = (1, N)$ are the finite element shape functions,

$F_\alpha(\mathbf{x})$, $\alpha = (1, M)$ are the enrichment functions,

$\mathbf{b}_I^\alpha$ is the nodal enriched degree of freedom vector associated with the elastic asymptotic crack-tip function that has the form of the Westergaard field for the crack tip. The finite element shape functions form a partition of unity: $\sum_I N_I(\mathbf{x}) = 1$. In particular case, for the crack, the enriched displacement approximation, using Heaviside and near tip functions, following [5–7], is written as:

$$\mathbf{u}^h(\mathbf{x}) = \sum_{I \in N_{nu}} N_I(\mathbf{x}) \left(\mathbf{u}_I + \underbrace{H(\mathbf{x}) \mathbf{a}_I}_{I \in N_{ua}} + \underbrace{\sum_{\alpha=1}^{4} F_\alpha(\mathbf{x}) \mathbf{b}_I^\alpha}_{I \in N_{ub}} \right), \tag{2}$$

where:

$\mathbf{u}_I$ is the nodal displacement vector associated with the continuous part of the finite element solution,

$\mathbf{a}_I$ is the nodal enriched degree of freedom vector associated with the Heaviside (discontinuous) function. The $\mathbf{x} \equiv (x, y)$ denotes Cartesian coordinates in 2D space. We denote by N_u the set of all nodes in the domain, and N_α the subset of nodes enriched with the Heaviside function, and N_b is the subset of nodes enriched with the NT (near tip) functions.

2.1. Enrichment functions

The enrichment is able to take a local form only by enriching those nodes whose support intersects a region of a crack. Two distinct regions are identified for the crack geometry, precisely, one of them is the crack interior and the other is the near tip region as it is shown in Figure 3. In the figure is shown a region of a crack for enrichment by H and NT functions. The circled nodes are enriched with a discontinuous function, while the squared nodes are enriched with NT functions. It can be noticed that this shape of enriching near the crack tip, is used in [5–6]. In this paper we modified the modality of the nodes enriching near the crack tip (see next sections).

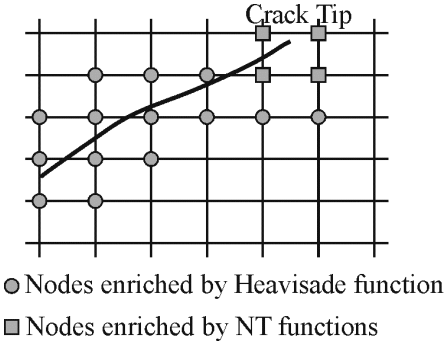

Fig. 3. Regions for standard enrichment near the edges of the crack [4–5]

- *Generalized Heaviside function*. The interior of the crack (Γ_c is the enrichment – domain) is modelled by the generalized Heaviside enrichment function $H(\mathbf{X})$, where $H(\mathbf{X})$ takes the value +1 above the crack and –1 below the crack [5–7]:

$$H(\mathbf{X}) = \begin{cases} 1 \text{ if } (\mathbf{X} - \mathbf{X}^*) \cdot \mathbf{n} \geq 0 \\ -1 \text{ if } (\mathbf{X} - \mathbf{X}^*) \cdot \mathbf{n} < 0 \end{cases}, \tag{3}$$

where:

$\mathbf{X}$ is the sample (Gauss) point,

$\mathbf{X}^*$ (lies on the crack) is the closest point to $\mathbf{X}$,

n is unit outward normal to crack at $\mathbf{X}^*$ (Figure 4). It can be seen that in the first published works [1–2] above shape modelling of the discontinuity was not used. The formulation (3) begins to use due to practical numerical reasons.

- *The near-tip crack functions*. The crack tip enriched functions ensure that the crack terminates precisely at the location of the crack-tip. The linear elastic asymptotic crack-tip fields serve as suitable enrichment functions for providing the correct near-tip behaviour, and in addition, their use also leads to better accuracy on relatively coarse finite element meshes in 2D [2], [5–7].

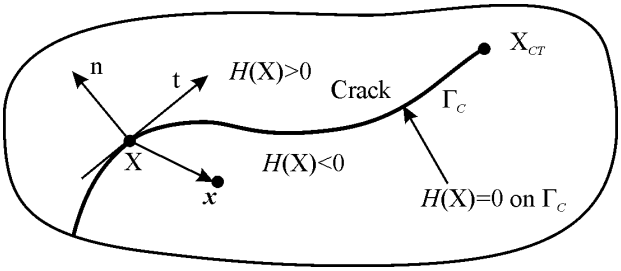

Fig. 4. Illustration of the values of the Heavisade function above and below the crack

The crack tip enrichment functions in isotropic elasticity have form of the Westergaard field for the crack tip:

$$F(\mathbf{x}) = \{F_1, F_2, F_3, F_4\} = \left[\sqrt{r}\cos\frac{\theta}{2}, \sqrt{r}\sin\frac{\theta}{2}, \sqrt{r}\sin\frac{\theta}{2}\sin\theta, \sqrt{r}\cos\frac{\theta}{2}\sin\theta\right] \tag{4}$$

where r and θ denote polar coordinates in the local system at the crack tip. It can be noted that the second function of the set (4) is discontinuous over there crack faces [1], [2]. The discontinuity over the crack faces can be obtained using other functions like Heaviside function (3), which have discontinuity. Let the element which contain the crack tip is denoted as CT element. In the papers [4–6] the discontinuity behind the tip in the CT element is accomplished by second function of the set (4). In this paper (see Figure 6), the discontinuity in the CT element we have achieved with Heaviside function (3).

2.2. Level set reparation of the crack

In this paper a crack is presented using the set of the linear segments. The crack is described by means of the tip position and level set of a vector valued mapping. A signed distance function $\psi(\mathbf{x})$ is defined over computational domain Ω using:

$$\psi(\mathbf{x}) = sign\left[\mathbf{n}\cdot\left(\mathbf{X}-\mathbf{X}^*\right)\right]\min_{\mathbf{x}\in\Gamma_c}\left|\mathbf{X}-\mathbf{X}^*\right|, \tag{5}$$

where:

n is the unit normal to Γ_c,

$\mathbf{X}^*$ is the closest point to **X** (Figure 4). The crack is then represented as the zero level set of the function $\psi(\mathbf{X})$, i.e.:

$$\psi(\mathbf{X}) = 0. \tag{6}$$

The position related to the crack tip is defined through the following functions:

$$\gamma(\mathbf{X}) = (\mathbf{X}-\mathbf{X}_{CT})\cdot\mathbf{t}, \tag{7}$$

where:

t is the unit tangent to Γ_c at the crack tip Λ_c,

$\mathbf{X}_{CT}$ is coordinate of Λ_c. The value $\gamma(\mathbf{X}) = 0$ corresponds to the crack tip. We defined LS functions $\psi(\mathbf{X})$ and $\gamma(\mathbf{X})$ in the whole computational domain. The crack and the crack tip are represented like:

$$\Gamma_c = \{\mathbf{X}:\psi(\mathbf{X},t) = 0 \ \wedge \ \gamma(\mathbf{X},t) \le 0\}. \tag{8}$$

In Figure 5, the definition of the $s(\mathbf{X})$ and $\gamma(\mathbf{x})$ around the crack is shown. For the crack representations linear interpolation has been used. The Heaviside step function (3) is modified using the LS function $\gamma(\mathbf{X}, t)$:

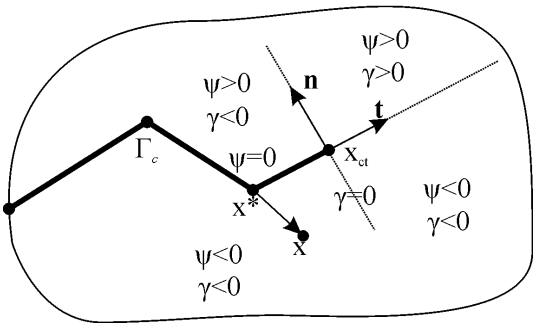

Fig. 5. Definition of the level set functions $\psi(\mathbf{X})$ and $\gamma(\mathbf{X})$ around the crack

$$H(\gamma(\mathbf{X})) = \begin{cases} -1 \text{ if } \gamma(\mathbf{X}) < 0 \\ +1 \text{ if } \gamma(\mathbf{X}) > 0 \end{cases}. \tag{9}$$

The near tip functions $F_\alpha(r, \theta)$, $\alpha = 1, 4$, that have form of the Westergaard field for the crack tip [3], also should be defined using the LS functions, to obtain polar coordinates in the local system at the crack tip (see Figure 6):

$$r(\mathbf{X}) = \sqrt{\psi^2(\mathbf{X}) + \gamma^2(\mathbf{X})} \text{ and } \theta(\mathbf{X}) = tan^{-1}\frac{\gamma(\mathbf{X})}{\psi(\mathbf{X})}. \tag{10}$$

Apart from the other authors [4–6] we used NT functions only ahead the crack tip ($\gamma(\mathbf{X}, t) > 0$), while behind the crack tip ($\gamma(\mathbf{X}, t) < 0$), we ensured discontinuity across the crack ($\psi(\mathbf{X}, t) = 0$), using only the step function $H\,\gamma(\mathbf{X})$). Therefore, the Westergaard field was used only for derivation of the asymptotic stress field ahead of the location near the tip i.e., $\gamma(\mathbf{X}, t) > 0$ (see Figure 6a, b).

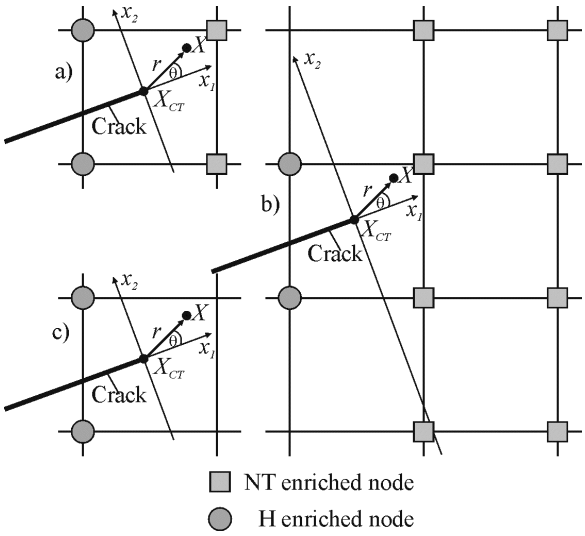

Fig. 6. The local enriched nodes of the element which contains the crack tip
a) standard (H+NT) enriched; b) enlarged $(H+NT)^*$ enriched; c) only (H) enriched

Since the NT functions are used for cracks in the linear-elastic materials, we have considered the results in the case when the enrichment is done only by the H function (Figure 6c). Enrichment by the H function is applied only behind the crack, hence discontinuity is occurred. This algorithm is very important for the Xfem application within elasto-plastic materials.

3. The weak form of the governing equations

To introduce a concept of discontinuous enrichment, we begin by considering the domain of the problem Ω bounded by Γ, with an internal boundary Γ_c as it is shown in

Figure 7. The boundary Γ is subdivided into two parts: Γ_u and Γ_t. The displacement is prescribed on Γ_u, and traction is prescribed on Γ_t. In addition to the external boundary, the crack surface presents an additional boundary inside Ω. The crack surface is denoted by Γ_c and is traction free; Γ_c consists of: Γ_c^+ and Γ_c^-, two coincident surfaces and crack surface is traction free.

The discrete weak form for the linear elasto-statics is:

$$\int_{\Omega^h} \sigma_{ij} \delta\varepsilon_{ij}^h \, \mathrm{d}\Omega = \int_{\partial\Omega^h} \overline{t}_i \;\; \delta u_i^h \mathrm{d}\Gamma \quad \forall \delta u_i^h \in U_0^{hh}, \tag{11}$$

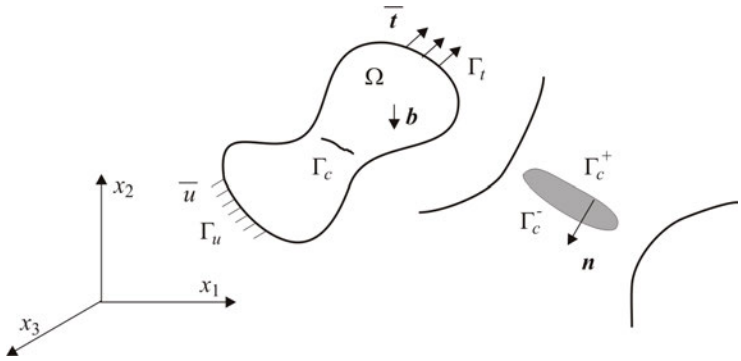

Fig. 7. The problem domain

where:

Ω^h is the finite element domain,

σ_{ij} is the Cauchy stress tensor,

u_i are the displacement components $u_i^h \in U_0^h$ and $\delta u_i^h \in U_0^{hh}$, are the approximating trial and test functions used in the X-FEM, $\overline{t}_i$ are traction components and the sum has repeated indices. The space U^{hh} is the enriched finite element space that satisfies the Dirichlet boundary conditions, and which include the basis functions that are discontinuous across the crack surfaces. The space U_0^{hh} is the corresponding space with homogeneous Dirichlet boundary conditions.

Substituting the X-FEM trial and test functions in to the above equations, and using the arbitrariness of nodal variations, the following discrete system of linear equations on an element-by-element is:

$$\begin{bmatrix} \mathbf{k}_{ij}^{uu} & \mathbf{k}_{ij}^{ua} & \mathbf{k}_{ij}^{ub} \\ \mathbf{k}_{ij}^{au} & \mathbf{k}_{ij}^{aa} & \mathrm{k}_{ij}^{ab} \\ \mathbf{k}_{ij}^{bu} & \mathbf{k}_{ij}^{ba} & \mathbf{k}_{ij}^{bb} \end{bmatrix} \begin{Bmatrix} \mathbf{d}_i^u \\ \mathbf{d}_i^a \\ \mathbf{d}_i^b \end{Bmatrix} = \begin{Bmatrix} \mathbf{f}_i^u \\ \mathbf{f}_i^a \\ \mathbf{f}_i^b \end{Bmatrix}, \tag{12}$$

where:

$\left\{\mathbf{d}_i^u \;\; \mathbf{d}_i^a \;\; \mathbf{d}_i^b\right\}^T$ – is vector of nodal unknowns,

$\left\{\mathbf{f}_i^u \;\; \mathbf{f}_i^a \;\; \mathbf{f}_i^b\right\}^T$ – external force vector,

$\mathbf{K}_e$ – elemental tangent stiffness matrix. The sub-matrices and vectors that appear in Equation (12) are defined as:

$$\mathbf{k}_{ij}^{rs} = \int_{\Omega_e} \left(\mathbf{B}_i^r\right)^T \mathbf{C}\mathbf{B}_j^s \mathrm{d}\Omega, \;\; (r, s = u, a, b), \tag{13}$$

$$\mathbf{f}_i^u = \int_{\partial\Omega_i^h \cap \partial\Omega_e} N_i \bar{\mathbf{t}}\, \mathrm{d}\Gamma, \tag{14}$$

$$\mathbf{f}_i^a = \int_{\partial\Omega_i^h \cap \partial\Omega_e} N_i \mathrm{H}\bar{\mathbf{t}}\, \mathrm{d}\Gamma, \tag{15}$$

$$\mathbf{f}_i^{b_\alpha} = \int_{\partial\Omega_i^h \cap \partial\Omega_e} N_i F_\alpha \bar{\mathbf{t}}\, \mathbf{d}\Gamma, \quad (\alpha = 1, 4). \tag{16}$$

In the above equations, N_i is the standard finite element shape function that is defined by i (i = 1, *nen*) of the finite element, where *nen* is the number of nodes in the connectivity of the finite element. The number of degrees of freedom is *ndof* = 2 in 2D elasticity. In Equation (18), $\mathbf{B}_i^u, \mathbf{B}_i^\alpha$ and $\mathbf{B}_i^{b_\alpha}$ are the strain interpolation matrices [5].

4. The EDI method for *J*-integral evaluation

Rice [8] defined a path-independent contour *J*-integral for two-dimensional crack problems in linear and nonlinear elastic materials. In general the structural integrity assessment of a cracked component requires a comparision of the crack driving force, as measured by the stress intensity factor K, and materials fracture toughness, K_c. An assessment involves either determining the critical loading to initiate growth of a known crack or in estabilishing the critical crack size for a specified loading [9]. J-integral founded practical application in determining stress intensity factor.

The contour *J*-integral is not the best suited form for finite element calculations. Therefore, it is transformed into an equivalent domain form. The contour integral is replaced by an integral over a finite-size domain. The standard *J*-contour integral given in [10] is rewritten, by introducing a weight function q (x_1, x_2) into the EDI. Hence, we define the following contour integral:

$$J_k = \int_\Gamma \left(W\delta_{kj} - \sigma_{ij}u_{i,k}\right)m_j q d\Gamma \qquad i, j, k = 1, 2, \tag{17}$$

where:

$\Gamma = \Gamma_0 + \Gamma^+ - \Gamma_S + \Gamma^-$ is the contour (Figure 8),

W is the strain energy density,

m_j is the unit vector outward normal to the corresponding contour (i.e. $m_j = n_j$ on Γ_0 and $m_j = -n_j$ on Γ_s),

q is the weight function defined as $q = 1$ inside the contour Γ and $q = 0$ for the domain outside Γ.

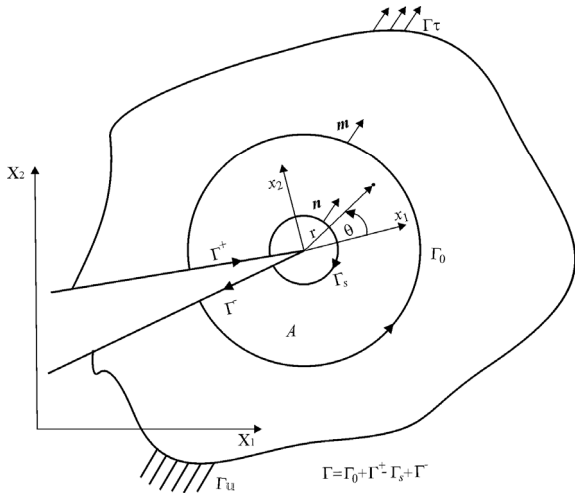

Fig. 8. Conversion of the contour integral into an equivalent domain integral

Taking the limit $\Gamma_s \to 0$ leads to [11–12]:

$$\begin{aligned}\lim_{\Gamma_S \to 0} J_k &= \lim_{\Gamma_S \to 0} \int_{\Gamma} \left(W\delta_{kj} - \sigma_{ij}u_{i,k}\right) m_j q d\Gamma \\ &= \lim_{\Gamma_S \to 0} \int_{\Gamma_0 + \Gamma^+ + \Gamma^- - \Gamma_S} \left(W\partial_{kj} - \sigma_{ij}u_{i,k}\right) m_j q d\Gamma \\ &= \lim_{\Gamma_S \to 0} \int_{\Gamma_0 + \Gamma^+ + \Gamma^-} \left(W\partial_{kj} - \sigma_{ij}u_{i,k}\right) m_j q d\Gamma - \lim_{\Gamma_S \to 0} \int_{\Gamma_S} \left(W\delta_{kj} - \sigma_{ij}u_{i,k}\right) m_j q d\Gamma.\end{aligned} \tag{18}$$

Applying the divergence theorem to Equation (18), we obtain the following expression:

$$J_k = \int_A \left(\sigma_{ij}u_{i,k} - W\delta_{kj}\right) q_{,j} dA + \int_A \left(\sigma_{ij}u_{i,k} - W\delta_{kj}\right)_{,j} q dA \qquad i, j, k = 1, 2, \tag{19}$$

where A is the area enclosed by G.

4.1. Numerical evaluation of the J-EDI method

When the material of the considered structure is homogeneous and there are no body forces, the finite element implementation of Equation (19) becomes very similar to equation of the contour integral. The only difference is the introduction of the weight function q when Equation (19) is used. With the isoparametric finite element formulation the distribution of q within the elements is determined by a standard interpolation scheme using the shape functions:

$$q = \sum_{i=1}^{m} N_i Q_i, \tag{20}$$

where:

Q_i are values of the weight function at the nodal points,

m is the number of nodes. The spatial derivatives of q can be found using the usual procedures for isoparametric elements. The equivalent domain integral in 2D can be calculated as a sum of the discretized values of Equation (19) [10], [13]:

$$J_k = \sum_{\substack{elements \\ in \\ A}} \sum_{p=1}^{p} \left[\left(\sigma_{ij} \frac{\partial u_i}{\partial X_k} - W \delta_{kj} \right) \frac{\partial q}{\partial X_j} \det\left(\frac{\partial X_m}{\partial \eta_n} \right) \right]_p w_p \quad i, j, k, m, n = 1,\ 2, \tag{21}$$

Note that the addend in the Equation (19) must vanish for linear-elastic materials. The terms within $[\,.\,]_p$ are evaluated at the Gauss points, using that the Gauss weight factors for each point are w_p. The present formulation is for a structure of homogeneous material in which no body forces are present. For the numerical evaluation of the above integral, the domain A is set from the set of elements about the crack tip.

5. Numerical examples

To illustrate the versatility and effectiveness of the enriched approximation, stress intensity factors are calculated using standard FEM and Xfem that are incorporated in our in-house software [14]. In this example we determined the stress field near the tip and the stress intensity factor for the opening mode of fracture (K_I). In Figure 9, the rectangular plate with a centered crack is shown. The plate is subjected to uniform uniaxial tensile stress σ_{yy} at two ends. The right hand half of the model is analyzed.

In the standard FEM, eight nodes elements and 2 × 2 Gauss quadrature are used. The four nodes elements over the entire domain and 6 × 6 Gauss quadrature only in the part of the domain with enriched nodes were used in the extended Xfem framework. The numerical results of the stress field near the crack tip are obtained using both approaches, where two meshes were utilized (40 × 40 and 80 × 80). The numerical simulation was performed using three version of X-FEM at the both meshes:

- nodes are enriched by only using the Heavisade function (40 × 40 (H); 80×80 (H)), (see Figure 6c);
- nodes are enriched by using the Heavisade function behind the crack tip and standard NT enriched functions ahead the crack tip (40 × 40 (H + NT), 80×80 (H + NT)), (see Figure 6a);
- nodes are enriched by using Heavisade function behind the crack tip and enlarged NT enriched functions ahead the crack tip (40 × 40 (H + NT)*, 80×80 (H + NT)*), (see Figure 6b).

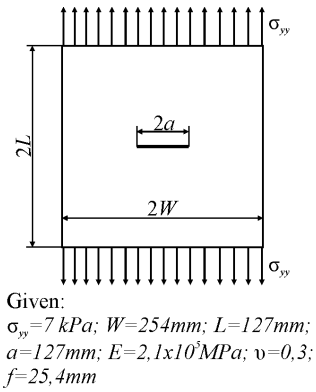

Fig. 9. The centered crack in the rectangular plate

The stress field near the crack tip for the linear-elastic materials is asymptotic and for this example theoretical result is available. The stress distribution, in the Gauss points, near the tip of the centered crack, is shown in the Figure 10.

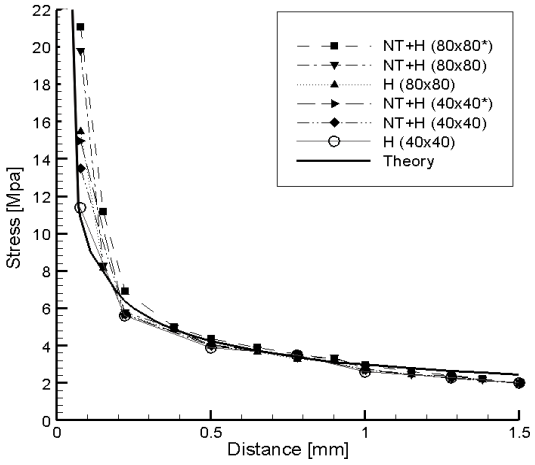

Fig. 10. Stress field σ_{yy} around the crack tip

All numerical results tend to theoretical value. Also, it can be seen that stress in the Gauss's points closest to the crack tip, increases, i.e., tends to the asymptotic value. It can be noticed that the influence of mesh density is bigger than for including the standard NT and enlarged NT functions. Hence, bigger mesh density with H enrichment gives better results than minor mesh density with (H+NT) and (H+NT)* enrichments. On the other hand, if we compare the models with the same mesh density, better results are obtained using standard (H+NT) end enlarged (H+NT)* enrichment.

The numerical results for the stress intensity factor of the first mode are compared to the theoretical values. The theoretical values are obtained using the following equation:

$$K_I^{\text{teor}} = \sigma F(a/b, h/b)\sqrt{\pi a}. \tag{22}$$

In Equation (22) correction factor F (a/b, h/b) for the given geometry, is taken from [7] as F (0.5, 0.5) and in this case it has the value ≈ 1.9. According to the applied loading and chosen correction factor, theoretical value of the stress intensity factor is $K_I^{\text{teor}} = 7.52 Psi\sqrt{in}$. The results for the stress intensity factor are shown in the Table 1, obtained by integration of the J-integral using the J-EDI method, corresponding to the different integration domain r_c. The radius of integration domain r_c is defined in % of the length of the crack a.

Table 1. Comparing the theoretical and the numerical results for the stress intensity factor

r_c (%a)	K_I FEM4 40 × 40	K_1 FEM8 40 × 40	K_I Xfem(H) 40 × 40	K_I Xfem (H + NT) 40 × 40	K_I Xfem(H + NT)* 40 × 40	K_I Xfem(H), 80 × 80
10	11.41	7.68	7.40	7.52	7.53	7.53
15	11.61	7.65	7.52	7.55	7.52	7.53
20	11.62	7.65	6.76	6.89	7.02	7.52
25	10.41	7.40	7.51	7.56	7.54	7.52
30	11.67	7.56	7.51	7.53	7.54	7.53
35	11.69	7.60	7.50	7.51	7.52	7.52
40	11.70	7.57	7.49	7.50	7.51	7.51
Av vel.	11.44	7.59	7.39	7.44	7.45	7.51
N/A %	52%	0.88%	1.73%	1.06%	0.99%	0.03%

The results for the stress intensity factor are obtained using: standard FEM with 4 node discretization (FEM4), standard FEM with 8 node discretisation (FEM8), Xfem with only H enrichments (Xfem(H)), Xfem with H+NT standard enrichments (Xfem(H + NT)), and Xfem with enlarged NT enrichments (Xfem(H + NT)*). In this example the same size of elements are used in standard Xfem as well as in the extended Xfem. The difference is that the quarter of the rectangular plate with the central crack is used in the standard FEM, and the half of the test model is used in the ex-

tended Xfem. The results obtained using the FEM and the Xfem are compared to theoretical values and it is shown in Table 1. One can note that numerical experiment is carried out by using the less favourably mesh (compared to 80 × 80). Evaluation is given as N/A % (Numerical*100/Analitical).

In Figure 11, the stress field of the half model, around the central crack, that is obtained by using Xfem is shown. Crack overlaps the elements edges, and there is no physical separation of the joint sides of elements. In this case, the discontinuity at the crack faces is modelled by using enrichment functions. In this figure, it can be noticed that, within the extended Xfem framework, the stress concentration is located well, i.e., placed at the real crack tip.

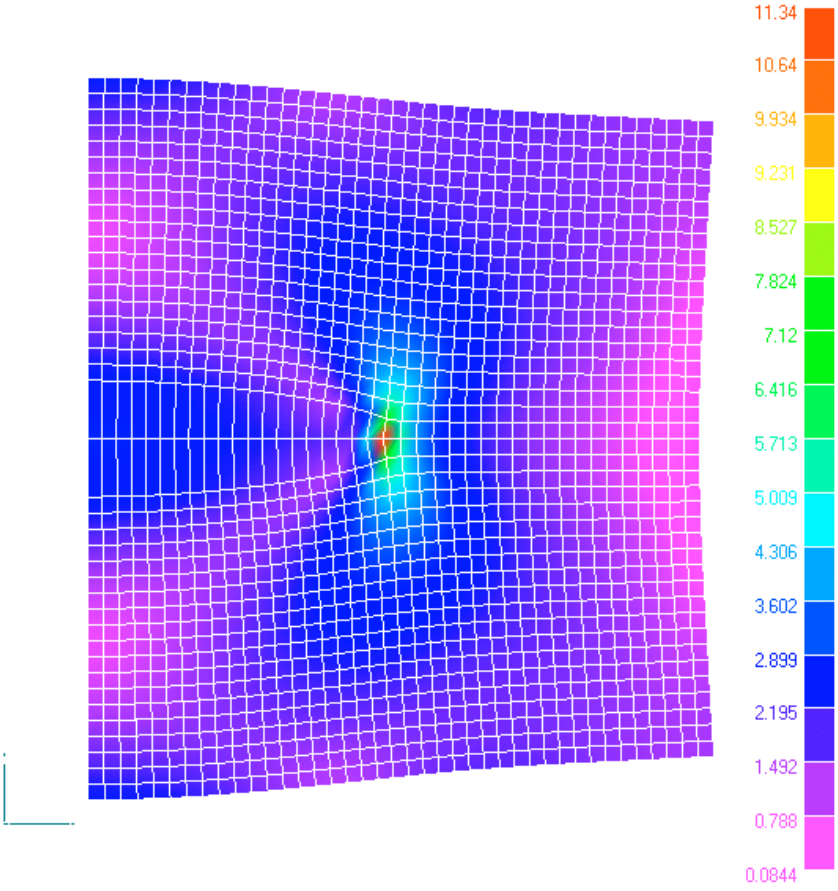

Fig. 11. The stress field around the central crack

In the Figure 12, the displacement field around the central crack obtained by extended Xfem is shown. It is worthy to stress that, without explicitly geometrical crack

modelling, we obtained discontinuity in the displacement field over the crack faces by using the Heaviside function.

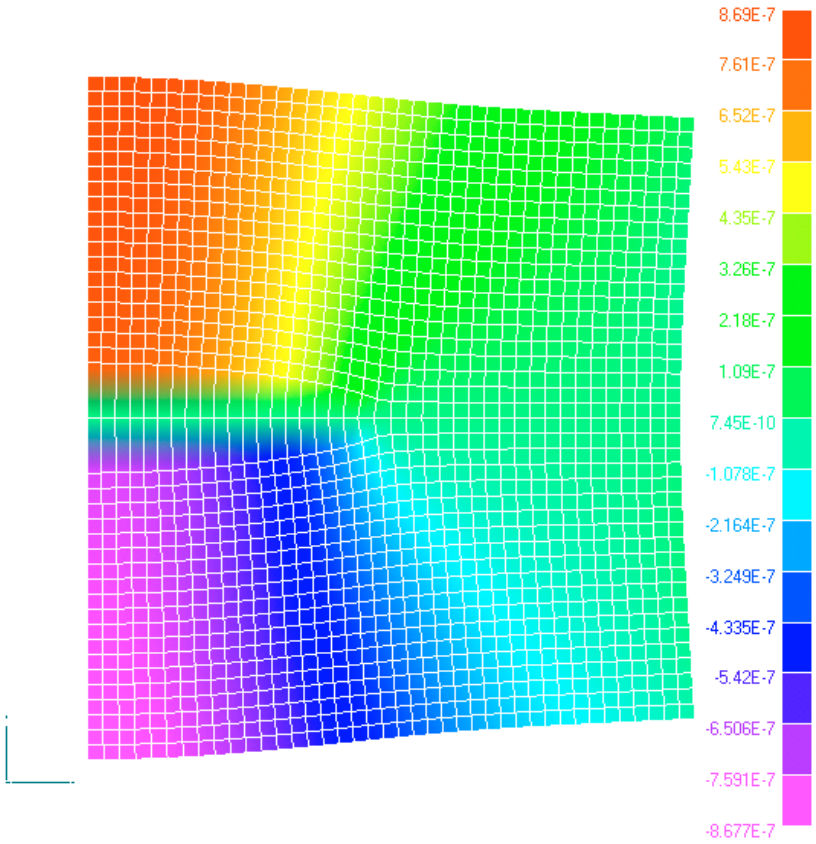

Fig. 12. The displacement field around the central crack obtained

6. Conclusion

The essential idea in Xfem method is to add enrichment functions to the approximation that contains a discontinuous displacement field. The crack is described by means of the position of the tip and level set of a vector valued mapping. The developed LS functions are used to determine values of NT functions. We also modified the enriching of corresponding elements. The crack is presented as discontinuity in displacements within the element. Xfem does not require projection between the mesh and crack geometry, and allows arbitrary crack in the finite element mesh. The methodology adopted for crack modelling belongs to the aspect enriching of the extended finite element method (Xfem).

In this study analysis was carried out on the ways of enriching around the crack tip, and the size of finite elements of the value of stress field near the crack tip and stress intensity factor around of the crack. At the same benchmark example, impact size of finite element mesh is analyzed and ways of enriching in the Xfem. On the basis of analysis it can be concluded that at the accuracy of results greater impact has mash refinement than enrichment with NT functions. Gained results for the SIF and stress field are more similar to analytical solutions using Xfem variations with H enriching on the 80 × 80 finite element mesh than to Xfem variation with H+NT enriching on the 40 × 40 finite element mesh. In this way, we came to the conclusion that the attribute of Xfem algorithm without using Near Tip enriching functions gives satisfactory results when used enough tiny mesh of finite elements and thus opens the possibility of future application of the Xfem in the zone of plasticity.

References

[1] Belytschko T., Black T.: *Elastic crack growth in finite elements with minimal remeshing*, International Journal for Numerical Methods in Engineering, Vol. 45, No. 5, 1999, pp. 601–620.

[2] Moes N., Dolbow J., Belytschko T.: *A finite element method for crack growth without remeshing*, International Journal for Numerical Methods in Engineering, Vol. 46, No. 1, 1999, pp. 131–150.

[3] Sedmak A.: *Applying fracture on structural integrity*, (in Serbian), University Belgrade, Serbia, ISBN 86-7083-471-5, 2003.

[4] Melenk J. M., Babuska I.: *The partition of unity finite element method: Basic theory and applications*, Computer Methods in Applied Mechanics and Engineering, Vol. 39, No. 1, 1996, pp. 289–314.

[5] Daux C., Moes N., Dolbow J., Sukumur N., Belytschko T.: *Arbitrary cracks and holes with the extended finite element method*, International Journal for Numerical Methods in Engineering, Vol. 48, No. 12, 2000, pp. 1741–1760.

[6] Sukumur N., Prevost J.H.: *Modelling quasi-static crack growth with the extended finite element method, Part I: Computer implementation*, International Journal of Solids and Structures, Vol. 40, 2003, pp. 7513–7537.

[7] Jovičić G.: *An extended finite element method for fracture mechanics and fatigue analysis*, (in Serbian), PhD thesis, University of Kragujevac, Serbia, 2005.

[8] Rice J.R.: *A path independent integral and approximate analysis of strain concentration by notches and cracks*, Journal of Applied Mechanics, Vol. 35, 1968, pp. 379–386.

[9] Jaric J., Sedmak A.: *Physical and mathematical aspects of fracture mechanics, from fracture mechanics to structural integrity assessment*, IFMASS 8, COBISS.SR-ID 115216140, 2004.

[10] Lin C-Y.: *Determination of the fracture parameters in a stiffened composite panel*, PhD thesis, North Carolina State University, 2000.

[11] Kim J.-H., Paulino G.H.: *Mixed-mode J-integral formulation and implementation using graded elements for fracture analysis of no homogeneous orthotropic materials*, Mechanics of Materials, Vol. 35, No. 1–2, 2002, pp. 107–128.

[12] Enderlein M., Kuna M.: *Comparison of finite element techniques for 2D and 3D crack analysis under impact loading*, International Journal of Solids and Structures, Vol. 40, No. 13–14, 2003, pp. 3425–3437.
[13] Kojic M., Jovicic G., Zivkovic M., Vulovic S.: *Numerical programs for life assessment of the steam turbine housing of the thermal power plant*, Special Issue: From Fracture Mechanics to Structural Integrity Assessment, editors: S. Sedmak, Z. Radaković, University of Belgrade, Serbia, 2004.
[14] Kojic M., Jovicic G., Zivkovic M, Vulovic S.: *PAK-FM&F – software for fracture mechanics and fatigue based on the FEM and X-FEM*, Manual, University of Kragujevac, Serbia, 2003–2005.

Ulepszenie algorytmu do numerycznego modelowania pęknięć

Rozszerzona metoda elementów skończonych eXtended (XFEM) jest ostatnio uznawana, jako skuteczne i efektywne narzędzie do modelowania numerycznego w mechanice powstawania pęknięć. W artykule przedstawiono szczególe zastosowania algorytmu XFEM we własnym oprogramowaniu bazującym na metodzie elementów skończonych. Celem badań było zweryfikowanie standardowego algorytmu XFEM w celu stworzenia możliwości przyszłej aplikacji tego algorytmu w obszarze plastycznym. W celu oceny dokładności obliczeń, wyniki liczbowe współczynników intensywności naprężeń zostały porównane z teoretycznymi i danymi z elementów skończonych. Uzyskane wyniki liczbowe wykazały dobrą zgodność ze wzorcami rozwiązań. Do wyliczenia wskaźników intensywności naprężeń użyta została metoda równoważnej całki J. Szczegółowo omówiono zagadnienia geometrii obliczeniowej związane z przedstawieniem pęknięcia i ulepszeniem aproksymacji w metodzie elementów skończonych.

ARCHIVES OF CIVIL AND MECHANICAL ENGINEERING

Vol. X 2010 No. 3

Mechanical properties of parts produced by using polymer jetting technology

A. KĘSY, J. KOTLIŃSKI
Technical University of Radom, Malczewskiego 29, 26-600 Radom, Poland.

A study investigating the effects of orientation of parts produced in a layer based process with photopolymer materials is presented. Tensile and hardness testing methods have been used. The test results show that the part producing orientation has an effect on the mechanical properties of the produced parts. The analysis has shown that this is due to the heterogeneity absorption of light energy by the photopolymer material during the jetting process.

Keywords: *rapid prototyping, polymer jetting technology, mechanical properties, fabricated parts*

1. Introduction

Rapid prototyping allows manufacturers and industrial designers to reduce product development cycles and shorten the time-to-market of new products in many industries. The technology has been adopted primarily in major markets such as automotive, heavy machinery, aerospace, electronics and consumer electronics, medical devices, consumer goods, footwear.

Rapid prototyping polymer jetting technology utilizes ultra-thin layer 3-dimensional printing system and photopolymer materials. The polymer jetting technology enables the production of 3-dimensional parts with smooth surfaces and fine details. Parts are completely manufactured during the process of production and can be handled immediately. A geometric model of conceptual design is created by means of CAD software which uses STL or SLC formatted files. The technology has been developed by Objet Geometries Ltd. company.

The production of parts using the polymer jetting technology can be applied in silicon moulding, rapid tooling, investment casting or vacuum forming.

The polymer jetting technology has been developed not only as rapid prototyping technology to produce functional prototypes [1–2] but it can also be applied in rapid manufacturing [3]. In these cases it is very important for the design process to know the properties of materials that could be applied.

In the paper orientation effects of parts made from photopolymer by means of the polymer jetting technology have been presented. In order to assess the mechanical properties of the produced parts tensile and hardness testing methods are used. These

kinds of tests should be taken into consideration during the layer based process when mechanical properties of produced parts are important. The polymer jetting technology can be used for manufacturing of functional prototypes.

2. Mechanical properties of polymer parts produced by means of layer technology

Mechanical properties of parts produced by means of the polymer jetting technology have not been investigated widely so far, but a lot of work has been done in order to define parameters for the layer technology, that is the laser sintering technology. The laser sintering technology is similar to the polymer jetting technology because it applies a layer based system to create complex 3-dimensional parts and uses photopolymer materials. In the technology CO_2 laser traces out and selectively sinters a layer of photopolymer powder material on the part being produced [4–5].

Gibson and Shi [6] examined anisotropy in polymer parts made by means of the laser sintering technology. Tensile test bars were produced in different kinds of orientation using a nylon material. The parts produced in the *X*-axis orientation showed a higher average tensile strength value than those in the *Y*-axis orientation. The test bars produced in the *Z*-axis orientation were of the worst tensile strength value. However, in the test bar shape was not compatible with the ISO standards.

In the work [7] the effect of the produced model orientation by the laser sintering technology for the nylon-12 material was examined. The researcher uses the tensile, flexural and compression testing methods. The tensile tests showed a maximum difference of 16% in strength for test bars produced in the *X*, *Y* and *Z*-axes orientation. The test bars produced in the *X*-axis orientation showed the highest strength while the test bars produced in the *Z*-axis showed the weak strength value.

3. Polymer jetting technology

In the polymer jetting technology process layers are produced in the horizontal direction (*Z*-axis) as shown in Figure 1. A jetting bridge (with 8 jetting heads) slides back and forth along the *X*-axis similar to a line printer. Very thin photopolymer drops are jetted in super-thin layers of just 16 μm onto an internal tray [8]. After creating each layer UV bulbs (located alongside the jetting bridge) emit UV light and immediately cause hardening of each layer. The internal tray moves down with a precise step and the jetting bridge continues creating, layer by layer, until the produced part is completed. Advanced software tools enable all heads of jetting bridge to jet identical amounts of material on the internal tray, synchronously. This results in ultra-smooth surfaces. Precise mechanics, electronics and software features allow to produce most parts with accuracy from 100 μm to 300 μm according to geometry, part orientation and part size [8].

A raster process is used to produce models in the polymer jetting technology machine. It enables the production of models in slices of 65 mm not point-by-point. Several

parts can therefore be created in the same amount of time. The combination of the raster process with the high-speed mechanical movement reduces the production time.

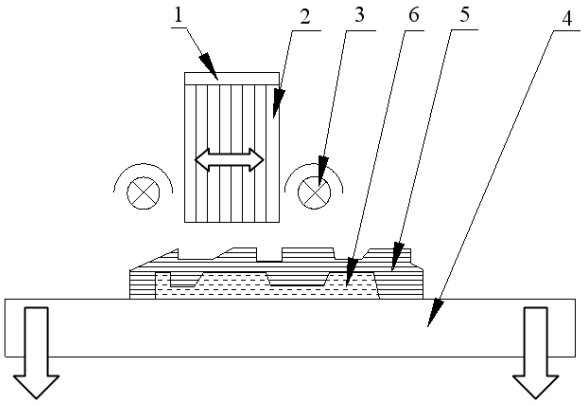

Fig. 1. Scheme of Polymer jetting technology process: 1 – jetting bridge, 2 – jetting head, 3 – UV bulb, 4 – internal tray, 5 – produced part, 6 – supporting material

In order to cope with complicated geometries, such as cavities, overhangs, undercuts, delicate features, and thin-wall sections, geometry of the support structure is pre-programmed. Supporting material ensures no hard grid edges. When the model is completed, the supporting material is easy to be removed by water, leaving a smooth surface. Two different materials are used for model building: one for the actual part, and the other one for support.

An integral part of the polymer jetting technology is a group of proper materials (photopolymer resins). It includes several types of flexible or rigid and transparent as well as opaque model materials with multiple colours. A single support gel-like material is used for all the types of materials the parts are produced.

Parameters of the polymer jetting technology machine are presented in Table 1.

Table 1. Parameters of the Polymer jetting technology [8]

	Parameter of model	Value of parameter
1.	Ultra-thin layer thickness	16 μm
2.	Built resolution *XYZ*	42 × 42 × 16 μm
3.	Accuracy	100 – 300 μm
4.	Net build size *XYZ* (Eden 500V machine)	500 × 400 × 200 mm
5.	Minimal wall thickness	0.6 mm

4. Experimental tests

It is important to show how the fabrication parameters of the polymer jetting technology influence the material properties of produced parts. This was achieved by carrying out experimental measuring.

4.1. Experimental tests methodology

The tensile strength and the shore hardness of test bars which had been produced in different orientation were measured.

All the test bars were produced using the polymer jetting technology machine Eden 260 with photopolymer FullCure 720 material (resin in a transparent colour). The process parameters applied were typical for this technology and were kept the same for the all test bars. The test bar used for this research is presented in Figure 2.

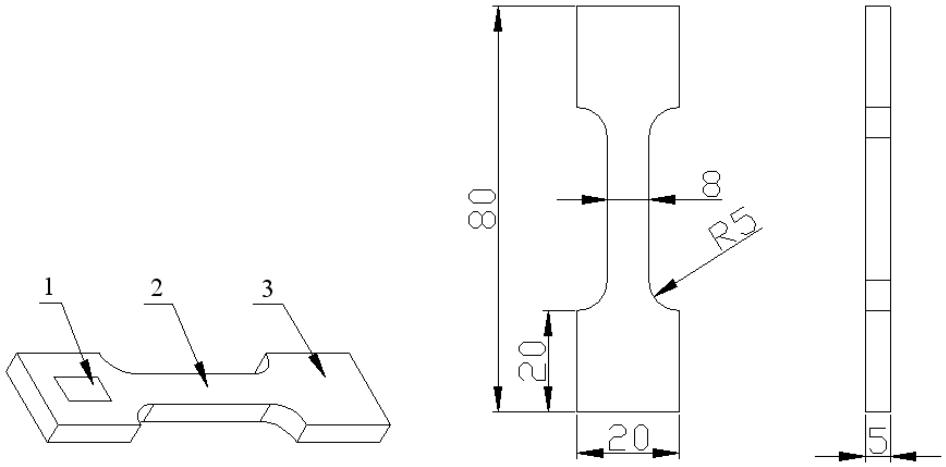

Fig. 2. Test bars geometry: 1 – hardness measure field, 2 – narrow part, 3 – clamp part

Figure 3 shows the *X*, *Y* and *Z*-axes test bars orientation during the production. The orientation of the test bars was chosen to assess the variations in mechanical properties between the 1st (*XY*), 2nd (*YZ*) and 3rd (*XZ*) orientation. A total of 30 test bars were produced for the test with 10 test bars for each orientation. The orientation of the test bar during the fabrication is presented in Figure 4.

The Walter and Bai AG (FS-LFM-100 type) with a 10 kN load cell was used to conduct the mechanical property test. Figure 5 shows the test bar during tensile process and Figure 6 shows the test bars after a tensile process.

All the tests were conducted in the laboratory in the temperature and humidity at 22 °C and 40% relative humidity.

The tensile test and measure of the shore hardness were compatible with the ISO standards (ISO 527-1; ISO 527-2; ISO 868) [9–11] and were conducted to observe what effect the test bars orientation had on the test results. For the tensile test the speed of 5 mm/min was used. The shore hardness H_d was measured in 5 points on the clamp part of the test bar as shown in Figure 2. The stoltman type D durometer was applied to measure the shore hardness.

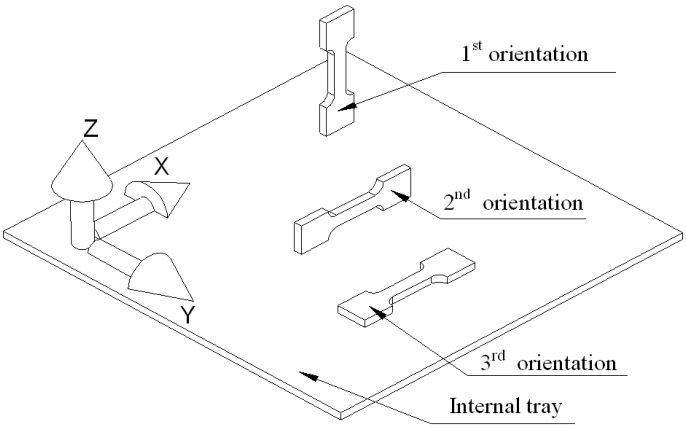

Fig. 3. Build orientation of test bars: 1st orientation (test bars number 1–10), 2nd orientation (test bars number 11–20), 3rd orientation (test bars number 21–30)

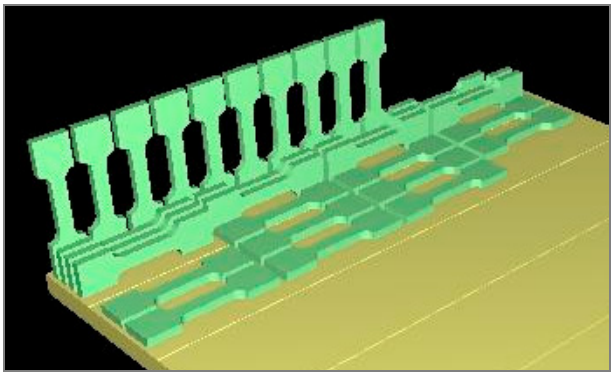

Fig. 4. View of internal trial with test bars before production process

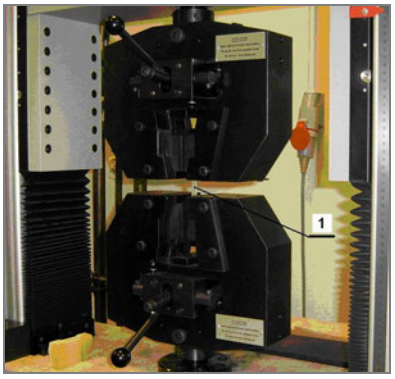

Fig. 5. View of the test bar during tensile process, 1 – test bar

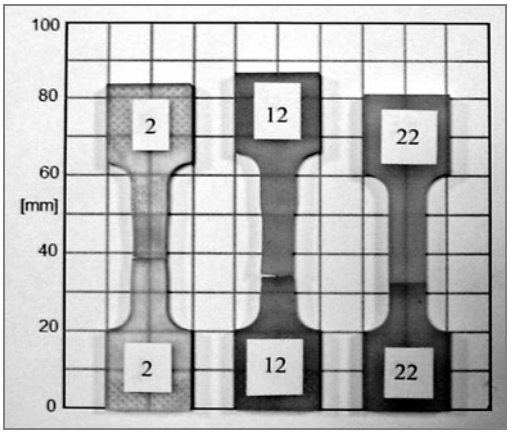

Fig. 6. View of test bars after tensile process: for the 1st orientation (test bar number 2), for the 2nd orientation (test bar number 12), for the 3rd orientation (test bar number 22)

4.2. Results of experimental tests

Figure 7 shows the characteristics obtained from the tensile test for the bar produced orientation. The analysis of the characteristics of the tensile test shows that the bars produced in the 1st and the 2nd orientations show different results than for the 3rd orientation. For the 1st and the 2nd orientations a clear yield point occurs and for the 3rd orientation brittle rupture occurs. The characteristics made for the 1st and the 2nd orientations are typical for plastics compound filled and reinforced by small rods while the characteristic for the 3rd orientation with brittle rupture is typical for unfilled plastics (ISO 527-1; ISO 527-2) [9–10]. Thus, it can be assumed that the tensile strength for the 1st and the 2nd orientations is defined by the yield point σ_y and for the 3rd orientation by the breaking stress σ_B, Figure 8.

Based on above characteristics and the test bar measurements following parameters:

– tensile strength – for the 1st and the 2nd orientations the yield point σ_y, for the 3rd orientation the breaking stress σ_B,
– the elongation at break ε_B,
– reduction of the area at fracture υ defined by formula:

$$-\upsilon = \frac{S_0 - S_u}{S_0} 100\%, \tag{1}$$

where:

S_0 – cross-sectional area of narrow part of test bar before break [mm^2], see Figure 2,

S_u – cross-sectional area of narrow part of test bar at the break point [mm^2] were calculated (ISO 527-1) [9].

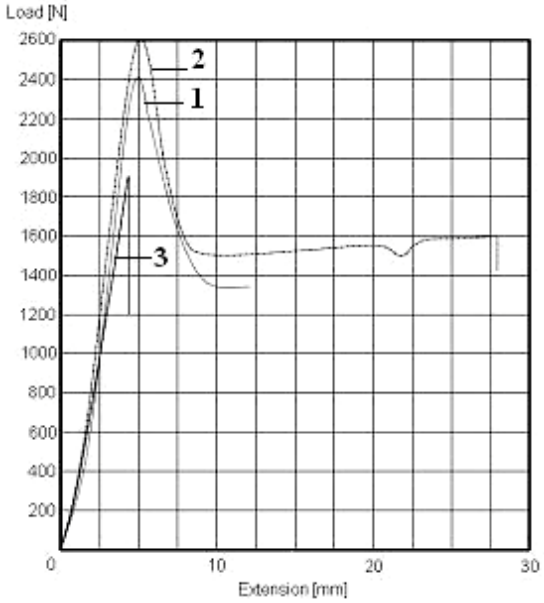

Fig. 7. Characteristics obtained from the tensile test for: 1 – the 1st orientation, 2 – the 2nd orientation, 3 – the 3rd orientation

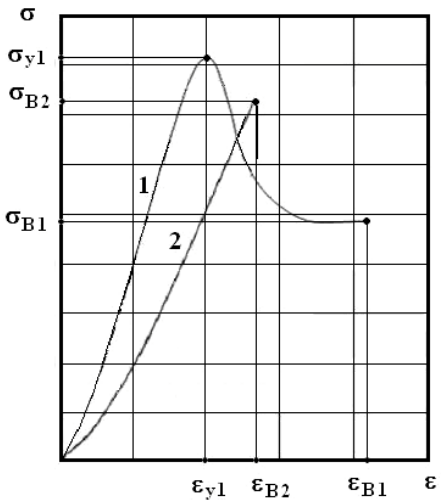

Fig. 8. Tensile strength for different materials: 1 – plastics compound filled and reinforced by small rods, 2 – unfilled plastics, σ – ensile strength, σ_y – yield point, σ_B – breaking stress, ε – elongation

A multi-sample statistical analysis of measured data was conducted (ISO 2602) [12]. The confidence level was set to 95%.

The results of the mechanical properties investigated are shown in Figures 9–11 and in Tables 2 and 3. They show average results from 30 test bars produced in each orientation. The results of the hardness measurements are shown in Table 4 and in Figure 12.

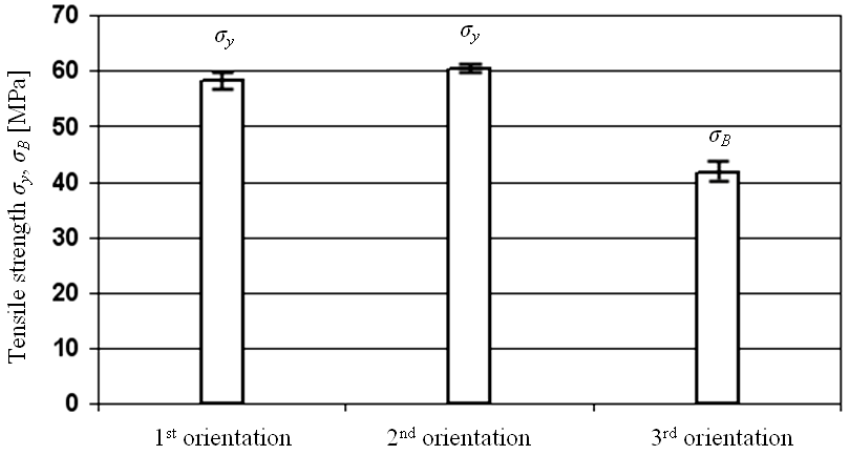

Fig. 9. Tensile strength σ_y and σ_B against produced orientation

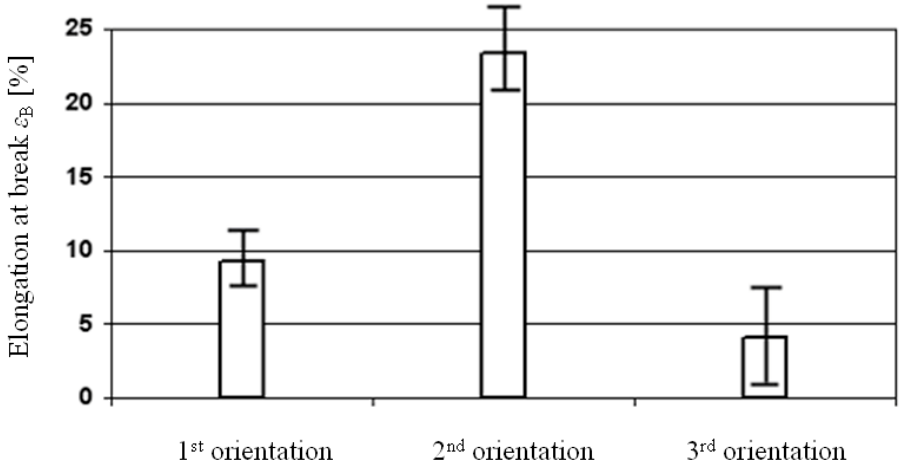

Fig. 10. Elongation at break ε against produced orientation

The tensile test results for parts which were produced in the 2nd orientation produced the highest tensile strength, elongation at break ε_B, reduction of the area at fracture υ values while the lower values were obtained from the parts produced in the

1st orientation. Although the lowest values come from the ones produced in the 3rd orientation, the results of hardness measurements from practical point of view are similar for all orientations.

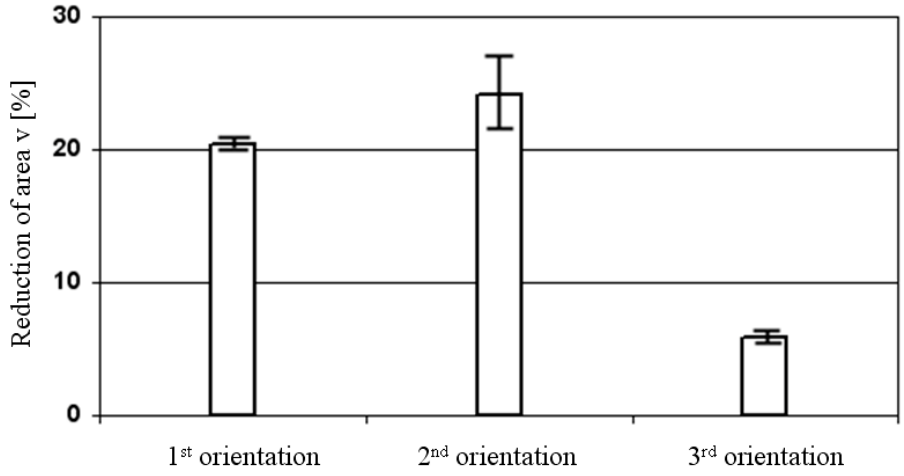

Fig. 11. Reduction of area at fracture υ against produced orientation

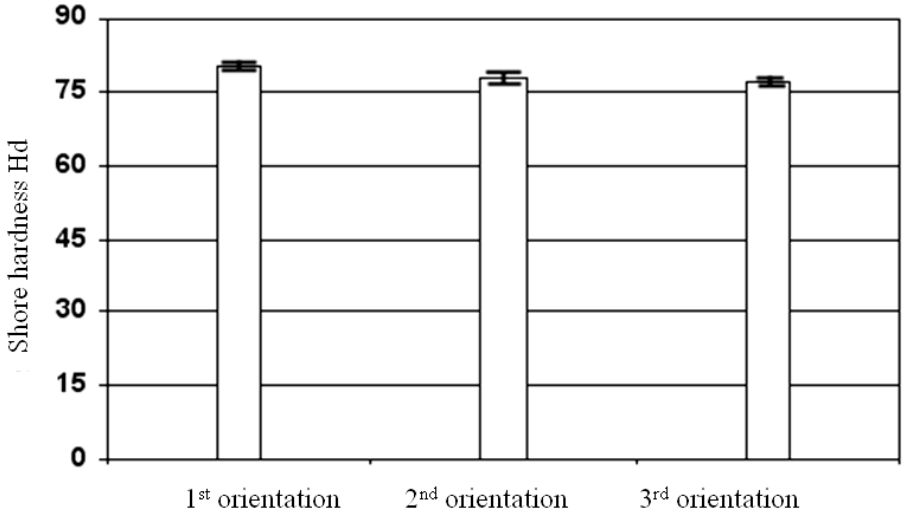

Fig. 12. Shore hardness H_d of testing bars against produced orientation

From Table 3 it can be found out that the reduction of the area at fracture υ and the elongation at break ε_B values are heavily influenced by the produced orientation of the test parts with a maximum difference 75.7% and 65.6% respectively. The tensile

strength values are not so strongly affected by the produced orientation of the test parts with only 29.4%. The Shore hardness strength values are not affected by the produced orientation of the test parts.

Table 2. Tensile properties of the test bars in different build orientations

Orientation	Parameter	Tensile strength		Elongation at break ε_B [%]	Reduction of area at fracture υ [%]
		Yield point σ_y [MPa]	Breaking stress σ_B [MPa]		
1st orientation Test bars number 1–10	Mean value $\bar{x}$	58.28	–	9.26	20.38
	Standard deviation s	1.42	–	3.25	1.82
	Confidence interval m	57.26–59.29	–	6.92–11.6	19.07–21.69
2nd orientation Test bars number 11–20	Mean value $\bar{x}$	60.44	–	23.44	24.12
	Standard deviation s	0.4	–	8.04	5.85
	Confidence interval m	60.05–60.83	–	17.65–29.23	19.91–28.33
3rd orientation Test bars number 21–30	Mean value $\bar{x}$	–	41.65	8.04	5.85
	Standard deviation s	–	3.72	0.25	1.16
	Confidence interval m	–	38.97–44.33	3.98–4.34	3.07–4.75

Table 3. Difference of mean value of tensile properties for the test bars in different build orientation between the 2nd orientation and other orientations [%]

Difference between orientations	Tensile strength σ	Elongation at break ε_B	Reduction of area at fracture υ
2nd orientation and 1st orientation	3.6	60.4	15.5
2nd orientation and 3rd orientation	29.4	65.6	75.7

Table 4. Hardness of testing bars in different build orientation

Orientation	Parameter	Shore hardness H_d
1st orientation Test bars number 1–10	Mean value $\bar{x}$	80.23
	Standard deviation s	0.45
	Confidence interval m	79.91–80.55
2nd orientation Test bars number 11–20	Mean value $\bar{x}$	77.78
	Standard deviation s	1.4
	Confidence interval m	76.03–77.53
3rd orientation Test bars number 21–30	Mean value $\bar{x}$	77.18
	Standard deviation s	0.31
	Confidence interval m	76.96–77.4

5. Model explaining mechanical anisotropy

The anisotropy of mechanical properties of parts produced by means of polymer jetting technology could be explained on the basis of the analysis of the bonding between layers assuming that the bonding stress between the layers for each orientation is constant. This way of consideration is clear for the 3rd orientation because in this orientation the tested force is perpendicular to the layers surface. But this effect does not explain the differences between orientation 1st and 2nd because for these orientations the surface of connection between all layers is the same, so the testing force should be the same.

In the polymer jetting technology UV light hardens each layer. The light emitted by two UV tube bulbs runs parallel to a jet line of the jetting heads. During the jetting process sides of created layer parallel to bulbs absorb more light energy than the layer surface because:

– the distance from the bulb to an edge is less than the distance from the bulb to some points of the top surface, see Figure 13,

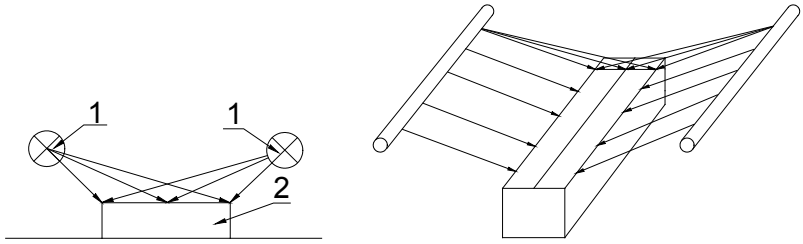

Fig. 13. Scheme of distribution of light energy for the test bars surfaces, different distance:
1 – UV bulbs, 2 – produced part

– the bulbs lighten the top surface and additionally the sides of the created layer, see Figure 14,

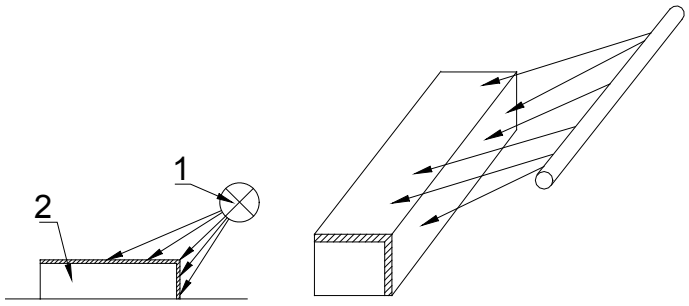

Fig. 14. Scheme of distribution of light energy for the test bars surfaces, additionally lighted the sides:
1 – UV bulbs, 2 – produced part

– the sides of the created layer are lit during the jetting process and additionally when the light is doused on the top surface by jetting photopolymer, see Figure 15.

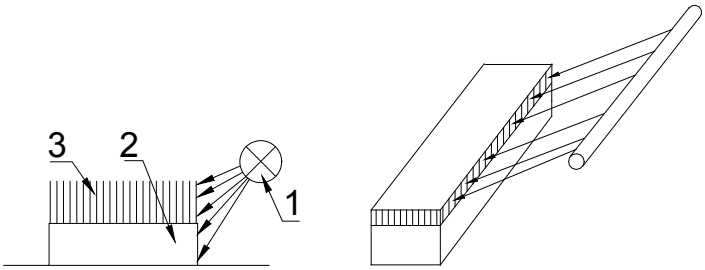

Fig. 15. Scheme of distribution of light energy for the test bars surfaces, sides additionally lighten during jetting process: 1 – UV bulbs, 2 – produced part, 3 – jetting photopolymer

Because of the above reasons the edges that are parallel to *X*-axis of the created test bar are dense and harder than other parts of the test bar and at the same time more resistant. The edges function as reinforcement rods. As a result the tensile strength for a test bar is higher than tensile force acting along the edge direction that is for the 1st and 2nd orientation. For the 2nd orientation a surface of tensile bar side is higher than for the 1st orientation so for the 2nd orientation a tensile resistance is the highest. For the 3rd orientation the edges are perpendicular to the direction of tensile force and reinforcement rods effect does not occur. So the material of the narrow part of test bars can be modelled as a compound filled by the same rods.

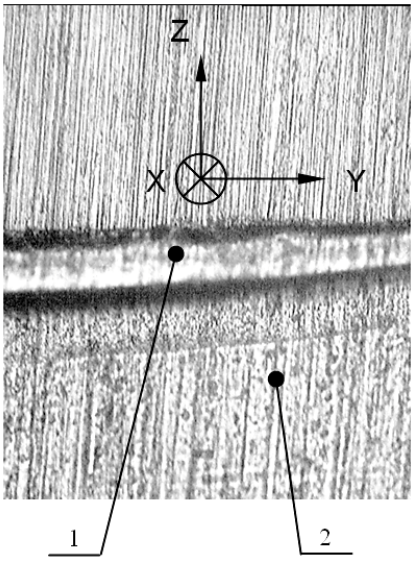

Fig. 16. Photo of cross sections of test bars narrow part: 1 – skin, 2 – base material

The model described above which explains mechanical anisotropy of parts produced by the polymer jetting technology is confirmed by runs of tensile characteristics from Figure 7 and by the photo of cross section of one the test bar presented in Figure 16. The photo was obtained by means of Carl Zeiss-Jena Neophot 21 metallographic microscope with multiplication 100. The photo shows dark belts run parallel to the edge. This is the result of differences in test bar structure near the edge and different density and hardness of the material.

6. Conclusion

The experimental results show the evidence of anisotropy for test bars produced by means of the polymer jetting technology from the photopolymer FullCure 720 material. This behaviour occurs due to the produced orientation of the test bars. The test bars produced in the 2nd orientation have the highest mechanical properties whilst these produced in the 3rd orientation have the smallest mechanical properties. The photo of the test bar cross section shows that the edges of test bars parallel to the direction of jetting bridge movement are more dense and harder than the central part. This is because during the jetting process the created layer edges absorb more light energy than the layer surface. The material of the test bars can be modelled as a compound filled and reinforced by rods.

The test results show that the orientation of the produced parts in the internal tray of the polymer jetting technology machine is the main factor which influences their mechanical properties.

References

[1] Kesy Z., Kesy A., Pawelski Z., Jackson M., Parkin R.: *Mechatronics design of impellers for hydrodynamic torque converters and hydrodynamic clutches*, Proceedings of the MX2006: 10th Mechatronics Forum International Conference, Philadelphia, USA, 2006, on CD, Paper No. 033101.

[2] Kotlinski J., Kesy A., Kesy Z., Jackson M., Parkin R.: *Dimensional deviations of machine parts produced in the laser sintering process*, Int. J. Rapid Manufacturing, Vol. 1, No. 1, 2009, pp. 88–98.

[3] Hopkinson N., Dickens P.: *Analysis of rapid manufacturing – using layer manufacturing processes for production*, Proc. Inst. Mech. Eng., Part C, Journal of Mechanical Engineering Science, Vol. 217, No. 1, 2003, pp. 31–39.

[4] Chua C.K., Leong K.F., Lim C.S.: *Rapid prototyping principles and applications*, Jon Wiley and Sons, Inc., New York, USA, 2003.

[5] Grimm T.: *User's guide to rapid prototyping, society of manufacturing engineers*, Derbon, Michigan, USA, 2004.

[6] Gibson I., Shi D.: *Material properties and fabrication parameters in selective laser sintering process*, Rapid Prototyping Journal, Vol. 3, No. 4, 1997, pp. 129–136.

[7] Ajoku U., Salesh N., Hague R.J.M., Erasenthiran P.: *Investing mechanical anisotropy and end-of-vector effect in laser-sintered nylon parts*, Journal of Engineering Manufacture, Vol. 220, No. 7, 2006, pp. 1077–1086.
[8] Objet Geometries Ltd. Company, Eden 250, Eden 260, Eden 350/350V Technical Specifications.
[9] International Standard Organization, ISO 527-1: *Plastics – determination of tensile properties-part 1*.
[10] International Standard Organization, ISO 527-2: *Plastics – determination of tensile properties-part 2*.
[11] International Standard Organization, ISO 868: *Plastics and ebonite – determination of indentation hardness by means of durometer (shore hardness)*.
[12] International Standard Organization, ISO 2602: Statistical interpretation of tests results – estimation of the mean – confidence interval.

Właściwości mechaniczne części wytwarzanych metodą *polymer jetting technology*

W artykule przedstawiono wyniki badań wytrzymałości przy statycznym rozciąganiu oraz twardości próbek wykonanych metodą szybkiego prototypowania – *polymer jetting technology*. Próbki różniły się ustawieniem w maszynie do szybkiego prototypowania podczas ich wytwarzania. Badania wykazały, że istnieją istotne różnice w wytrzymałości próbek w zależności od ich ustawienia podczas wytwarzania.

ARCHIVES OF CIVIL AND MECHANICAL ENGINEERING

Vol. X 2010 No. 3

Testing procedures in evaluation of resistance of innovative shear connection with composite dowels

W. LORENC, E. KUBICA, M. KOŻUCH
Wrocław University of Technology, Wybrzeże Wyspiańskiego 27, 50-370 Wrocław, Poland.

The article constitutes an introduction to the issue associated with modern steel-concrete composite girders having open continuous connectors of the composite dowels type. The way of fabrication of the steel portion of the composite girders has been presented as well as the details connected with experimental investigations on the new type of composition which demands broader approach of researches than attempts of determining the load-bearing capacity used so far, known as POST. The steel connector constitutes an integral part of the steel part of composite beam, in which it is subjected apart from the local longitudinal shear acting between steel and concrete, to the global effects of bending and axial loading as well. Thus, the stress criteria describing the composite dowel's behaviour have to be established and it is much more than pure load-bearing capacity criteria used in present. The test procedures combining the concept of the load-bearing capacity for the concrete part of the connector and the elasticity of its steel part lead to an efficient designing of the composite structures.

Keywords: *composite structures, composite dowels, continuous shear connection, testing procedures*

1. Innovative shear connection

In civil engineering, especially in bridge structures, are starting to be applied the composite structures, in which the connection steel-concrete is achieved by the continuous line of the cut along the I-beam's web [1]. As the result of this operation, two tee beams are produced with a specially formed web (convex and concave cuts), which allows to create efficient integration between steel and concrete under the longitudinal shear. The composite structures contains continuous, open steel dowels produced from mentioned above tee steel section and the concrete, filling up the space between steel girders and additionally reinforced in the transversal direction. Presented herein idea of the composite beam is shown in Figure 1.

1.1. Production engineering of the steel component

The tee steel beam used in the considered structure is produced as a half from the hot-rolled I-beam (although corresponding cross-section can be created by welding). The cut can be conducted with any methods that give a cut surface with a quality not worse from that obtained by automatic oxygen cutting (for instance plasma or laser

cutting). The quality of the cut surface is significant especially when the fatigue strength has to be determined. The line of the cut should be get after a single operation guaranteeing the obtainment of two equal tee cross-sections. Otherwise, an account of the deformation of beams caused by residual stress, the repeat of programming of the cutting device is practically impossible. At present in the structures a MCL shape is applied as easy to produce and having required strength parameters [2, 4–5]. The way of MCL cut is presented in Figures 2–4.

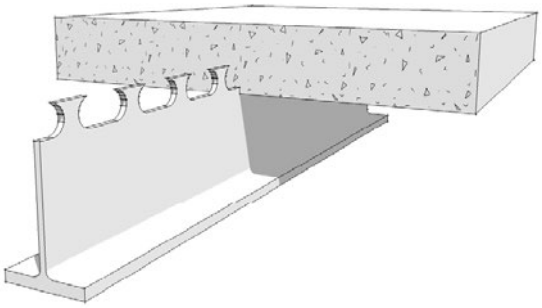

Fig. 1. Composite beam with innovative shear transmission by composite dowels (draw. G. Nillson)

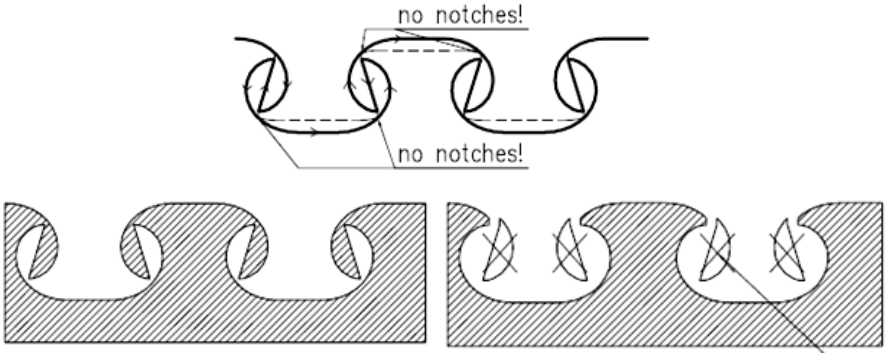

Fig. 2. Cutting line for MCL shape

Fig. 3. Steel plate after gas cutting-remaining steel parts to be removed by hand cutting

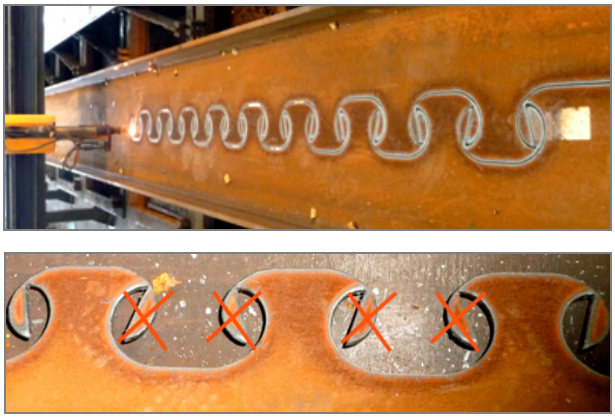

Fig. 4. I-Beam IPE500 during cutting and MCL shape after gas cut

The effect of residual stresses relieved during the cut and the process of making a recommended camber are described in the work [8].

1.2. Issues of dimensioning

The steel-concrete connection executed by described previously way requires the computational personal touch for estimating its resistance, different from that used when mechanical connectors are applied. The composite dowel constitutes an integral part of the steel component and its stressing affects the global stress state in the entire unit. Thus, it is not possible to separate the problem of dimensioning of the composite beam (due to effects tied with the distribution of normal stress in the composite cross section) from the dimensioning of the connector itself under the longitudinal shear between the steel and concrete. The computational approach should comprehensively describe both mentioned above issues. Additionally the degree of complexity of such a connection is forcing into applying the non-linear analyses (FEM) taking into account the material and geometrical nonlinearities resulting from the contact effects between steel and concrete. It is also essential to carry out extensive destructive tests for different types of elements. Some destructive tests at present applied for the evaluation of the resistance of connectors of the composite dowels type are presented below.

2. Testing procedures

2.1. Push-out standard test (POST)

POST (push-out standard test) constitutes a basic destructive type of test of the composite dowels carried out according to principles given in Eurocode 4 [9], Figure 5. It allows to determine the load-bearing capacity of the shear connection, which is usually sufficient for the standard shear mechanical connectors (headed studs for

instance) when the characteristic resistance has to be determined. Similarly (by the test POST) the fatigue strength under the cyclic load is determined. In the case when composite dowels are used, the POST test allows to conclude about: the strength of the concrete part of the connection, the load-bearing capacity of the steel part and the connection's stiffness. However for the steel part this test is not fully conclusive owing to the stress state in the steel connector, which can not be determined, although the stress in an elastic range of the connector's behaviour is deciding about its resistance, especially when the fatigue strength has to be determined.

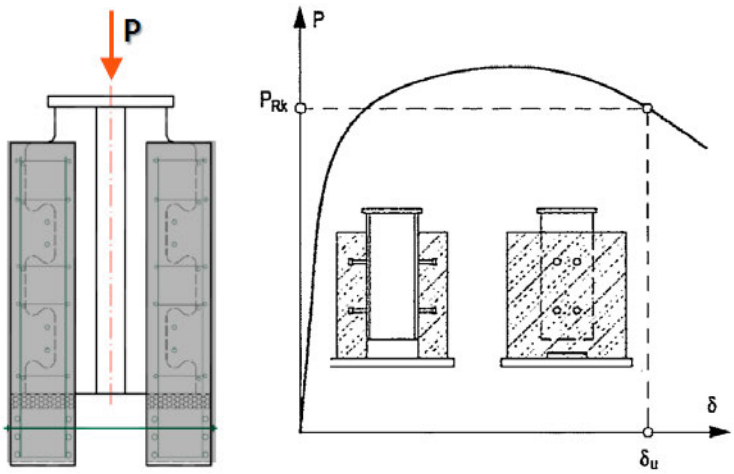

Fig. 5. Specimens with composite dowels (at the left side) and standard force-slip diagram for push-out test (at the right)

On the basis of force-slip diagram executed for the composite dowel one may determine the design resistance of the connection, but two cases have to be here separated. If the strength is reached due to shear of the steel connector, then the information about its load-bearing capacity and the ductility is given. Thus, the studies upon the effect of the shape, dimension, spacing, steel grade, etc., on the connection's resistance and its ductility can be carried out, including the value of the both slip and uplift. On the contrary, the concluding about the connector's resistance in the elastic range, which determines its fatigue strength under cyclic loads is here difficult. But if the strength is reached due to the destruction of the concrete part, then the load-bearing capacity can be determined and in consequence the design resistance according to EC4 [9] can be calculated. The procedures of dimensioning and determining the resistance of the concrete part of the composite dowels were given by Seidl [7]. Additionally, the POST tests allow to conclude about the degradation of concrete dowels under cyclic loads, which is understood as an irreversible increment of the slip of the connection caused by cyclic loads. This effect can be defined as a value of slip after n cycles of loading, diminished by the slip's value of the first

cycle under determined level of loading, which depends on the both web's thickness and the value of cyclic load acting on the connector. Force-slip relationship under the cyclic load is depicted for example in Figure 6 and 7. The bigger amplitude of the force per one connector, the quicker is the progress of concrete dowel's degradation, similarly the lesser thickness of the web, the higher is the slip's increment under the constant level of the load (although the web's thickness affects the load-bearing capacity of the connector).

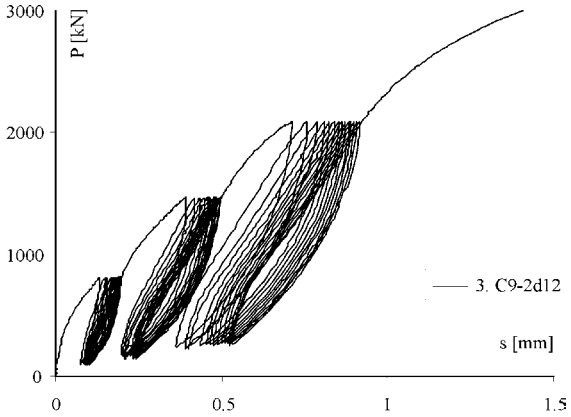

Fig. 6. Force-slip behaviour for POST specimens with composite dowels under cyclic loads-influence of force amplitude

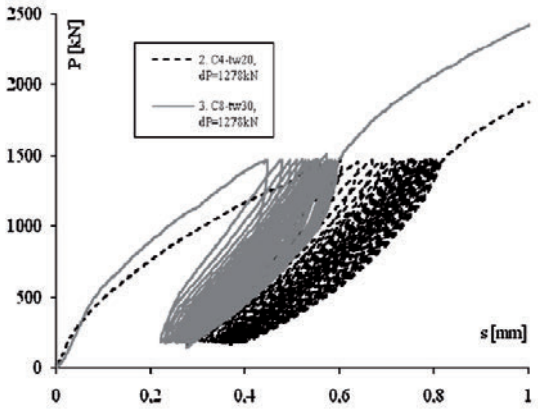

Fig. 7. Force-slip behaviour for POST specimens with composite dowels under cyclic loads-influence of web thickness (gray line-web thickness of 30 mm, black dashed line – 20 mm)

A similar analysis might be carried out upon the effect of the connector's dimension on the degradation of concrete. A suitable relationship are shown in Figure 8, where the black continuous and dashed lines describe standard dimension dowels, whereas the

gray dashed line is tied with that twice as much smaller, spaced two times closer for the same length of shear connection.

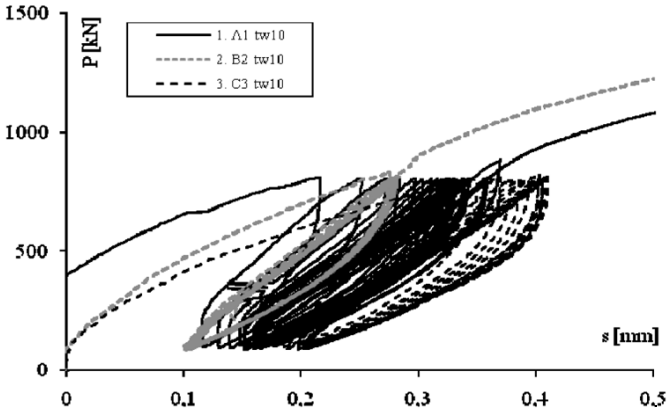

Fig. 8. Force-slip behaviour for POST specimens with composite dowels under cycling loads-influence of dowel size (description in text)

It can be seen that connectors with a smaller dimensions are less sensitive to degradation of the concrete. It results from the beneficial distribution of the stress per one connector's surface. The smaller contact stress (higher concentration of connectors providing the same resistance per the unit length) the smaller increment of the slip between steel and concrete.

The effect of the degradation of concrete in the composite dowel can be described as:

$$\Delta s = f\left(\frac{\Delta P}{P_{ult}}\right) \cdot \ln(n), \tag{1}$$

where:

n denotes the number of cycles of amplitude ΔP,

P_{ult} is the load-bearing capacity of the connector.

2.2. New push-out test (NPOT)

Tests of NPOT type constitute an attempt of transition from the load-bearing capacity obtained by POST to the stress approach as necessary when the elastic resistance and fatigue strength of the steel dowels have to be determined. The NPOT is modified form of POST method, in which the transmission of forces has been reversed in such a way, that the steel part responsible for the transmission of the longitudinal shear is in terms of a total tension. This operation allows to determine stresses in the steel connector under conditions close to that occurring in beam

members subjected to the positive bending moment, where the steel part is under tension and the concrete under compression. In order to guarantee such a flow of internal forces in the specimen, the compression force is applied by a hydraulic jack trough an additional steel part welded from the bottom side to the steel sheet with connectors has been forced to tension. The idea of NPOT procedure is shown in Figure 9.

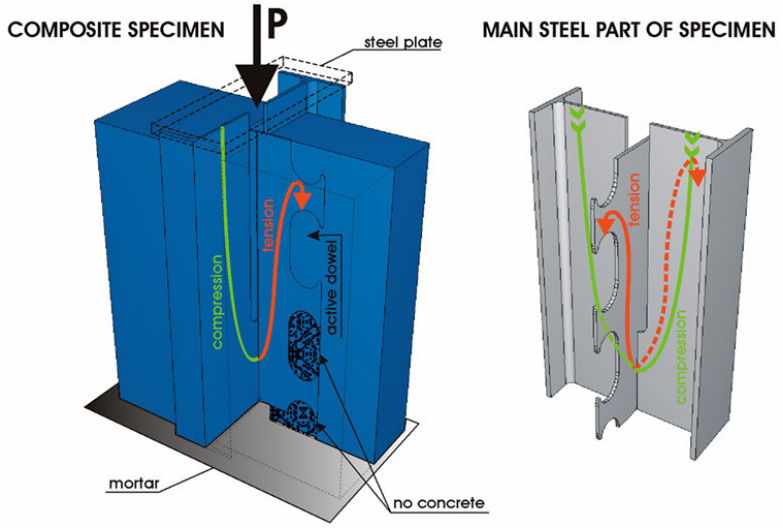

Fig. 9. Construction of NPOT specimens-flow of internal forces

Tests of NPOT specimens enable the initial analysis of behaviour of steel dowel with a determined shape by means of small-dimensioned elements (simplification in comparison with examinations carried out a beam members), under static and cyclic load as well. The obtained map of the connector's strains, employing the electro-resistance strain gauges, enables the both verification and calibration of FE models.

Models of NPOT were used, while examined at the Wroclaw University of Technology, for the comparison of different shapes of connectors and afterwards for the optimization of the shape used for further destructive tests on beam members and POST examinations.

2.3. Beam tests

The most extended test, which is confirming the resistance of the composite dowels, is the beam examination under the static and cyclic loads. This type of experimental investigations is very essential especially when fatigue behaviour needs to be verified (and in consequence the resistance in elastic range). The idea of elastic

resistance of the steel connector is based on the analysis of stresses results obtained from numerical FE models. It is assumed that the connector's resistance is achieved when the ultimate stress is exceeded (i.e. yield stress and von Misses stresses or the fatigue strength and the main stresses) under certain combination of external loads. This concept can by employed for checking the fatigue limit state (FLS) because on this base the maximum normal stress σ_1 directly received in the most stressed point of connector. The connector constitutes an integral part of the steel cross-section and participates in carrying the internal forces caused by global loads (bending moment and axial force in the beam), moreover is a member producing the steel-concrete composite structure and has to resist the longitudinal shear load allowing composite actions can take place. Additionally, the increase of distance between the level of connectors in beam's cross section and its axis of inertia causes the increase of global stresses in the considered connector. The formula describing stress in the connector in the elastic range is as follow:

$$\sigma_{\max} = k_c \cdot \sigma + \beta \cdot \tau, \tag{2}$$

where:

σ – normal stress in the beam cross-section on the level of the connector base (root) caused by global effects of the both bending moment and axial load in an elastic state,

τ – shear stress in the web,

k_c – coefficient which denotes normal stress concentration at the connector's base resulting from its geometry (geometrical notch),

β – is associated with the stress concentration coming from the effects of local longitudinal shear.

Coefficient k_c and β depend entirely on the connector's shape and may by determined by FE analysis. Considering the steel connector in terms of different loads, it is possible to create an interactive envelope of the connector's resistance, on the basis of coordinates showing the relationship between the dimensionless connector's stressing from global but also local effects (Figure 10). Each quadrant of the diagram is corresponding with different combination of the sign of forces acting on the connector caused by the local and global actions.

The envelopes 1 and 2 in Figure 10 show the hypothetical curves for different shapes of connectors.

In order to confirm the correctness of the assumed methods of the connector's dimensioning, the composite beams are subjected for instance to four – point bending, in which the strains are recorded by means of SGs. The scheme of beams meant to destructive tests at Wroclaw University of Technology has been shown in Figures 11 and 12, whereas the location of SGs being attached to the connectors has been shown for an example in Figures 13 and 14.

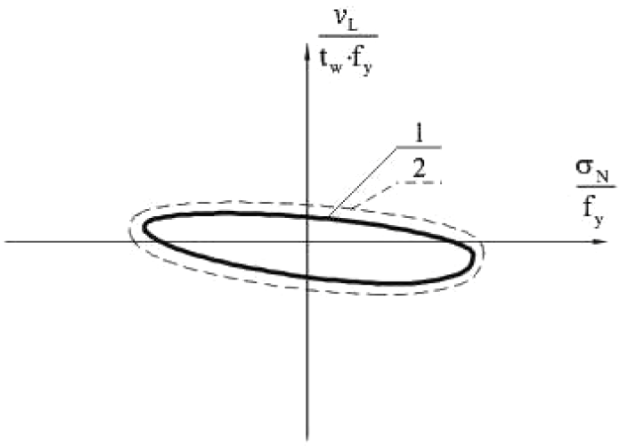

Fig. 10. Interactive envelope of the steel connector's resistance in the elastic range – pictorial diagram (description in text)

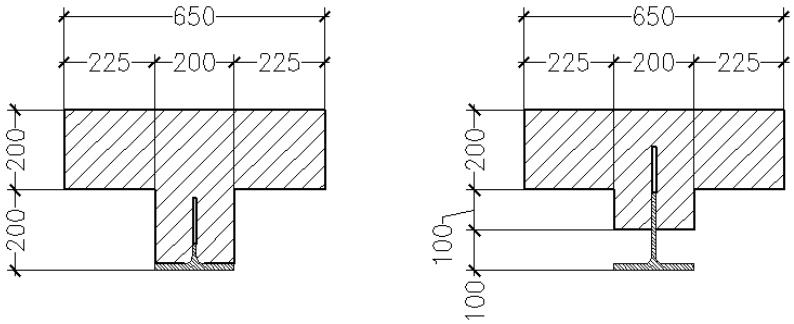

Fig. 11. Basic beam's cross section subjected to 4-point-bending tests

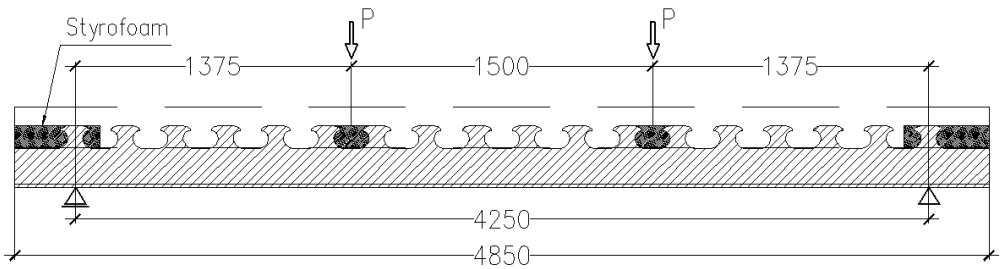

Fig. 12. General view of static system for 4-point-bending tests

Basing on the measured strains obtained from the proposed arrangement of SGs, the FE model can be calibrated and afterwards the map of strains gained numerically can be confirmed in the chosen discrete points. This map forms a basis for

determining the interactive formulas of the elastic resistance. The additional employment of (apart from standard SGs) of so called SGs chains (10 SGs per about 25 mm) allows to record an extra concentration of stresses at the geometric notches. Exemplary diagram of the concentration of stresses at the steel dowel's root is shown in Figure 15.

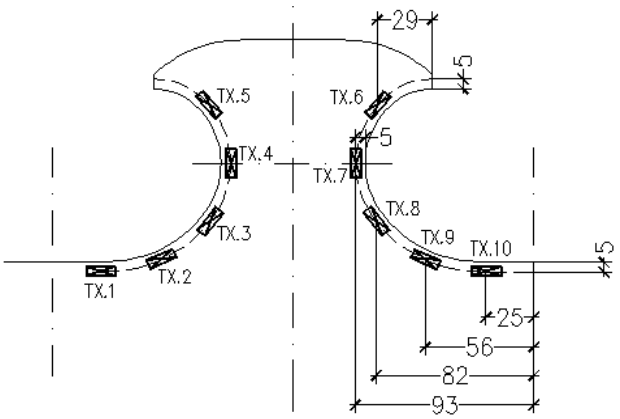

Fig. 13. Localization and numbering of Strain Gauges on one chosen steel dowel

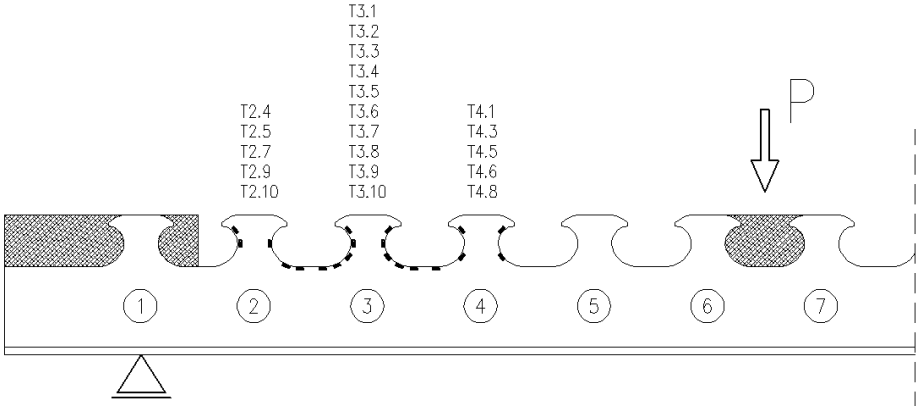

Fig. 14. Proposal of placing SGs on steel dowels (one part of beam is shown)

Additionally the experimental investigations carried out on beams allow to assess the effect of uplift on the steel connector's resistance. In the elastic range the effect of uplift is not resulting from the mechanics of force transmission between steel and concrete , but is conditioned by the one kinematically allowed mechanism of the slip between steel and concrete components, and thus can by defined as a function of the slip and results from the geometry of the dowel's root. Since slips in the elastic

range of behaviour of the steel connector are very small, the effect of uplift is negligible.

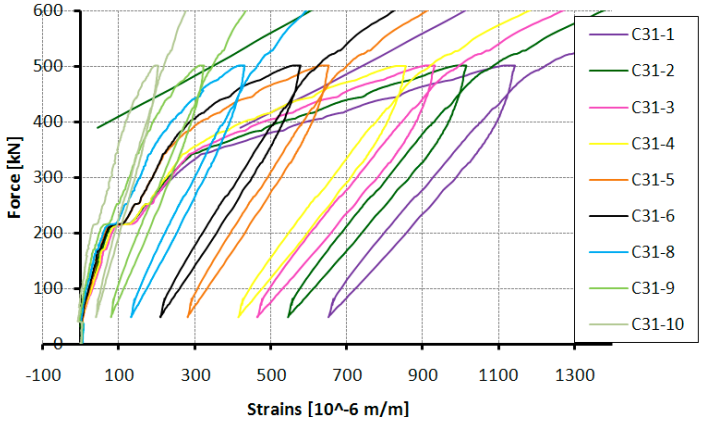

Fig. 15. Concentration of stresses at the dowel's root visible by means of chain of SG's measures

2.4. Finite element method (FEM)

FEM is an economic and efficient method for parametrical studies to optimize the design unlike time-consuming experimental tests [3, 6], like described above POSTs, NPOTs and beam tests. However, even basic numerical models are complex (Figure 16), the behaviour is high-grade nonlinear and influenced by many parameters.

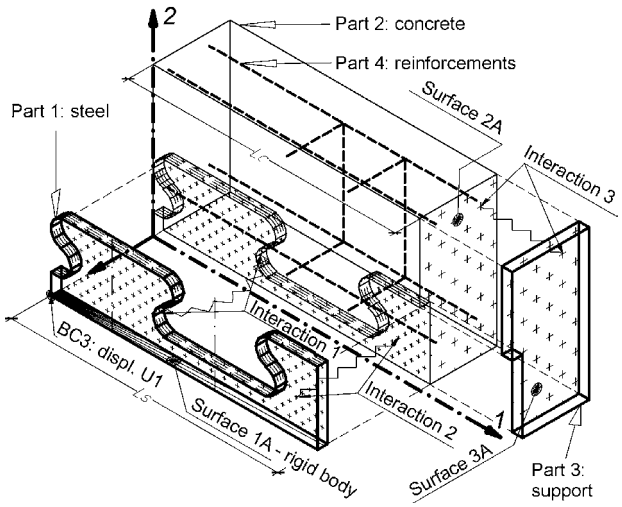

Fig. 16. One-dowel model (1D) – parts and interactions [3]

A numerical model is generated with the objective of analyzing the structural behaviour of the connection and determining the failure mechanisms. The numerical simulation of the connection with CD is complicated because of its complex geometry combined with a multiplicity of nonlinearities. To establish an elementary model is complex, especially due to the concrete part of the connection which appears high-graded non-linear in whole load range. The following aspects are focused: the material nonlinearities, the contact interactions and the complex geometry. Investigating on the behaviour of the model is possible by comparing it with experimental results. FEM is currently a basic tool to precise calculation of coefficients applied in Equation 2.

3. Final remarks

The concept outlining the resistance of the composite dowels was developed on the basis of numerical analyses supported by experimental measurements and is not introduced in a readable analytic method. Preparing of such a method is complicated due to complexity of the exact solution of the nonlinear issues including also contact problems. The issue of the concrete resistance is even more complex. Thus the rational application of destructive test methods and appropriate numerical models is very essential. Therefore the extended experimental investigations are employed in comparison with that given in EC4. The steel dowels required the stress approach, when their resistance is examined. Due to economic aspects of tests, the NPOT type was employed apart of the POST type, as the small dimension elements enabling the stress analysis for the connector in conditions closely corresponding to that in real composite beams in bending. The final verification of the correctness of different methods used in the analysis of the behaviour of composite dowels is achieved by means of destructive tests an full-scale beams, under static and cyclic loads by the SGs as tool approving the distribution of stresses in composite dowels.

References

[1] Lorenc W., Kołakowski T., Kosecki W., Seidl G.: *VFT-WIB® prefabricated composite girders with innovative shear connection*, Nowoczesne Budownictwo Inżynieryjne, No. 6, 2008, pp. 70–73.

[2] Hechler O., Lorenc W., Seidl G., Viefhues E.: *Continuous shear connectors in bridge construction*, Composite Construction VI conference, USA, Colorado, 2008.

[3] Lorenc W., Ignatowicz R., Kubica E., Seidl G.: *Numerical model of shear connection by concrete dowels*, Recent Developments in Structural Engineering Mechanics and Computation, Millpress, 2007, Rotterdam, Netherlands.

[4] PreCo-Beam: *Prefabricated enduring composite beams based on innovative shear transmission*, Technical Reports, Research fund for coal and steel, Contract N° RFSR-CT-2006-00030, 01.07.2006–30.06.2009.

[5] Berthellemy J., Seidl G.: *Les poutres préco – une solution économique pour les petites portées, objet d'un programme de recherche européen*, Ouvrage d'art 54, Sétra, 03.2007.
[6] Fink J., Petraschek TH., Ondris L.: *Push-out test parametric simulation study of a new sheet-type shear connector*, in: Projekte an den zentralen Applikationsservern, Berichte 2006, Zentraler Informatikdienst (ZID) der Technischen Universität Wien, Wien, 2007, pp. 131–153, http://www.zid.tuwien.ac.at/projekte.
[7] Seidl G.: *Behaviour and load bearing capacity of composite dowels in steel-concrete composite girders*, Instytut Budownictwa Politechniki Wrocławskiej, Raport serii PRE nr 4.2009, Rozprawa doktorska.
[8] Kubica E., Rykaluk K., Lorenc W., Kożuch M.: *Forming of cut hot – rolled I – beams subjected to composite girders*, Zespolone konstrukcje mostowe. Teoria, badania, projektowanie, realizacja, utrzymanie, wzmacnianie, Kraków, 2009, pp. 289–300.
[9] EN 1994-1-1 Eurocode 4: *Designing of composite steel – concrete structures 1-1: General rules and rules for buildings*.

Metody oceny wytrzymałości łączników w innowacyjnym zespoleniu belek stalowo-betonowych

Niniejsze opracowanie dotyczy metod badawczych pozwalających określić nośność zespolenia typu *composite dowels*. Omówiono szczegółowo problematykę badań nowego rodzaju zespolenia, które wymaga szerszego podejścia badawczego niż stosowane dotychczas próby nośności granicznej typu POST. Łącznik stalowy, pracujący jako integralna część stalowej belki zespolonej, partycypuje w przenoszeniu obciążeń nie tylko od lokalnego ścinania podłużnego między stalą i betonem, ale również podlega wytężeniu od globalnych efektów zginania i działania sił osiowych. Wymusza to opracowanie kryteriów naprężeniowych opisujących pracę łącznika, stąd też problematyka badawcza łączników wykracza poza stosowane do tej pory wyłącznie kryteria nośności granicznej. W tekście referatu przedstawiono procedury badawcze, które w połączeniu z koncepcjami nośności granicznej w odniesieniu do części betonowej łącznika, oraz sprężystej w odniesieniu do łącznika stalowego, prowadzą do sprawnego wymiarowania zespolenia w rzeczywistych konstrukcjach.

ARCHIVES OF CIVIL AND MECHANICAL ENGINEERING

Vol. X 2010 No. 3

Numerical simulation of piercing using FEA with damage and SPH method

M. MABOGO, G.J. OLIVER
Department of Mechanical Engineering, Cape Peninsula University of Technology, PO Box 1906 Bellville 7535, South Africa.

J. ROŃDA
Department of Applied Computer Science and Modelling, AGH University of Science and Technology, Al. Mickiewicza 30, 30-059 Kraków, Poland.

The Smoothed Particle Hydrodynamic (SPH) method as implemented in the commercial code LS-DYNA has been used to solve the problem of piercing a hole in a stamped shock absorber seat. The results are compared to those produced by dynamic analysis using conventional finite element methods with material erosion as implemented in LS-DYNA. The SPH method is suitable for modelling of cracking and tearing phenomena occurring in actual production of the spring seat for some material and process parameters. The SPH stress levels need to be closely interpreted in contour plots than for the FEA results though as high stresses remain in the disconnected volumes. A rate dependent plasticity model is used in the simulation with data produced by mechanical tests of the materials used.

Keywords: *smoothed particle hydrodynamic, finite element analysis, piercing, cracking, tearing, spring seat*

1. Introduction

The main aim of the paper is to highlight advantages of the Smoothed Particle Hydrodynamics (SPH) analysis in comparison with the Finite Element Analysis (FEA). These numerical methods are compared for the piercing process widely used in manufacturing. The piercing of a drainage hole is treated here as the benchmark problem.

The fully formed and pierced shock absorber spring seat is shown in Figure 1. Currently the piercing process, which forms part of a progressive tool, has a failure rate of 70% as a result of the tearing near the valve seat neck for the TM380 material. This is due to the high stresses the part is subjected to over the small distance between the drainage hole and the valve seat neck. Failure of the forming process can vary from unwanted deformation around the hole to tearing of the spring seat. Conventional finite analysis with solid continuum elements can hardly be applied to model both the piercing and tearing. In the finite element analysis shown here criteria for damage and failure modify the stiffness of the working piece as was done in e.g. [5] or [6]. The adaptive finite element methods [11] are usually applied to model continuum damage.

When the conventional FEA in LS-DYNA was used, some elements were deleted in the region susceptible to failure. For the case, when the Smoothed Particle Hydrodynamics (SPH) method was used, there was no need for additional modelling to simulate material removal or separation. SPH can be used also to model high velocity impacts of solids [10] because it is capable to model large deformations. Local effects such as cracking or shear bands can be modelled easily when using SPH method [14]. An overview of the novel applications of SPH in simulating materials processing is given by Cleary et al. in [2]. The LS-DYNA package with SPH was used for high speed cutting simulation by Limido et al. [7].

Fig. 1. Shock absorber spring seat

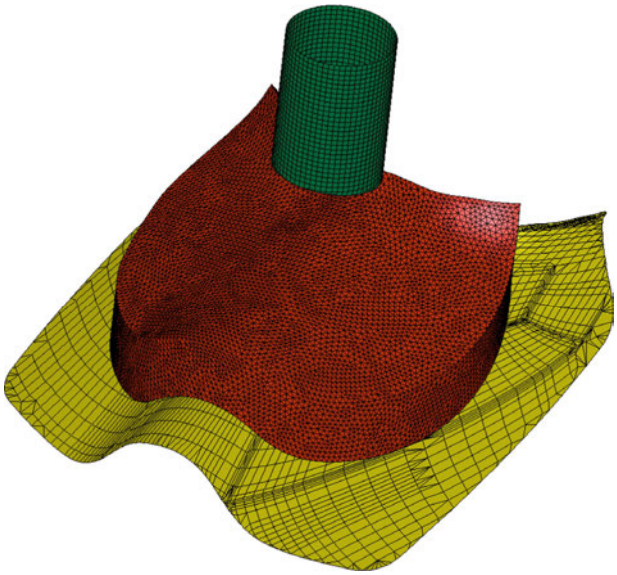

Fig. 2. The finite element meshes for the punch surface, the blank and supporting die surface

2. Piercing problem formulation

2.1. Formulation of elastic-plastic problem

The piercing problem can be formulated in the Eulerian framework because the thickness of the blank is small and displacements of material points are also small in the direction of the tool motion. In this framework, the elastic-plastic problem is defined by the following set of equations and relations:

- The balance of momentum in the material description is written as

$$\rho_o \ddot{u}_i(x_i,t) + \sigma_{ij,j}(x_i,t) + \rho_o b_i(x_i,t) = 0, \tag{1}$$

where:

$u_i(x, t)$ – is the displacement,

$\sigma_{ij}(x_i, t)$ – are body forces per unite volume,

x_i – the Cauchy stress, x_i is the position of a space point,

t – time.

- The strain rate decomposition is defined by

$$\dot{\varepsilon}_{ij} = \dot{\varepsilon}_{ij}^e + \dot{\varepsilon}_{ij}^p, \tag{2}$$

where:

$\dot{\varepsilon}_{ij} = \dfrac{d\varepsilon_{ij}}{dt} = \dfrac{1}{2}\dfrac{d}{dt}\left(\dfrac{du_i}{dx_j} + \dfrac{du_j}{dx_i}\right)$ – the total strain rate,

$\dot{\varepsilon}_{ij}^e$ – the elastic fraction of strain rate,

$\dot{\varepsilon}_{ij}^p$ – the plastic part of strain rate.

- The stress evolution is described by the elastic-plastic constitutive equation

$$\dot{\sigma}_{ij} = C_{ijkl}\dot{\varepsilon}_{kl}, \tag{3}$$

where:

C_{ijkl} – the elastic-plastic modulus.

- The Maxwell–Huber–Hencky–von Misses yield criterion with strain hardening and without damage effects is expressed as

$$\phi(s_{ij}) = \sigma_v^2 - \sigma_y^2 \le 0, \tag{4}$$

where:

$\sigma_v \equiv \sqrt{\frac{3}{2} s_{ij} s_{ij}}$ is the Misses stress,

s_{ij} – the deviator of the Cauchy stress defined by $s_{ij} = \sigma_{ij} - \frac{1}{3}\sigma_{kk}\delta_{ij}$,

σ_y – the yield stress called also the current yield limit.

• This yield limit is defined by

$$\sigma_y = \beta[\sigma_{y0} + f_h(\varepsilon^p_{\text{eff}})], \tag{5}$$

where:

σ_{y0} – the initial stress limit or the threshold stress,

f_h – the hardening function,

$\varepsilon^p_{\text{eff}}$ – the effective strain is related to the material deformation history as it is calculated as the time integral of nonlinear function of the plastic strain rate

$$\varepsilon^p_{\text{eff}} = \int_0^t \left(\frac{2}{3} \dot{\varepsilon}^p_{ij} \dot{\varepsilon}^p_{ij} \right)^{\frac{1}{2}} d\tau. \tag{6}$$

• The factor β in the expression (5) accounts for strain rate effects (viscosity) following the Cowper–Symonds [3] model which scales the yield stress by the strain rate and is given by the formula

$$\beta = 1 + \left(\frac{\dot{\varepsilon}}{C} \right)^{\frac{1}{r}}, \tag{7}$$

where C and r are material parameters defined in [3].

• The hardening function f_h in the expression (5) can be defined by using experimental data from a true stress σ_{true} vs. true strain $\varepsilon_{\text{true}}$ curve by the following steps

$$E_h = \frac{\sigma_{\text{true}} - \sigma_{y0}}{\varepsilon_{\text{true}} - \frac{\sigma_{\text{true}}}{E_Y}} \Rightarrow E_{tan} = \frac{E_h E_Y}{E_h + E_Y}, \Rightarrow f_h(\varepsilon^p_{\text{eff}}) = E_{tan}\varepsilon^p_{\text{eff}}, \tag{8}$$

where:

E_Y – the Young modulus of elasticity,

E_h – the true hardening modulus which fulfils also the relationship $E_h = \frac{E_{tan} E_Y}{E_Y - E_{tan}}$ if $E_Y > E_{\text{tan}}$.

• The true stress and strain are defined as follows:

– $\sigma_{\text{true}} = s\,(1 + \varepsilon_e)$ where ε_e is the nominal strain (called also the engineering strain), and s is the nominal (or correspondingly engineering) stress.

– The relationship between true strain and engineering strain is given by $\varepsilon_{\text{true}} = \ln(1 + \varepsilon_e)$.

The piercing problem formulation includes also the effect of material failure or damage of the blank [11], and there are two ideas to incorporate such effects in the analysis of elastic-plastic continuum:

• the concept applied e.g. by Lee et al. [6], where the Lemaitre damage variable, reducing the material stiffness, is evaluated,

• the technique, utilized by e.g. Casalino at al. [1] and known as the "killing elemental stiffness" procedure that consists in setting the element stiffness to zero in the material damage region.

Moreover, some material models, which incorporate damage parameters, are available in LS-DYNA. In this program it is also possible to choose so-called material erosion algorithm based on the concept of instantaneous damage associated with a number of choices for the damage criterion used for the elimination of some elemental stiffness contributions from the global stiffness matrix. In our calculations the criterion assessing, when the blank material loses continuity, can be written as

$$\sqrt{\frac{3}{2} s_{ij} s_{ij}} \geq \sigma_f, \tag{9}$$

where σ_f – the maximum stress at failure.

The contact algorithm is used in LS-DYNA to investigate the penetration of a slave node through a master element. It is commonly assumed, that the punch is rigid and a penalty function based method is used to apply a fictitious force to resist penetration that leads to the elimination of the penetration. A penalty scale factor of 0.1 is used for the piercing simulation to reduce the contact stiffness. Friction is included in the contact with both static and dynamic friction coefficients defined by the generalized Coulomb friction model. The frictional algorithm evaluates a yield force, and then computes the incremental movement of the slave node updates the interface force and checks the force against the yield condition. The force is scaled if it exceeds the yield force. The actual coefficient of friction that is smoothed combination of static and dynamic friction coefficients given by

$$\mu = \mu_d + (\mu_s - \mu_d) e^{-c|v|}, \tag{10}$$

where:

μ_s and μ_d are appropriately static and dynamic friction coefficients,

v – the relative velocity,

c – a decay constant.

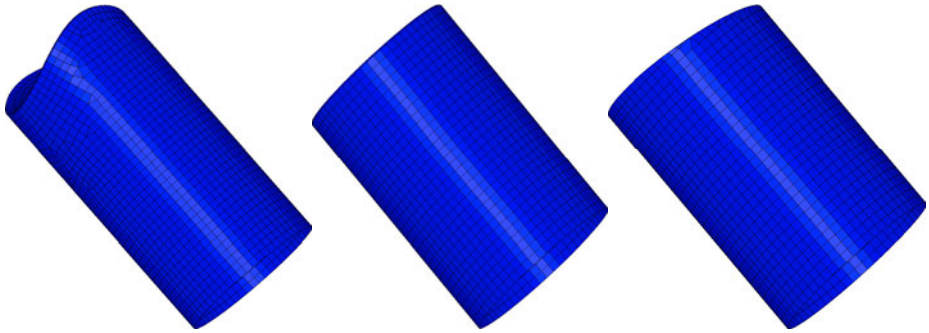

Fig. 3. The finite element meshes of the three different punches used:
(from the left to right) concave punch, shear punch, flat punch

The boundary conditions for piercing problem [15] can be split as follows:

• boundary conditions on the surface ${}^t\Gamma_u$ where the boundary displacements are given by $u_i = \phi_i$ (**x**, ξ), for points $\mathbf{x} \in {}^t\Gamma_u$ and time $\xi \in (t_n, t_{n+1})$,

• boundary conditions on the blank material surface ${}^t\Gamma_f$ defined by the normal vector **n** where the displacement **u** = 0 and external continuous force, e.g. clamping force, $f_j^{(cl)}$ is prescribed and equals to $t_j^{(n)} = \frac{1}{3}\sigma_{ij}\delta_{ik}n_k$,

• boundary conditions on the contact surface ${}^t\Gamma_C$ with friction expressed in terms of tangent and normal surface forces: f^n and $f^{(t)}$.

The initial conditions are given by $u_I(\mathbf{x}, 0) = 0$ and $\dot{u}_I(\mathbf{x}, 0) = 0$.

2.2. Smoothed particle hydrodynamics

Smoothed particle hydrodynamics is a grid-less method developed in papers by Lucy [9] and Gingold and Monaghan [4] and described in further papers by Monaghan [12–13]. In this method the governing equations describing the deformation process occurring during piercing are solved in the domain of individual particles with constraints.

Traditionally, authors describing the SPH method follow the original paper by Monaghan [12] and use notation in fundamental SPH formulas appropriate for the Eulerian analysis of motion, although formulating a problem for motion of material particles.

SPH is based on an integral transform of the form:

$$Tf(\mathbf{x}) = \int_\Omega K(\mathbf{x}, \mathbf{x}')f(\mathbf{x}')d\mathbf{x}', \tag{11}$$

where $K(\mathbf{x}, \mathbf{x}')$ is a function of two variables, that is called integral kernel, and is a kind of mathematical operator, where the input is a function $f(\mathbf{x})$ and the output is another function $Tf(\mathbf{x})$. Particularly, the kernel K can be the Dirac delta function

$$\delta(\mathbf{x}-\mathbf{x}')=\begin{cases}\infty & \mathbf{x}=\mathbf{x}' \\ 0 & \mathbf{x}\neq\mathbf{x}'\end{cases} \tag{12}$$

and then the integral transformation is defined by

$$Tf(\mathbf{x})=\int_{\Omega} f(\mathbf{x}')\delta(\mathbf{x}-\mathbf{x}')d\mathbf{x}'. \tag{13}$$

For SPH [8] the Dirac function is replaced with a smoothing function $W(\mathbf{x}-\mathbf{x}', h(\mathbf{x}))$ of the form

$$W(\mathbf{x}-\mathbf{x}', h(\mathbf{x}))=\frac{1}{h(\mathrm{x})^3}\theta(\mathbf{x}-\mathbf{x}'), \tag{14}$$

where the vector $\mathbf{x}'$ is a position vector of an arbitrary particle in the neighbourhood of the particle assigned to the position vector $\mathbf{x}$, and $h(\mathbf{x})$ is the smoothing length which varies in space time and determines the area of influence of the kernel [7].

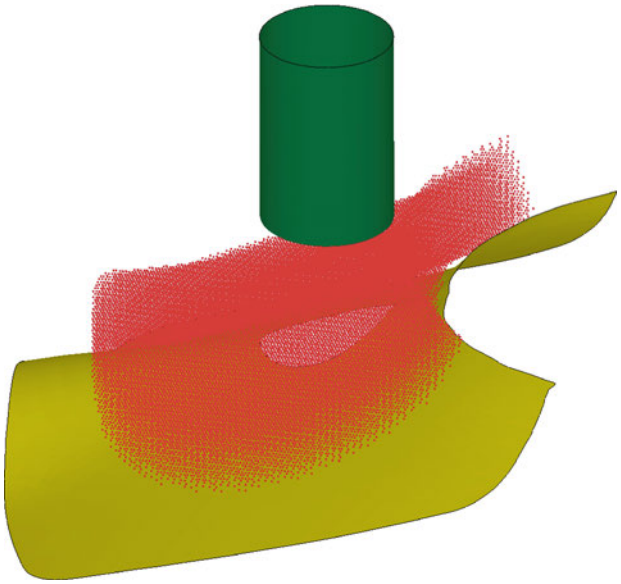

Fig. 4. The punch surface, SPH volumes and supporting die surface

The interpolating function, θ is usually taken as the cubic B-spline

$$\theta(\bar{u}) = C \times \begin{cases} 1 - \frac{3}{2}\bar{u}^2 + \frac{3}{4}\bar{u}^3 & \text{for } |\bar{u}| \le 1 \\ \frac{1}{4}(2 - \bar{u})^3 & \text{for } 1 \le |\bar{u}| \le 2, \\ 0 & \text{for } 2 \le |\bar{u}| \end{cases} \tag{15}$$

where:

C – a normalization constant,

$\bar{u}$ – represents the variable that is interpolated and for SPH it can be applied as the difference between the position vector assigned to an optional particle and vectors assigned to it's neighbours [8]. Now, due to the spline approximation and expressions: (14), and (15), the kernel W is possessed of useful properties: the "weighting" function property, the δ-Dirac property and fulfils the compact support condition:

$$\int_{\Omega} W(\mathbf{x} - \mathbf{x}', h(\mathbf{x})) = 1, \tag{16}$$

$$\lim_{h \to 0} W(\mathbf{x} - \mathbf{x}', h(\mathbf{x})) = \delta(\mathbf{x} - \mathbf{x}'), \tag{17}$$

$$W(\mathbf{x} - \mathbf{x}', h(\mathbf{x})) = 0 \text{ when } |\mathbf{x} - \mathbf{x}'| > h\,. \tag{18}$$

Then the integral transformation defined by (13) can be written in the form

$$Tf(\mathbf{x}) \approx \int_{\Omega} f(\mathbf{x}') W(\mathbf{x} - \mathbf{x}', h(\mathbf{x})) d\mathrm{x}', \tag{19}$$

and the transformation for a gradient of $f(\mathbf{x})$ is written as

$$T[\nabla \cdot f(\mathbf{x})] \approx \int_{\Omega} [\nabla \cdot f(\mathbf{x}')] W(\mathbf{x} - \mathbf{x}', h(\mathbf{x})) d\mathbf{x}'\,. \tag{20}$$

Replacing the integrals in the relations (19) and (20) by sums, the conservation equations for the piercing problem can be expressed as

Conservation of mass

$$\frac{d_{(I)}\rho}{dt} = {}_{(I)}\rho \sum_{(J)=1}^{(N)} \frac{{}_{(J)}m}{{}_{(J)}\rho} ({}_{(J)}v_k - {}_{(I)}v_k) \frac{\partial_{(IJ)} W}{\partial_{(I)} x_k}, \tag{21}$$

Conservation of momentum

$$\frac{d_{(I)}v_k}{dt} = \sum_{(J)=1}^{(N)} {}_{(J)}m\left(\frac{{}_{(I)}\sigma_{kl}}{{}_{(I)}\rho^2} - \frac{{}_{(J)}\sigma_{kl}}{{}_{(J)}\rho^2}\right)\frac{\partial_{(IJ)}W}{\partial_{(I)}x_k}, \tag{22}$$

Conservation of energy

$$\frac{d_{(I)}E}{dt} = \frac{{}_{(I)}\sigma_{kl}}{{}_{(I)}\rho^2}\sum_{(J)=1}^{(N)} {}_{(J)}m\left({}_{(J)}v_k - {}_{(I)}v_k\right)\frac{\partial_{(IJ)}W}{\partial_{(I)}x_k}, \tag{23}$$

where:

$_{(I)}$ and $_{(J)}$ are taken for *I*-th and *J*-th particles,

$_{(J)}m$ – the mass of the particle,

$_{(J)}\rho$ – the density of particle, the smoothing function for particles,

labelled by (*I*) and (*J*), is defined by $_{(I,J)}W = W\,(_{(I)}x - {}_{(J)}x,\, h)$

The same contact algorithms used for the continuum model can be used for the SPH model with the SPH particles or elements acting as the slave element in contact.

3. Numerical results

The piercing problem is solved by FEA (finite element analysis) and SPH for three different shapes of the punch and two different materials.

Results produced by SPH method for three different punches: flat, concave, and shear, for TM380 steel are presented in Figures 5–7. SPH results for the HR190 steel are only shown for the flat punch in Figure 8.

The same three punches are also used when solving the problem by applying FEA. Numerical results for FEA for two different materials: TMS380 steel, and HR190 steel, are presented in Figures 9–14.

Regrettably, numerical results obtained for SPH and FEA, can not be evaluated against results of experimental tests, conducted by our industrial partners, because they does not permitted us to publish results produced solely for them.

The meshes of the solid blank material, punch and die used for the simulation are shown in Figure 2. The blank is meshed with 397 001 solid tetrahedral elements comprised of 86 749 nodes. Solid elements are used rather than shell elements because the analysis is confined to a relatively small region so that the plate is relatively thick. The meshes of the rigid dies used for the three punch types are shown in Figure 3. The rigid punch and supporting die are composed of 13 786 shell elements for the discretization of contact areas.

The SPH analysis focuses on the flat punch for piercing the TM380 steel as this is the one used to produce the physical specimens exhibiting the aforementioned failures. The SPH results show that the softer material, i.e. HR190 steel, is less sus-

ceptible to cracking during piercing. This becomes clear, when comparing Figure 5 and Figure 8 where there is a tear opening up in the former but nothing significant in the latter.

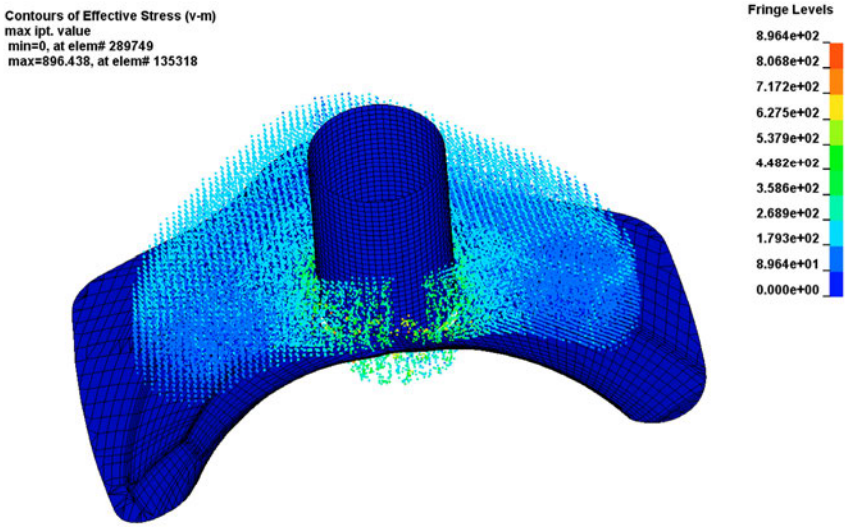

Fig. 5. SPH Results for TM380 steel using the flat punch

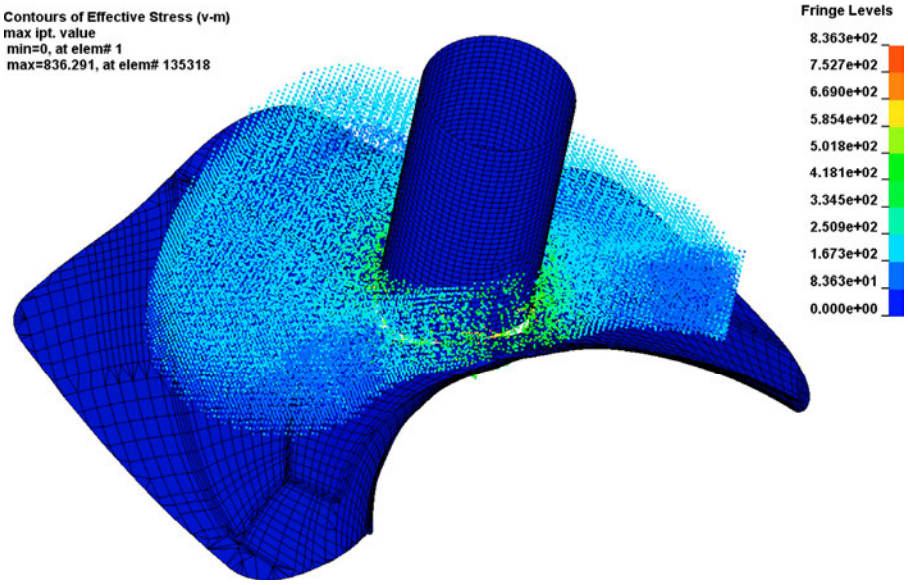

Fig. 6. SPH Results for TM380 steel using the concave punch

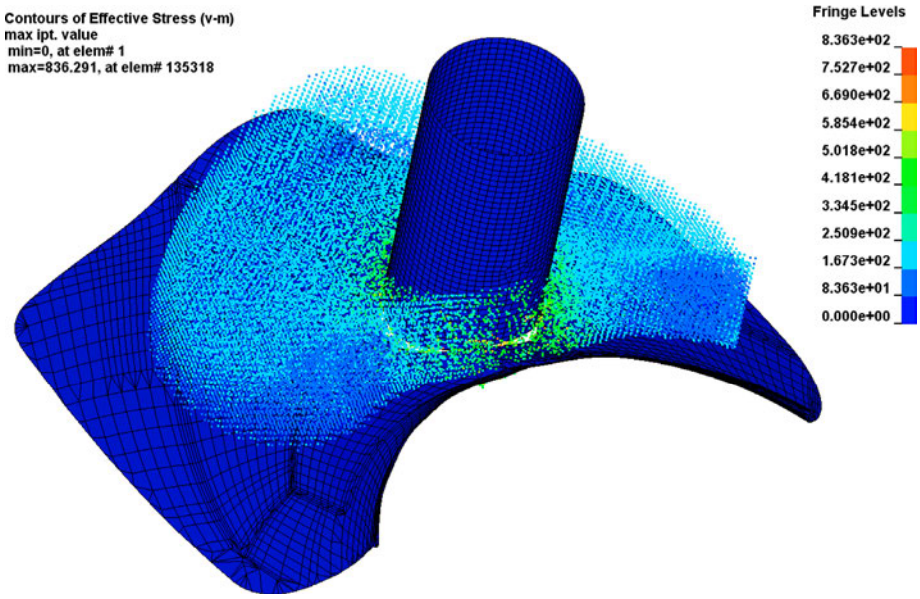

Fig. 7. SPH Results for TM380 steel using the shear punch

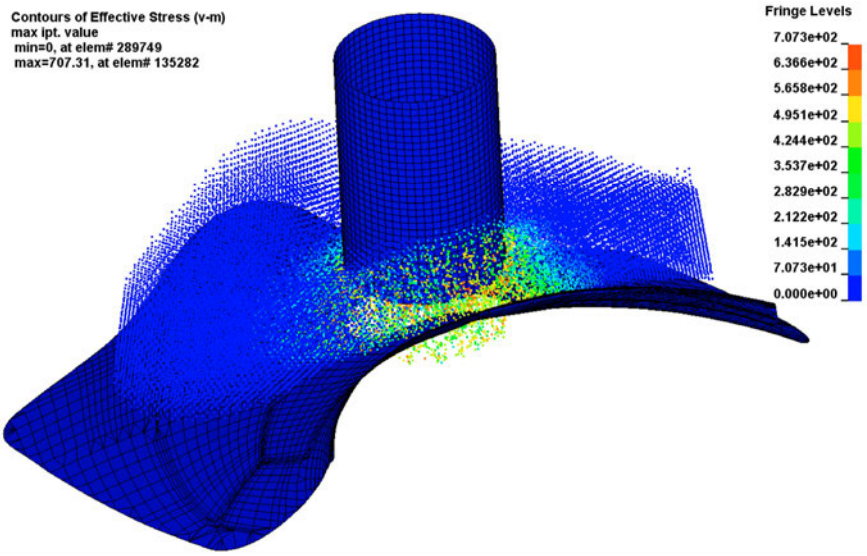

Fig. 8. SPH Results for HR190 steel using the flat punch

All three punch geometries produce some cracking or tearing for the TM380 steel as can be seen in Figures 5–7 with the most significant tear occurring for the flat punch and a smaller tear starting for the shear punch. The concave punch seems to cause

failure in two significant cracks rather than one single tear. Figures 5–7 show a separation of SPH cells corresponding to the separation of material which indicates tearing. This separation is most clearly visible at the centre of Figure 5 in the vicinity of the punch above the blank holder.

In contrast, FEA analysis with damage does not show the same crack initiation or tears for the TM380 material for any of the punches as can be seen in Figures 9–11.

As the damage model used in FEA is suitable to model the material removal during the piercing operation, as shown in Figures 9–14, the problem with the modelling of the cracks would lie in the fact, that there is not enough strain localization effects in the constitutive equations to produce a high enough stress in the expected failure zone to cause failure. From the presented results it can be seen, that one would have to develop a more sophisticated model of a material with damage effects to improve this kind of FEA analysis, whereas the material model presently available in LS-DYNA and used together with SPH method is suitable to reproduce the same effect as observed in the appropriate manufacturing process.

Table 1. Maximums of Misses stress, plastic strain and fraction of erode volume for TM380 steel

Punch shape	Max. Misses stress	Max. plastic strain	Max. fraction of erode volume
Flat punch	668 MPa	0.399	0.0663
Concave punch	569 MPa	0.399	0.0614
Shear punch	663 MPa	0.382	0.0573

Table 2. Maximums of Misses stress, plastic strain and fraction of erode volume for HR190 steel

Punch shape	Max. Misses stress	Max. plastic strain	Max. fraction of erode volume
Flat punch	589 MPa	0.390	0.0565
Concave punch	556 MPa	0.405	0.0563
Shear punch	583 MPa	0.397	0.0476

One would reason that the punch producing the least amount of volume fraction of removed material, and still able to penetrate the blank, would do the least damage and have the best dimensional conformity. The volume fraction of removed material evaluated in FEA is summarized in third columns of Tables 1 and 2. This shows that the flat punch is the worst performing punch, the concave punch is better in the case of the softer material and the shear punch significantly better than both for both the harder and softer steels. This can be ascribed to the graded contact corresponding to the slope of the punch, which produces higher levels of localized shear.

The shear punch is the best punch for maintaining dimensional conformance as can be seen in Tables 1 and 2 by the amount of material eroded. The concave punch however, produces the lowest levels of stress for both the harder and softer materials. This might have implications for the wearing of the punch and the residual stresses around the hole.

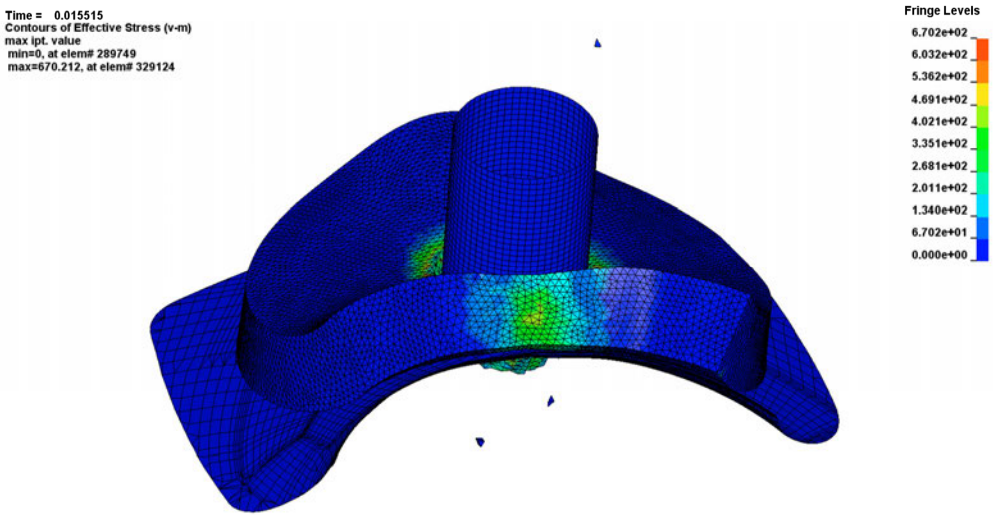

Fig. 9. Stress contours for FEA of piercing for the flat punch and TM380 steel

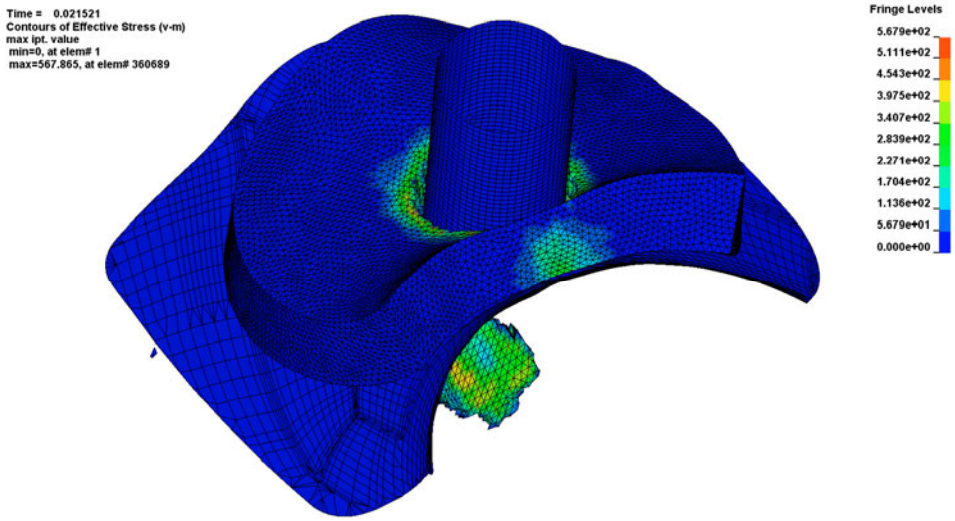

Fig. 10. Stress contours for FEA of piercing for the concave punch and TM380 steel

In terms of computational cost there was a significant increase in time increments for establishing initial contact required for the concave punch in the case of the softer material. The analysis is taking almost twice as long in terms of 'real world' time (the wall time). The fact that it this problem only arose with the softer material indicates that it is related to the cost of computation of initial plastic yield for the punch, which has an initially sharper contacting surface over the other geometries.

For the concave punch, the maximums for the Misses stress and erode volume are significantly lower than for other punch geometries. This indicates that the concave punch does not draw the material as much as the other punches and the strain energy dissipates more readily.

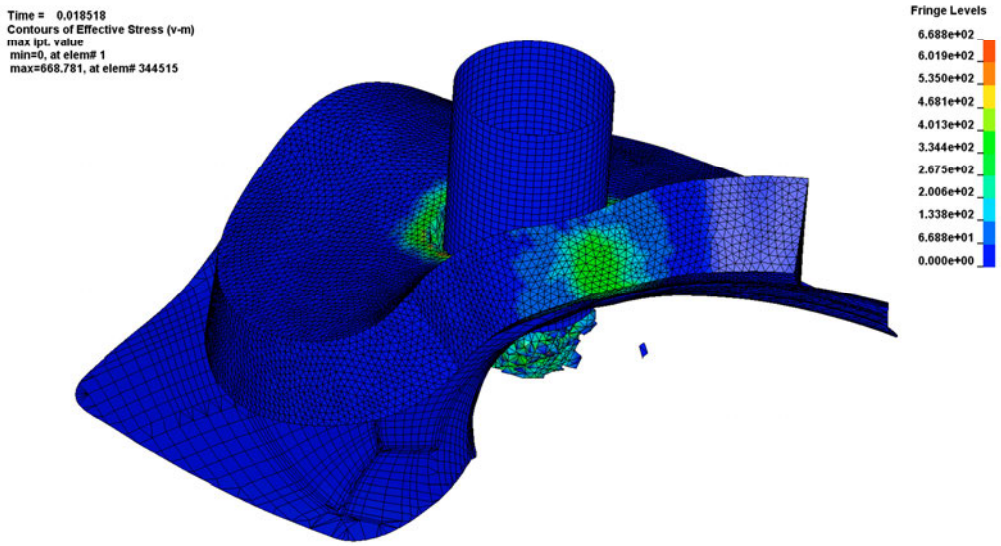

Fig. 11. Stress contours for FEA of piercing for the shear punch and TM380 steel

It is more difficult to determine the residual stress of the remaining material for SPH analysis, as stresses are much higher than for the FEA results for the TM380 material, where tearing has occurred but the higher stresses appeared in the ejected material. On the other hand, SPH results for the HR190 steel shows stress levels comparable to the FEA.

4. Conclusions

We have shown numerical results obtained both for FEA and SPH analysis for piercing of elastic-plastic blank with incorporated damage effects. FEA with damage or tearing effects is combined with deletion of finite elements in the region, where the physical slug of material is produced when a hole is produced. The simulation was conducted for three different punch geometries and two materials. Two steels: TM380, and HR190, were selected for analysis. The former material is comparatively harder than the latter.

The FEA does not produce the localized damage in the forms of tears or cracks in the vicinity of the hole close to the valve seat. The stresses in this area are relatively high but still below the threshold that would indicate potential failure. The energy is

dissipated by the removal of the slug, containing a portion of energy, without producing the strain localization that is not sufficient to induce failure in the material separation region.

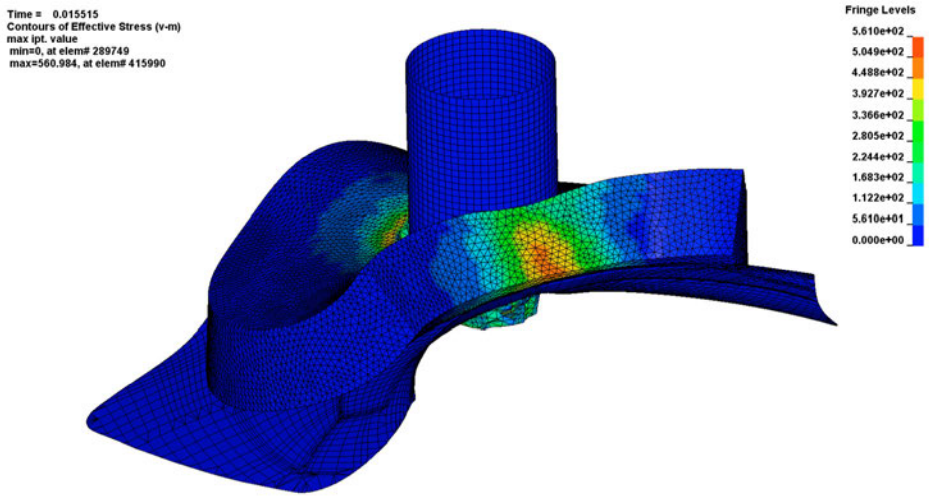

Fig. 12. Stress contours for FEA of piercing for the flat punch and HR190 steel

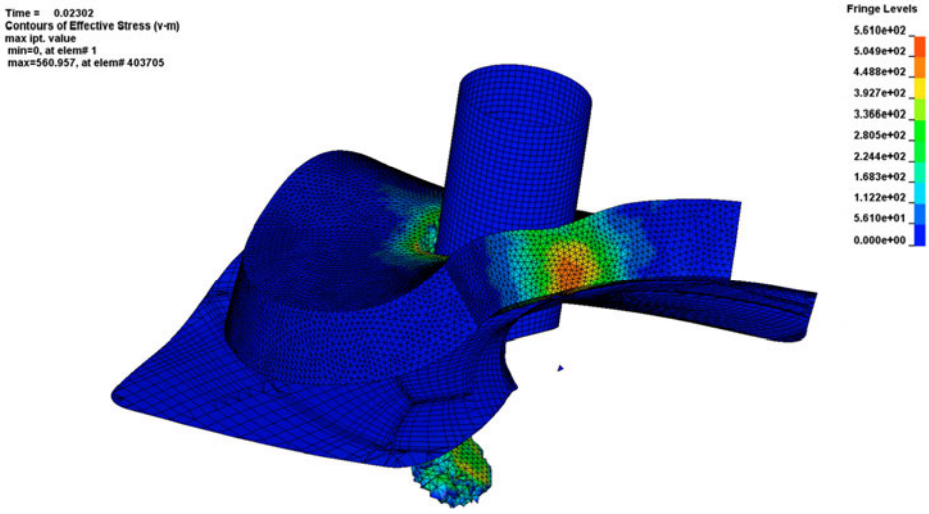

Fig. 13. Stress contours for FEA of piercing for the concave punch and HR190 steel

The three punch geometries are selected for the piercing simulation: the flat punch, the concave punch, and the shear punch. The flat punch, which is currently used by

industry, has been found as the worst in terms of the residual von-Misses stresses induced in the finished part and the dimensional conformance.

The shear punch is performed slightly better, although with some additional computational cost in numerical solution due to the greater initial yielding of the softer material. The concave punch performed the best of the three, especially in terms of volume fraction of material removed as well as in terms of the smallest residual stresses for both materials.

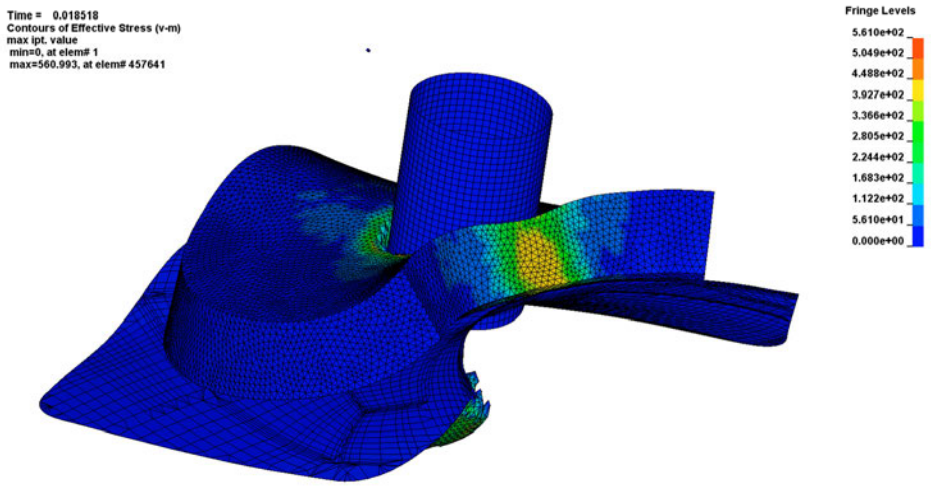

Fig. 14. Stress contours for FEA of piercing for the shear punch and HR190 steel

The observed failures in the production of physical parts are better simulated with the use of SPH method. Cracking and tearing has been produced in the area of the blank identified as being susceptible to this. SPH results also confirmed that the softer HR190 material would not produce significant failures in this region as found in production. Where material becomes disconnected from the structure in the SPH method it appears that an over prediction of stress levels occurs. Therefore, one should very carefully study the actual levels of stress for the part which is still connected and where stress can still be released throughout the blank structure. Aside from this caveat, SPH method appears to give comparable result to FEA results and is suitable to model the strain localization that produces crack tearing.

References

[1] Casalino G., Rotondo A., Ludovico A.: *On the numerical modelling of the multiphysics self piercing riveting process based on the finite element technique*, Advances in Engineering Software, Vol. 39, No. 9, 2008, pp. 787–795.

[2] Cleary P.W., Prakash M., Ha J.: *Novel applications of smoothed particle hydrodynamics (SPH) in metal forming*, Journal of Materials Processing Technology, Vol. 177, No. 1–3, 2006, pp. 41–48.
[3] Cowper G.R., Symonds P.S.: *Strain hardening and strain rate effect in the impact loading of cantilever beams*, Brown University, Deprtment of Applied Mathematics Report, Vol. 28, 1957.
[4] Gingold R.A., Monaghan J.J.U.: *Smoothed particle hydrodynamics: theory and application to non-spherical stars*, Mon. Not. R. Astron. Soc., Vol. 181, 1977, pp. 375–389.
[5] Hambli R., Reszka M.: *Fracture criteria identification using an inverse technique method and blanking experiment*, International Journal of Mechanical Sciences, Vol. 44, No. 7, 2002, pp. 1349–1361.
[6] Lee S.W., Pourboghrat F.: *Finite element simulation of the punch less piercing process with Lemaitre damage model*, International Journal of Mechanical Sciences, Vol. 47, 2005, pp. 1756–1768.
[7] Limido J., Espinosa C., Salaun M., Lacome J.L.: *SPH method applied to high speed cutting modelling*, International Journal of Mechanical Sciences, Vol. 49, No.7, 2007, pp. 898–908.
[8] Liu G.R., Liu M.B.: *Smoothed particle hydrodynamics*, World Scientific, 2003.
[9] Lucy L.B.: *A numerical approach to the testing of fusion process*, Astronomical J., Vol. 88, No. 12, 1977, pp. 1013–1024.
[10] Mehra V., Chaturvedi S.: *High velocity impact of metal sphere on thin metallic plates: A comparative smooth particle hydrodynamics study*, Journal of Computational Physics, Vol. 212, No. 1, 2006, pp. 318–337.
[11] Min J.B., Tworzydło W.W., Xiques K.E.: *Adaptive finite element methods for continuum damage modelling*, Computers and Structures, Vol. 58, No. 5, 1995, pp. 887–900.
[12] Monaghan J.J.: *Smoothed particle hydrodynamics*, Annual Review Astronomical Astrophysics, Vol. 30, 1992, pp. 543–574.
[13] Monaghan J.J.: *SPH without tensile instability*, Journal of Computational Physics, 2000, Vol. 159, No. 2, pp. 290–311.
[14] Nguyen V.P., Rabczuk T., Bordas S., Duflot M.: *Meshless methods: A review and computer implementation aspects. Mathematics and computers in simulation*, Vol. 79, No. 3, 2008, pp. 763–813.
[15] Ronda J.: *Nonstationary contact problems*, Reports of the Institute of Fundamental Technological Research, IPPT PAN, Warsaw, Vol. 1, 1990.

Symulacja numeryczna wycinania otworów z użyciem metody elementów skończonych z efektami zniszczenia i metody wygładzonej hydrodynamiki cząstek

Metoda wygładzonej hydrodynamiki cząstek (MWHC), zaimplementowana w kodzie systemu LS-DYNA, została użyta do rozwiązania zagadnienia wycinania otworów w wytłaczanym amortyzatorze siedzenia samochodowego. Wyniki tego rozwiązania zostały porównane z wynikami otrzymanymi z rozwiązania przy zastosowaniu konwencjonalnej metody elementów skończonych wzbogaconej przez uwzględnienie efektów erozyjnych w materiale, która również została zaimplementowana w LS-DYNA. Metoda MWHC nadaje się do modelowania efektów pękania i rozdzierania, jakie występują w czasie obróbki amortyzatora siedzenia w procesach przemysłowych.

Analiza wyników MWHC pozwala zaobserwować, że najwyższy poziom naprężeń występuje w usuwanych fragmentach wytłoczki. W związku z tym warstwice pól naprężeń określone w MWHC powinny być bardziej zagęszczone niż w MES. W obliczeniach zastosowano model konstytutywny materiału lepko-plastycznego, którego parametry materiałowe zidentyfikowano na podstawie prób wytrzymałościowych wykonanych w laboratorium Cape Peninsula University of Technology.

ARCHIVES OF CIVIL AND MECHANICAL ENGINEERING

Vol. X 2010 No. 3

Composite adhesive joints of hardmetals with steel

Z. MIRSKI, T. PIWOWARCZYK
Wrocław University of Technology, Wybrzeże Wyspiańskiego 27, 50-370 Wrocław, Poland.

Newest developments in the field of gluing and processing of plastics permit obtaining adhesive materials with profitable properties: high mechanical parameters, increased thermal conductivity, low electrical resistivity, increased rigidity, limited residual stresses or reduced creep [1–2]. This is possible by composite structure of adhesives, i.e. binders enriched with filling materials – additional phases of different kind, grain size and fraction. In the paper, effect of reinforcing adhesive materials with continuous and powdery fillers on shear strength of adhesive joints is discussed. Presented are also results of electron microscopy examinations and EDX analysis.

Keywords: *hardmetals, adhesive composites, shear strength, microscopic examination, EDX analysis*

1. Characteristics of adhesive composites

Composites are defined as composite materials consisted of at lease two separate and mutually insoluble phases with different properties, offering a better set of properties and structural features coming from each of the materials separately [1–4]. Composites are externally monolithic materials, but have macroscopically visible boundaries between individual components.

Matrix of a composite is to bind the reinforcement and permit utilising its complete properties by effective conveyance of load from outside to the additional, reinforcing phase. Thanks to its flexibility, the matrix reduces stresses in composites and gives them specific operational, physical and chemical features [2]. The matrix facilitates forming composite bonds, affects their thermal properties and transmits stresses to the reinforcement.

Fillers can be divided into fibrous (continuous), used for manufacture of laminar materials, and powdery – spherical, irregular, flaky or in form of short cut fibres, see Figure 1 [1, 4]. Properties of composites depend on kind, size and fraction of filler, chemical and physical structure, as well as on adhesive abilities resulting from intermolecular distance of the couple matrix–reinforcement [1, 4]. A very important question is also proper orientation of fibres in individual layers of a composite or, in case of a powdery additional phase – its uniform distribution in the matrix. Besides reinforcing fillers, some chemically neutral additional phases are applied to reduce manufacturing costs of composites.

Usage of powdery fillers does not result in so large increase of mechanical parameters of composites as it is in the case of fibrous (continuous) fillers, but permits

an improvement or even reaching some selected usable properties. Fraction of the reinforcement can even reach ca. 80 vol% in relation to the matrix, provided that the additional phase is well glue-wettable [1, 4–6]. Apart from size and shape of powdery fillers, important is also the relation between the grain length and cross dimension. From among the most frequently used inorganic fillers, the following should be distinguished: powders of metals and alloys, various oxides, nitrides and carbonates, glass, graphite and silicon compounds [1, 4–5].

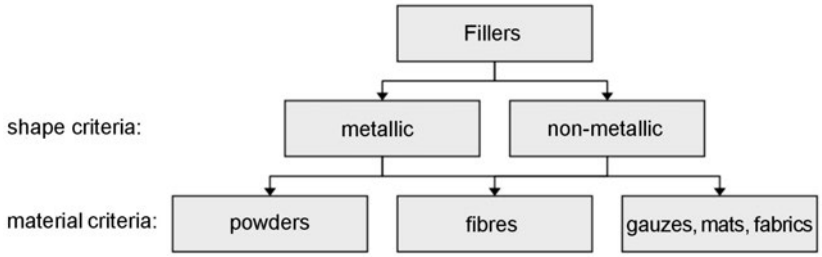

Fig. 1. Kinds of fillers depending on material and shape criteria [1]

2. Effect of fillers on properties of adhesive joints

Irrespective of their form, fillers are first of all used to eliminate the most significant shortcomings of adhesive joints, i.e. relatively low strength, irresistance to high temperatures, very low thermal and electrical conductivity. Properties of a composite are strictly related to kind and size of the particles, their volume fraction and distribution in the matrix [1, 4–5]. Unlike composites with plastic matrix, adhesives with composite structure include mostly powdery fillers as the additional phase. Maintaining suitable volume fraction guaranteeing profitable wettability, they increase mechanical strength of adhesive joints by improving forces of cohesive bonds. By selecting a suitable filler (chemical composition, granularity and shape), it is possible to design material properties which assume extreme values depending on forecast applications. A typical example is ability to conduct heat or electrical current. Adhesives of composite structure can demonstrate diametrically different characteristics – from typical insulators to materials with increased thermal conductivity coefficient or ohmic resistance corresponding to that of metallic conductors [1, 4, 7]. The other benefits resulting from applying adhesive bonds with composite structure are: improved impact strength, magnetic and processing properties, vibration damping ability, possibility of designing light but rigid structures, and resistance to unfavourable environmental conditions.

Generally, improvement of selected properties of adhesive bonds with composite structure is related to deterioration of other properties, so in fact the choice becomes a compromise solution. Nevertheless, the economical and operational benefits resulting from using such binders justify continuing research/development works in this field and predict its dynamic development.

3. Basic materials used in the research

Hardmetals grade B2 (acc. to PN-H-89500:1988), characterised by most advantageous ratio of abrasion resistance to ductility and coarse-grained structure with uniformly distributed cobalt and without additional phases, were chosen for testing. Size of the WC (α-phase) grains is within 1 to 7 μm, with some presence of grains up to 12 μm and single ones to 15 μm. Examination of the fractures revealed minimum gaseous porosity (pores up to 10 μm) of the lamines, which did not deteriorate their quality. Chemical analysis of the plates revealed cobalt content of 9.3 wt%. Chemical composition of the examined hardmetals is given in Table 1 [1, 8].

Table 1. Chemical composition of the examined hardmetals grade B2 [1, 8]

Co	Ni	Ti	Ta	Nb	WC
9.3	0.006	max 0.01	max 0.01	max 0.01	rest

For gluing with hardmetals, the unalloyed heat-treatable steel C45 (acc. to PN-EN 10083-2:2008) was selected, with chemical composition given in Table 2. The C45 steel is commonly used for tool holders and machine parts [1, 8]. Cubicoid test specimens were prepared with dimensions corresponding to those of the carbide shaped pieces (15 × 16 mm × ca. 80 mm long). The C45 steel is characterised by high strength accompanied by good ductility and crack resistance. The contained small alloying additives increase its hardenability and at the same time delay softening during tempering.

Table 2. Chemical composition of the examined heat-treatable steel C45, wt% [1, 8]

C	Mn	Si	P	S	Cr	Ni	Mo
0.42–0.5	0.5–0.8	max	max 0.03	max 0.035	max	max	max

Static shearing test of adhesive joints was carried out on a testing machine Instron model 3369 with travel rate V_b = 0.2 cm/min, on the test appliance shown in Figure 2. The device was placed on a cradle permitting axial loading of the specimen.

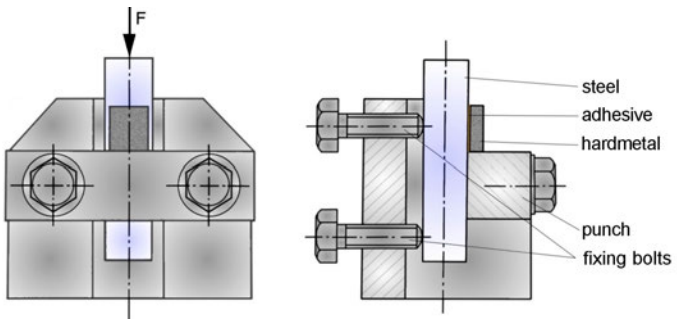

Fig. 2. Device for shearing test of adhesive joints of hardmetals with steel

4. Preparation of adhesive joints with composite bonds

Adhesive joints with composite-structure bonds were made of hardmetals grade B2 mechanically ground (Ra = 0.77 μm) and bodies of C45 steel prepared by milling (R_a = 1.75 μm). The alien phase in form of networks and powders was added to the matrix consisting of the anaerobic glue Loctite 638 or the two-component glue Agomet F330 based on methacrylate resin [9].

Initially, metallic woven gauzes with plain weave were applied. Nickel gauzes of wire dia. 0.15 mm and square mesh 1.0 mm^2 and steel galvanised gauzes of wire dia. 0.25 mm and mesh 0.25 mm^2 are shown in Figures 3a and 3b.

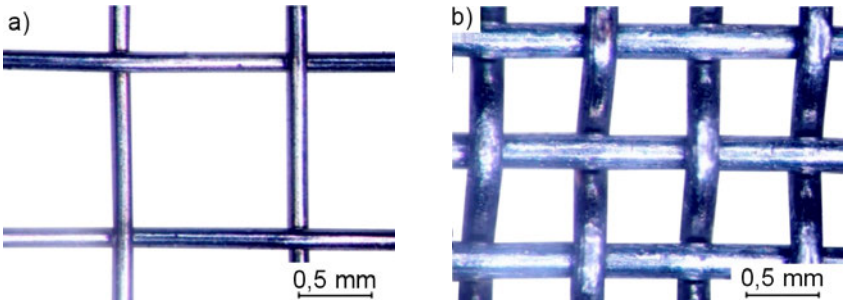

Fig. 3. Shape and size of nickel net (a) and galvanised steel gauze (b)

Another kind of reinforcement consisted of powders with granulation up to 200 μm. Selection of the powders considered variety of shapes and sizes, their availability and economic factors. Powders were manually mixed with glue, taking care not to introduce any air bubbles to the mixture.

The initial filler, producing conditions for designing the other reinforcing phases, was iron powder showing spheroidal grains with characteristic "accretions".

The remaining selected fillers were metallic powders NiCr, CuNiZn (argantan) and non-metallic powders SiC and graphite. The metallic powders were obtained by pulverising a stream of liquid metal with compressed gas: nitrogen (for CuNiB and NiCr) or air (for CuZnNi). Chemical compositions of the metallic powders were (in wt%):

– CuNiB: 0.05% B, 3% Ni, rem. Cu,
– NiCr: 80% Ni, rem. Cr,
– CuZnNi: 0.2% Si, 10% Ni, 48% Cu, rem. Zn.

Chemical compositions of all the powders were checked by local EDX analysis. Exemplary characteristic radiation spectra and results of analysis in wt% for iron powder are shown in Figure 4a and for NiCr alloy in Figure 4b. The analysis showed that the two reinforcing powders were respectively: pure iron and the alloy 77.8% Ni plus 22.2% Cr (wt%).

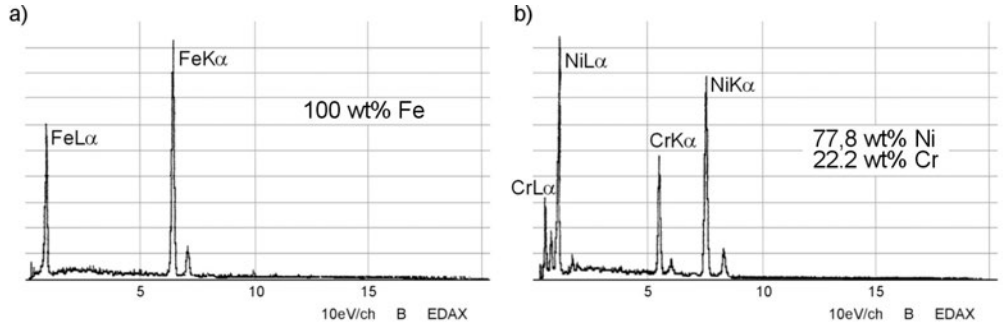

Fig. 4. Characteristic radiation spectra and EDX analyses in wt% for iron powder (a) and NiCr (b)

Kind, grain size, shape and bulk density of the applied powdery fillers are given in Table 3.

Table 3. Kind, grain size, shape and bulk density of the applied powdery fillers [1]

Kind of the filler	Grain size μm	Grain shape	Bulk density $kg/m^3 \cdot 10^{-3}$
Fe	<200	spheroidal, irregular	2.92
CuNiB	<100, single grains <200	spheroidal	6.35
NiCr	<120, single grains <200	spheroidal	5.09
CuZnNi	<160	jagged	3.38
SiC	<100	crystalline	1.76
Graphite	<200, single grains <500	flaky	2.91

Figures 5 to 10 show characteristic grains of powdery fillers used for reinforcing the glue matrix.

5. Static shearing test of adhesive joints with composite bonds

Tests carried out on adhesive joints with bonds modified with metallic woven gauzes of plain weave did give the expected results. For each kind of the adhesive reinforced with nickel or galvanised steel gauze, the shear strength values were much lower in comparison with analogical non-reinforced bonds (for Agomet F300 R_t = 27 MPa) and did not exceed 15 MPa. That resulted generally from missing interaction between the gauze wires and surface irregularities of the adhesive materials, as well as smaller quantity of adhesive present directly between the gauze wires and surfaces of the adhesive materials [10]. Cohesion forces of composite bonds reinforced with wire gauzes were much higher than the adhesion forces. The adhesive joint made with Agomet F330 reinforced with nickel gauze is shown in Figures 11a and 11b. Each time, the joints showed adhesive nature of fracture, with residues of adhesive and gauze on the steel surface, see Figure 12.

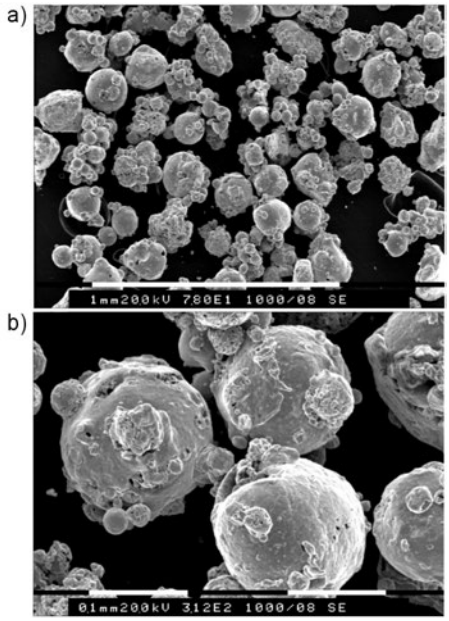

Fig. 5. Shape of iron powder grains (a, b)

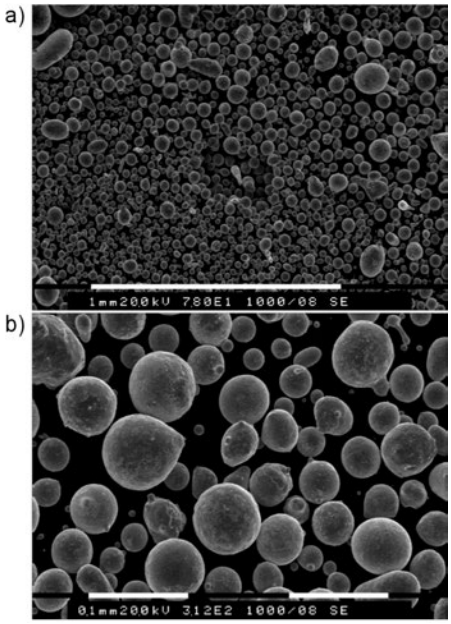

Fig. 6. Shape of CuNiB powder grains (a, b)

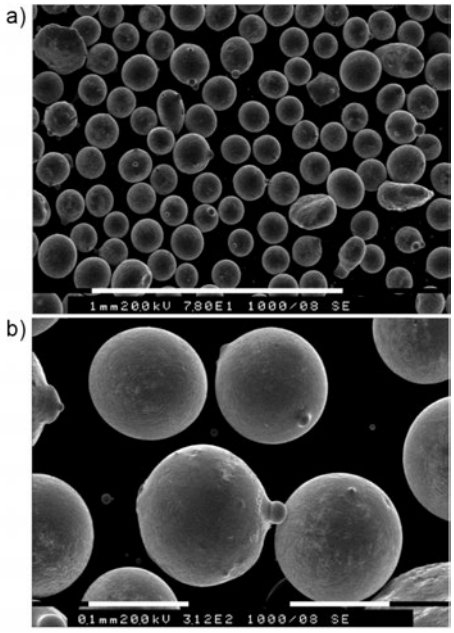

Fig. 7. Shape of NiCr powder grains (a, b)

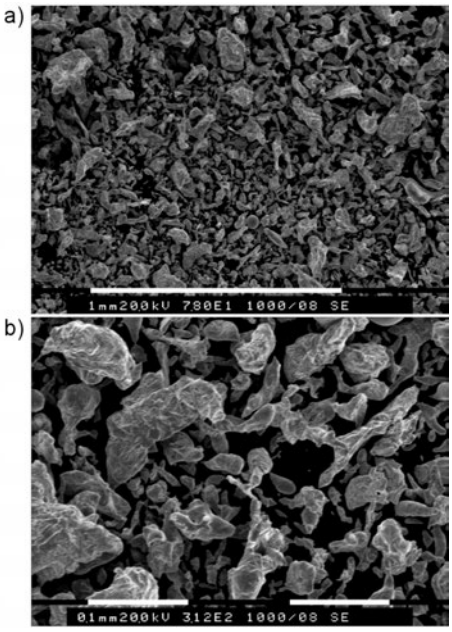

Fig. 8. Shape of CuZnNi powder grains (a, b)

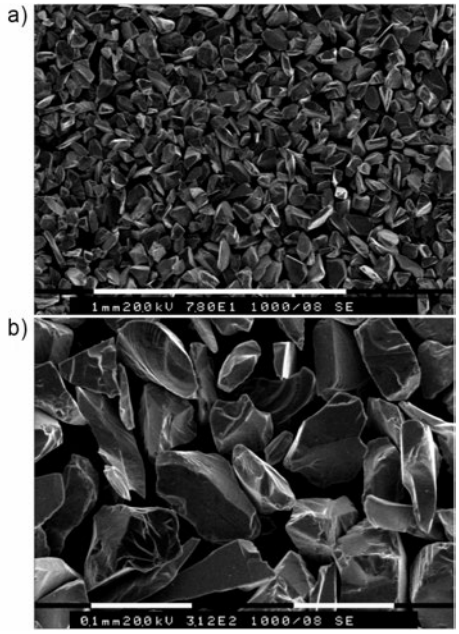

Fig. 9. Shape of SiC powder grains (a, b)

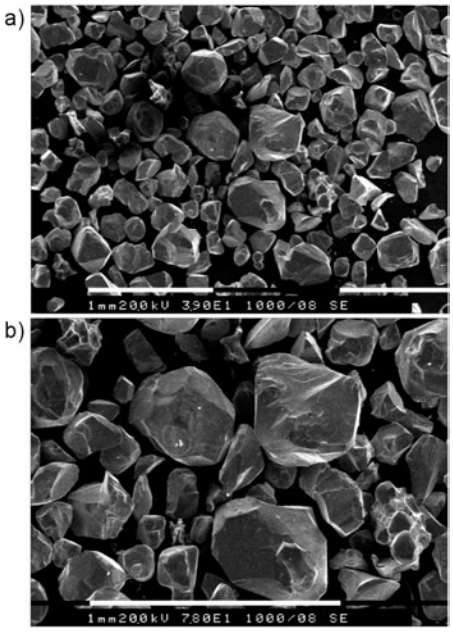

Fig. 10. Shape of graphite powder grains (a, b)

For powdery fillers, it was necessary to determine preliminarily the most profitable fraction of the additional phase for that the adhesive joint showed the highest mechanical strength. As the filler for initial tests, iron powder was selected, added in quantities of 20, 40, 60, 67 and 80 wt%. The joints were made with a glue gap s = 0.45 mm. Results of shearing test of adhesive bonds with various iron filler fraction are shown in Figures 13 and 14. For comparison, results for filler-free bonds are also shown.

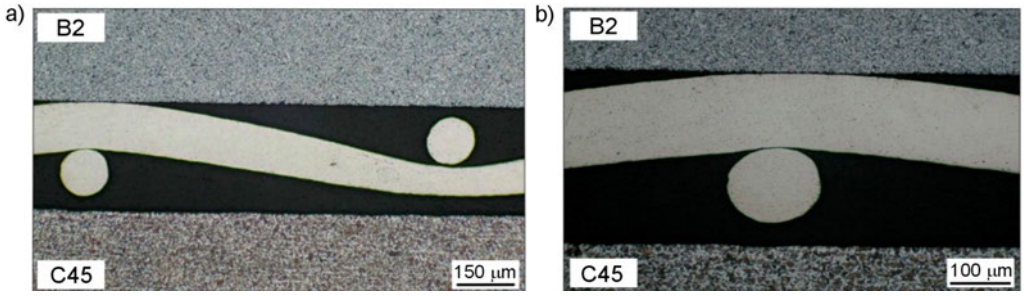

Fig. 11. Joints B2-C45 made with Agomet F330 reinforced with nickel gauze 0.15/0.15 mm (a, b)

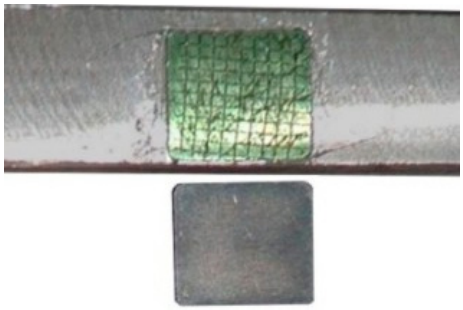

Fig. 12. Adhesive nature of fracture of adhesive joint with nickel gauze as reinforcing phase, adhesive base – Loctite 638

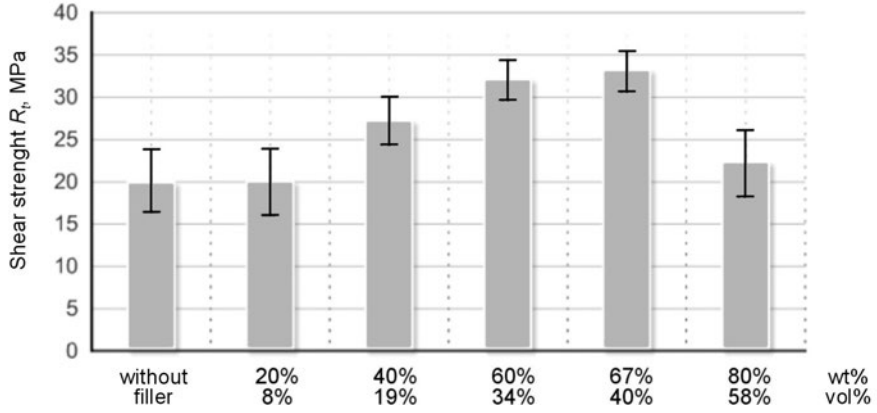

Fig. 13. Shear strength of adhesive bonds with various fractions of iron filler, Loctite 638

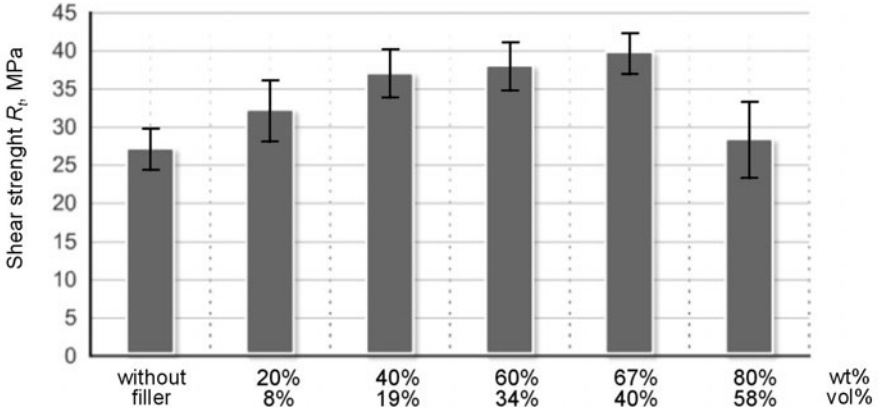

Fig. 14. Shear strength of adhesive bonds with various fractions of iron filler, Agomet F330

It results from the performed tests that the highest shear strength was obtained for the bonds containing 67 wt% of iron powder (40 vol%). With 67 wt% of filler in anaerobic glue, the shear strength increased by ca. 65% in comparison with filler-free bonds, and for methacrylic glue Agomet F330 the rise of R_t reached nearly 50%.

For further tests of reinforcing adhesive bonds with metallic and non-metallic fillers, the powder fraction of 40 vol% was selected. Due to variability of materials and shapes of the powdery fillers, joints with adhesive bonds containing 60 vol% of additional phase were also prepared for comparison.

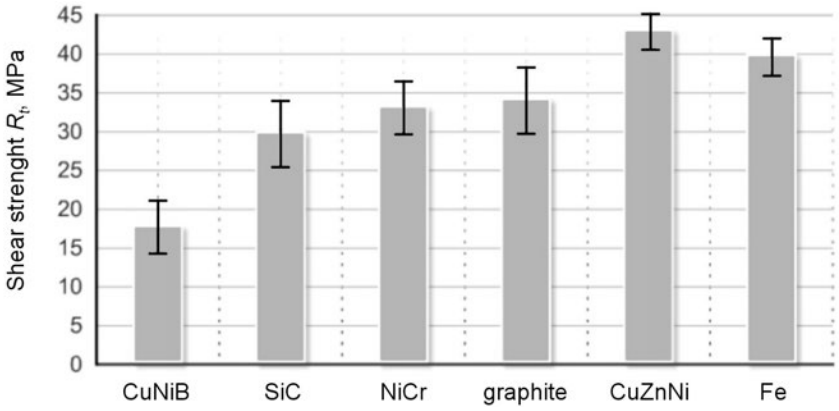

Fig. 15. Shear strength of adhesive joints with composite bonds depending on filler type in 40 vol%, glue Agomet F330, gap s = 0.45 mm

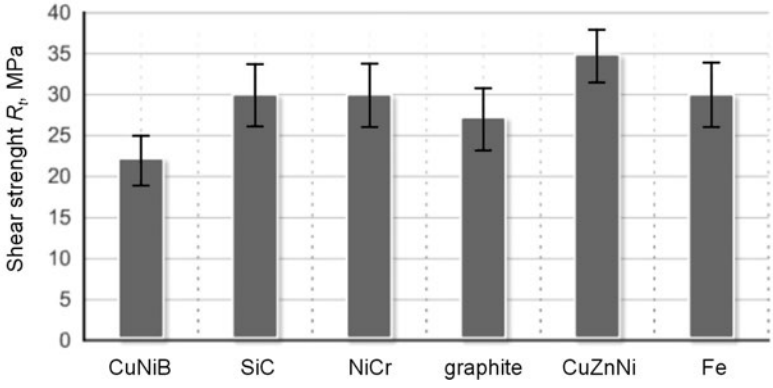

Fig. 16. Shear strength of adhesive joints with composite bonds depending on filler type in 60% obj., glue Agomet F330, gap s = 0.45 mm

Subsequent shearing tests of adhesive joints B2-C45 with composite bonds were performed using the methacrylic glue Agomet F330 only (with gap s = 0.45 mm) that permits obtaining higher shear strength in comparison with the anaerobic glue Loctite 638.

As fillers, CuNiB, NiCr, CuZnNi, SiC and graphite powders were used. Results of static shearing test for 40 vol% fraction of powdery fillers are shown in Figure 15 and for 60 vol% fraction – in Figure 16. For comparison, results for joints with adhesive bonds modified with iron powder are also shown.

The highest values of shear strength R_t = 43 MPa were obtained using the reinforcing phase in form of CuZnNi. This can be explained by irregular shape and the most developed powder surface, cooperating with surface irregularities of the adhesive materials, see Figures 17a and 17b.

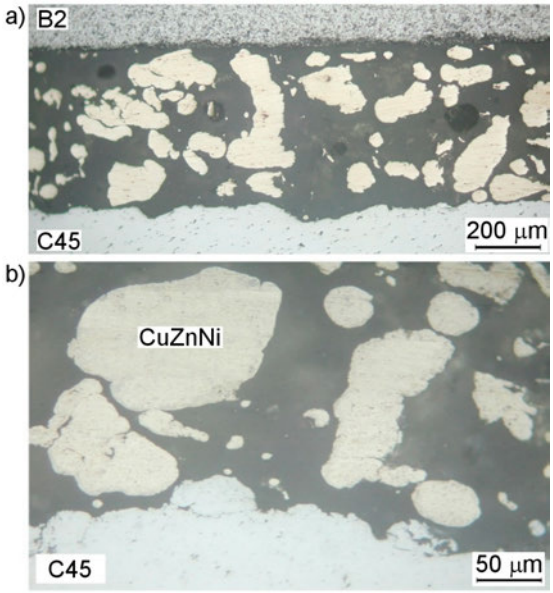

Fig. 17. Irregular shape of CuZnNi powder cooperating with surface irregularities of adhesive materials

Most of the fillers added in 40 vol% resulted in increased shear strength in comparison with filler-free bonds (up to 60% rise for CuZnNi). At 60 vol% of filler, a clear increase of shear strength could be obtained for CuZnNi powder only. For the remaining fillers, the obtained values were close to those for the filler-free bonds, i.e. R_t = 25–30 MPa, or even less for the CuNiB powder. Lower strength parameters for the bonds reinforced with the CuNiB powder can result from its high bulk density of $6.35 \cdot 10^{-3}$ kg/m^3, what makes its volume fraction in the adhesive bond lower than of the others by 55% in average. Volume and weight fractions of all the used powders are settled in Table 4. In most cases, the joints showed adhesion fractures, except for the bonds with the graphite filler showing cohesion-type fracture. Microscopic observations of composite bonds showing cohesion fracture confirm the literature data [11]: the fracture surface runs in the matrix, omitting the reinforcement.

Table 4. Comparison of volume and weight fractions of the applied powdery fillers [1]

Filler	Fe	CuNiB	NiCr	CuZnNi	SiC	graphite
40 vol%	67 wt%	81 wt%	69 wt%	69 wt%	54 wt%	66 wt%
60 vol%	82 wt%	90 wt%	83 wt%	83 wt%	73 wt%	81 wt%

Attempts to prepare adhesive bonds with 80 vol% of reinforcing phase failed, because for most of the composites some problems occurred with proper mixing the components and wetting the fillers with glue, and the obtained shear strength values were always lower than the analogical values obtained with no reinforcing phase.

6. Summary

Increase of cohesive interaction in adhesive bonds was examined using reinforcing fillers in form of metallic gauzes and powders of variable materials with differentiated grain shapes. Reinforcing adhesive bonds with plain-woven metallic gauzes is profitable for their cohesion, however at the same time the gauzes reduce the quantity of adhesive directly between the gauze wires and the joined surfaces, and moreover they do not interact with the material irregularities. This results in reduced shear strength of composite adhesive bonds by ca. 50% in comparison with non-reinforced specimens. This is a completely opposite interaction to that found in soldered joints. Joints of hardmetals brazed with C45 steel reach the shear strength increase up to 100% in comparison with non-reinforced specimens [10]. The reason is that a reinforced soldered weld participates in the joint deformation to a larger extent than an adhesive bond reinforced with a gauze.

Cohesive interaction of adhesive bonds with powdery fillers with granulation up to 200 μm was evaluated on the ground of static shearing test. At the first stage of the research, proper width of the glue gap for the iron filler was determined. The gaps in the adhesive joints were fixed with no distance or with spacers dia. 0.2 and 0.4 mm. The measured gaps were 0.25, 0.45 and 0.65 mm, respectively. The highest shear strength of 39.9 MPa was obtained for the joints with 0.45 mm gap and that gap was used in the further tests. In the case of powdery fillers, the shear strength values of adhesive joints depend mostly on fraction, kind and shape of reinforcement. In the performed examinations, the best results were obtained for the bonds with 40 vol% of CuZnNi powder with developed and jagged structure, for which twofold increase of shear strength was obtained in comparison with the filler-free bonds.

References

[1] Piwowarczyk T.: *Increase of adhesive and cohesive interaction in adhesives joints of sintered carbides with steel C45* (in Polish), Doctoral Thesis, Institute of Machine Engineering and Automation, Wroclaw University of Technology, Wrocław, 2008.

[2] *ASM international handbook committee: ASM metals handbook*, Vol. 21, Composites, American Society for Metals, USA, 2001.

[3] Dobrzański L.A.: *Materials science lexicon, basic settlement of polish, foreign and international standards* (in Polish), Metals, Polymers, Ceramics, Composites, Verlag Dashöfer, Warsaw, 1999.
[4] Wypych G.: *Handbook of fillers – A definitive user's guide and databook*, ChemTec Publishing, Second Edition, Toronto–New York, 2000.
[5] Żuchowska D.: *Constructional polymers*, WNT, Warsaw, 2000 (in Polish).
[6] Pilarczyk J.: *Poradnik inżyniera – spawalnictwo (Engineer's guide – welding) 2*, WNT Publ., Warsaw, 2005.
[7] Petrie E.M.: *Handbook of adhesives and sealants*, McGraw-Hill, New York, 2000.
[8] Mirski Z., Piwowarczyk T.: *Analysis of adhesive properties of B2 hardmetal surface*. Archives of Civil and Mechanical Engineering, Vol. IX, No. 2, 2009, pp. 93–104.
[9] Mirski Z., Piwowarczyk T.: *Klejenie metali (Metals gluing)* (in Polish), Przegląd Spawalnictwa (Welding Technology Review), No. 6, 2003, pp. 10–12, 17–18.
[10] Mirski Z., Piwowarczyk T.: *Porównanie technik klejenia i lutowania węglików spiekanych (Comparison of hardmetal gluing and soldering techniques)* (in Polish), Przegląd Spawalnictwa (Welding Technology Review), No. 9, 2007, pp. 102–108.
[11] Imielińska K., Wojtyra R.: *Effect of epoxy matrix modification with glass microglobules on post-impact strength of epoxy laminates reinforced with glass fibres*, Materials Engineering, No. 2, 2001, pp. 102–107.

Klejowe połączenia kompozytowe węglików spiekanych ze stalą

Najnowsze osiągnięcia w dziedzinie klejenia oraz przetwórstwa tworzyw sztucznych umożliwiają uzyskanie materiałów klejowych o korzystnych właściwościach: wysokich parametrach mechanicznych, zwiększonej przewodności cieplnej, małej oporności elektrycznej, zwiększonej sztywności, ograniczonych naprężeniach wewnętrznych czy redukujących proces pełzania [1–2]. Pozwala na to budowa kompozytowa klejów, tj. spoiw wzbogaconych udziałem napełniacza – dodatkowej fazy o różnej wielkości, rodzaju i udziale. W pracy omówiono wpływ zbrojenia klejów napełniaczami ciągłymi i proszkowymi na wytrzymałość na ścinanie połączeń klejowych. Przedstawiono również wyniki badań z wykorzystaniem mikroskopii elektronowej oraz analizy EDX.

ARCHIVES OF CIVIL AND MECHANICAL ENGINEERING

Vol. X 2010 No. 3

Problems with analyzing operational data uncertainty

T. NOWAKOWSKI
Wrocław University of Technology, Wybrzeże Wyspiańskiego 27, 50-370 Wrocław, Poland.

The paper deals with problem of uncertainty of information and data obtained during operation and maintenance processes of technical system. The notations of uncertainty are discussed. The classification of uncertainty mathematical models is shown based on generalized information theory by G.J. Klir. Three examples of analysis of operation data uncertainty are shown: comparison of reliability measures obtained from statistical data and expert opinions, analysis of uncertainty of expert opinions about failure reasons and possibilities of use fuzzy measures.

Keywords: *technical system, operation, data, uncertainty*

1. Introduction

The problem of uncertainty concerns various areas of human activity. Uncertainty is a term used, for example, in philosophy, statistics, economics, finance, insurance, psychology, or engineering. Examples of the areas where the uncertainty estimation is crucial are, among others [9]:

- investing on the financial markets, or at the stock exchange, making business decisions such as exchange interest rates,
- projecting/participation in games, particularly in gambling where randomness is the fundamental of the game,
- weather forecasting – common is taking into account the level of uncertainty in the forecasting,
- physics – in different situations, uncertainty has been applied as a law, for example in Heisenberg's uncertainty principle,
- metrology – uncertainty (accuracy, measurement error) of measurement is the central question in valuation of dispersion which can be ascribed to the result of measurement.

While evaluating the functioning of a technical object, fundamental is determination of measurement errors if this determination can be done through measuring conducted with the use of a measuring instrument. The measurement uncertainty usually consists of numerous factors. Some of them can be determined by means of statistical distribution of many measurement's results. Other factors are estimated on the basis of probability distributions known from other experiences or

other sources of information. The most common procedures of calculating the measurement uncertainty have been discussed in [4].

Measurement uncertainty depends on a number of factors [4]:

- incomplete definition of the measured quantity,
- imperfect realization of the measured quantity definition,
- incomplete knowledge of the environmental influence or of the imperfect measurement of the environmental conditions,
- instrument reading errors,
- inaccurate measuring instruments manufacture, their inaccurate functioning, etc.
- inaccurate data received from the external sources: the values attributed to the standards and reference materials, calculation constants,
- imperfection of the measuring method.

Traditionally, in the experimental research, distinguished are [3, 13]:

- systematic uncertainty – caused by not taking into account an important factor which influences the value of the measured quantity,
- random (statistical) uncertainty – influence of measuring instruments imperfection, their sensitivity and definition, as well as of the research method and other factors influencing the measurement result,
- major error resulting, for example, from passing erroneous information about the measurement result in other units, or from the error concerning the measurement range of the measuring instrument, etc.

The most relevant evaluation of an appliance's usefulness for performing the tasks set to it can be achieved in research carried out in real operational conditions. There are several kinds of research which are described as "operational" [7]. Normally, the notion of the "operational research" stands for the research on a machine's operation. The aim of such research is to evaluate characteristics of the machines operational process.

The research on the complete technical objects (systems) in their natural operational environment is carried out by means of the statistical methods (from the observation of randomly selected objects, conclusions about all the objects of a particular kind – of the general population – are drawn) or expert methods (data is provided by people regarded as experts).

Basic difficulties in conducting the experimental research result, among others, from [15]:

- conditions complexity of the environment where the examined objects work,
- the examined objects complexity, which makes application of the reductionism rules impossible,
- the absence of the generally accepted rules of conducting similar experiments.

The objective of the operational research is to obtain data necessary for determining the operational and reliability characteristics, or verifying the indicators values conformity with the requirements provided in the technical documentation or in trade agreements. The operational research program includes acquiring and processing

the data, as well as evaluating the research results and their use. The acquisition and processing of data requires developing a suitable information system. The structure of the system depends on the quantity and quality of the accessible sources of information describing the process of machine operation.

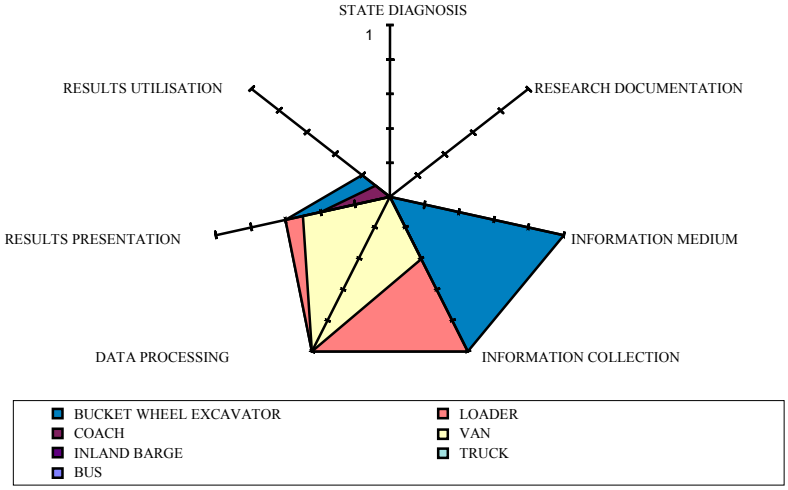

Fig. 1. Degree of computer aided of machine dependability tests

An example of a possibility of errors at particular stages of the operational research has been shown in Figure 1. Analysis of the reliability data uncertainty was based on research of 7 objects such as [7]: trucks, buses and coaches, barges, loaders, and excavators. The degree of particular computer enhanced stages of the reliability operational research has been presented. Value 1 means that a given research stage is fully computerized and its conduct features no human interference. At the stage of the state diagnosis and documentation of the research such enhancement was not introduced. It was decided that in a situation of high reliability of the computer work, the basic factor lowering the certainty of reliability evaluation is a possibility of introducing errors and mistakes by the human at the early stages of research.

2. The notion of uncertainty

Generalizing the problem of getting information about a technical system operation (information can, and sometimes has to, come not only from the measurements, but also from the historical statistical data or from the expert's opinion), the question of information uncertainty ought to be mentioned. The notion of information uncertainty has not been definitely determined. According to the classical Shannon's information theory (Figure 2), information is defined in terms of uncertainty reduction achieved by a relevant action [5].

Uncertainty is normally understood as:

- the degree of conformity with the reality [1],
- the absence of relevant information for undertaking the considered decision [14].

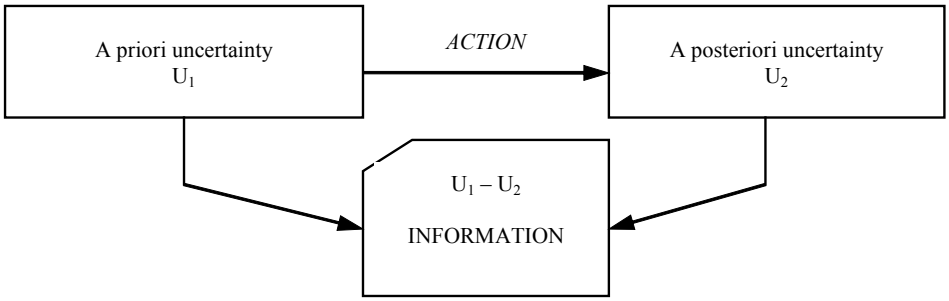

Fig. 2. Uncertainty-based definition of information [3]

The effect of using uncertain information may be such that the same results will be interpreted differently by different analysts. It is also thought [1] that information concerning the surrounding world is inaccurate, incomplete or uncertain. Inaccurate information means that there are no definite limits of values ranges, to which the variable included in considered information should belong.

Another problem is communicating uncertain information. Used is a term of concluding inference [7] if a relation between the uncertainty degree of premises and a degree of a conclusion's certainty is defined. The role of the concluding inference can be compared to the role of estimating the error by formulating an empirical problem.

Analysis of the information loaded with certain degree of uncertainty, in the literature of the problem ([1] for instance) is called uncertainty evaluation. Analyzing the influence of uncertainty of the hypotheses assumed for modelling, for example, characteristics of a technical system is called [1] sensitivity study.

The most important reasons of uncertainty of information characterizing an object are connected with [7, 15]:

- uncertainty concerning parameters (e.g., little statistical sample and a broad parameter interval, data extrapolation from one object to another),
- uncertainty concerning modelling (models of phenomena are approximate, particularly when it comes to the influence of the system environment's or of the human's),
- uncertainty resulting from the inexhaustive character of the phenomena analysis (the analyst cannot be totally sure whether all important factors concerning events and their interactions were taken into consideration).

In the literature devoted to the problem of information uncertainty describing the functioning of a technical system ([13] for example), it is common to distinguish two uncertainty categories: the epistemic uncertainty and the aleatory uncertainty. The epistemic uncertainty results from the lack of the basic knowledge on the core of the

analyzed problem. The aleatory uncertainty stems from the variability in a known-observable population, and represents "in-born" randomness of a phenomenon.

Distinctions between the aleatory and the epistemic uncertainty is considered [10] very useful from a practical viewpoint, because the epistemic uncertainties are generally reducible through obtaining more and more knowledge. Therefore, if we know what part of uncertainty in the external information comes from the epistemic sources of uncertainty, then we know that the uncertainty is, in general, removable (or at least reducible), while the part which results from the aleatory uncertainty is irreducible. Analysis of sensitivity is a tool for the research on how various uncertainties influence the external information, and whether it is possible to determine the range of reducing uncertainties coming from the epistemic sources.

So far, a general method of modelling uncertain information has not been developed. In the problem literature [7], mainly the numerical approach is exposed. Used are various categories of certainty factors. A crucial and difficult task is to determine the appropriate interpretation of the certainty degree measures applied.

Often, uncertainty is identified with risk [12]. The important differences between the notions of risk and uncertainty need to be emphasized. There are fundamental differences in dealing with the phenomena depending on which of the two approaches is really used. It may turn out that the measurement uncertainty or the real risk, as the two notions ought to be used, is applied in a far different way than the immeasurable problems, which are not at all an effect of uncertainty.

Risk is well defined, for instance [12], whereas the point of uncertainty cannot be specified in such a well-founded way. What is more, the uncertainty degree often cannot be reduced by adding/completing more information on phenomena from the research on the causes and effects [6].

There are other uncertainty measures, for example in [2]:

- stochastic, risk is uncertainty for which probability can be calculated (from the past statistics, for example) or at least mathematically estimated (by forecasting events scenarios),
- insurance, risk regards only the negative uncertainty (the one causing loss or damage),
- cognitive psychology, uncertainty can be real or can be only a question of perception such as expectations, threats, etc.

3. Mathematical models of uncertainty

In order to determine usefulness of particular uncertainty measures, three basic principles of uncertainty management have been formulated in the general information theory [5]:

- the minimum uncertainty principle,
- the maximum uncertainty principle,
- the invariable uncertainty principle.

The minimum uncertainty principle is basically arbitrary [5]. This principle makes it easier to select meaningful alternative solutions out of the set of solutions obtained through solving a problem, where certain amount of the starting information is inevitably lost (for example the problem of acceptable simplifications or obtaining contradictory solutions). According to this principle, accepted are only those solutions for which information loss is as little as possible. It means choosing the solutions of the minimum uncertainty.

The maximum uncertainty principle is important for the problems of the surplus concluding [5]. In this case of concluding, conclusions are not drawn from the conditions. It means that in the surplus concluding used is all information accessible from a particular data source, but it must be made sure that no extra information (not coming from the particular data source) was unintentionally added. Whatever conclusion drawn from the concluding should maximize the particular uncertainty in a range of limitations representing given conditions. This principle guarantees full recognition of our lack of knowledge when attempts are made at concluding beyond the information range defined in the given conditions, and at the same using all the information included in the conditions. The principle also guarantees maximum non-committance of concluding if the information not included in the conditions is taken into account.

The invariable uncertainty principle (also named the principle of keeping information) was introduced in order to facilitate the crucial modifications among various uncertainty theories. According to this principle, the amount of uncertainty and of the information connected to it should be saved in every modification of uncertainty from one mathematical model to another.

Generally, modelling the uncertainty consists in looking for certain measure which, in relation to a described quantity, would determine the dispersion/range of the quantity acceptable in a concluding process. Mathematical models of uncertainty are classified according to different criteria by different authors who deal with this problematic.

Table 1. Structure of uncertainty models [5]

Uncertainty theory			Formalized set theories		
			Classical	Nonclassical	
				Standard fuzzy set	Non-standard fuzzy set
					...
Monotonic measures	Additive	Classical probability theory	1	8	
	Non additive	Possibility and necessity measures	2	9	
		Sugeno λ-measures	3	10	
		Dempster – Schafer theory	4	11	
		Choquet measures of order n	5		
		Interval valued probability distributions	6	12	
		General lower/upper probabilities	7		

Fig. 3. Uncertainty theories [3]

Applied are for instance:

- relations between the accessible information and the object's state [8, 14],
- variability range of the data concerning the object [12],
- information theory (general) [2, 5].

In the general version of the information theory, two generalizations necessary to build a formalized uncertainty structure have been used, namely:

- generalizing the classical measure theory in the monotone measure theory,
- generalizing the classical set theory in the fuzzy set theory.

Such a two-dimensional possibilities structure of formalizing uncertainty models has been depicted in Table 1.

Columns of this matrix represent different kinds of formalization of the set theory, and particular lines refer to the monotone measure theory. Each element of the matrix represents a model/theory of uncertainty of a certain type. Numbering the matrix cells indicate 12 mathematical uncertainty models which are presently well developed.

Development, in a sense of generality of particular theories has been shown in Figure 3.

The classical uncertainty theories are [2, 5]:

- the possibility-based uncertainty theory,
- the probability-based uncertainty theory.

These theories are developed through the application of the fuzzy sets and the imprecise probability theory.

Each problem requires the employment of a different theory which would enable expressing our lack of knowledge and would protect us against ignoring accessible information whatsoever.

4. Examples of operational process uncertainty evaluation

4.1. Expert opinions versus statistical estimations

Analysis of the research data gathered in the process of machine operation [7] made it possible in the first place to relate uncertainty of the gathered information to the procedure of its gathering.

Comparison of the reliability measures estimated by an expert and calculated on the basis of the statistical data was carried out for the bucket ladder excavators operating in open coal mines in Poland. For this, indexes K_a and K_t were applied:

$$K_a = \lambda_e/\lambda_d, \tag{1}$$

$$K_t = T_e/T_d, \tag{2}$$

where:

λ_e – parameter of the object damage stream estimated by an expert,

λ_d – parameter of the object damage stream calculated on the basis of the SNK system database,

T_e – working time to the exchange of the object estimated by an expert,

T_d – working time to the exchange of the object calculated on the basis of the SNK system database.

The calculations were done for particular functional systems of the machine and the excavator as a whole. It was stated that the estimations and calculations are of the same value

$$H_1: K_a = 1; \quad H_2 : K_t = 1 \text{ for } \alpha = 0.05. \tag{3}$$

The test results have been set out in Figure 4.

The data proves the summary evaluation of the machines correct (the interval considered). The expert showed a tendency to optimistically evaluate the reliability of the object, namely estimated lower damage intensity and higher durability than it was shown in the calculations based on the statistical research. Apparently, the expert's opinion is better in relation to the failure damage than to the durability of particular units of the machine.

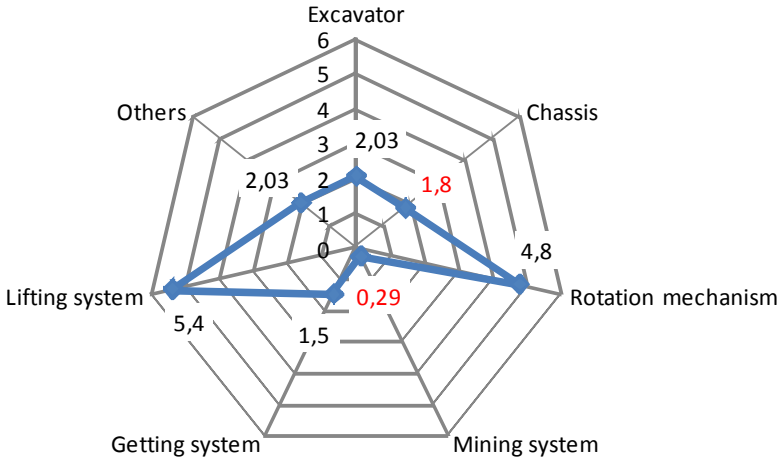

Fig. 4. Relations of estimations expert/statistical data of time to replacement

4.2. Failure occurrence foresight

Possibilities of the failure characteristics evaluation were specified on the basis of the statistical data from the operational research conducted on the city buses reliability [7]. The information gathered concerned, among others, such damage characteristics as: form, cause, and the way the damage was repaired. The results of the evaluation were compared to the subjective evaluation of the damage form.

For particular elements of the engine, experts determined various forms of its damage. Two kinds of errors are possible:

- determining the damage form which cannot occur in a particular element,
- disregarding the damage form which occurs in a particular element.

The experts' estimations (E) were compared with the operational research results (B). The analysis results were set out in Figures 5–7 in a form of indexes $N_{E,B}$ (E = 0, 1; B = 0, 1) determining:

- $N_{0,0}$ – the damage form, according to the expert, is impossible and did not appear in the research,

• $N_{1,1}$ – the damage form, according to the expert, is possible and appeared in the research,

• $N_{1,0}$ – the damage form, according to the expert, is possible but did not appear in the research,

• $N_{0,1}$ – the damage form, according to the expert, is impossible and appeared in the research.

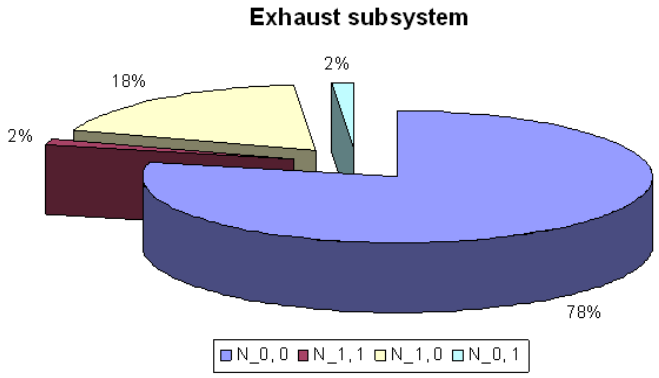

Fig. 5. Failure characteristics of exhaust subsystem

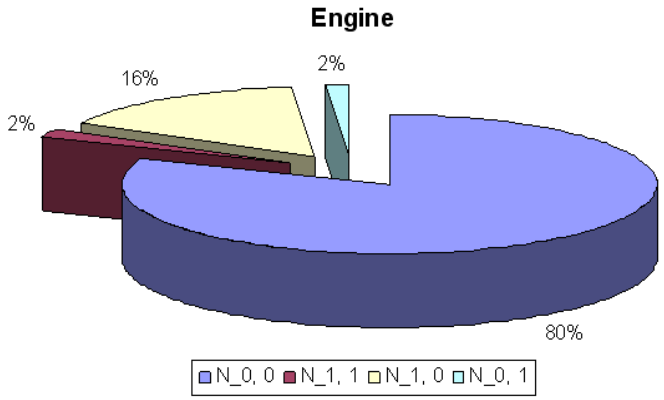

Fig. 6. Failure characteristics of engine

Cases $N_{0,0}$, $N_{1,1}$ indicate that the expert's evaluation is correct; case $N_{1,0}$ can be the expert's error, but it can also be caused by too short a time of the operational research; case $N_{0,1}$ is an error. The share of the correct expert's opinions exceeds 80%. The number of errors made falls in the range of 1–2%. Similar estimations were obtained in the operational research.

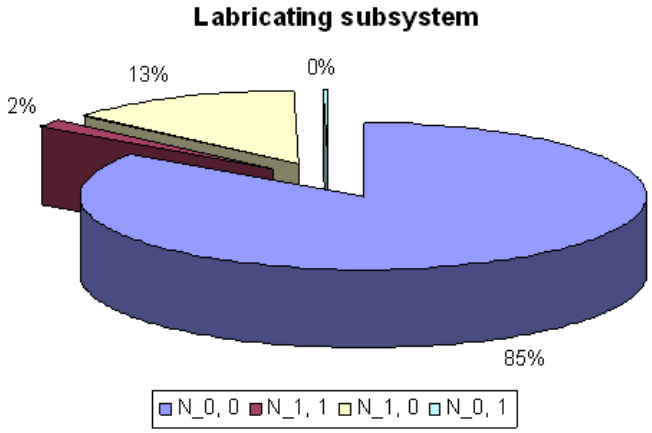

Fig. 7. Failure characteristics of lubrication subsystem

4.3. Uncertainty measures evaluation

A much more difficult problem is the attempts at deciding about usefulness of the mathematical uncertainty models. Positive are experiences with the application of the fuzzy sets logic in the quality evaluation of physical quantities, object and system states, as well as their comparison. The fuzzy logic is based on the application of fuzzy sets. The difference between a binary set and a fuzzy set consists in the fact that in a normal set each element either belongs to it or not, whereas in the case of a fuzzy set we have to do with a notion of membership to the set on certain level (affiliation level) [8, 13]. The membership function of a fuzzy set A is a function which attributes a membership level to each x element belonging to the numerical space of consideration X. The membership function's value is in a range from 0 to 1, where 0 means zero membership level to a particular set, and 1 – a full membership.

A fuzzy number L of $a - b$ type is represented by four (a, b, α, β). The first two parameters indicate the range in which the membership function reaches value 1; the third and fourth parameter indicates the left and right width of distribution. The membership function is defined as follows:

$$\mu_L(x)=\begin{cases}0, & x<a-\alpha,\\ (1/\alpha)(x-a+\alpha), & x\in[a-\alpha,a),\\ 1, & x\in[a,b],\\ (1/\beta)(b+\beta-x), & x\in(b,b+\beta],\\ 0, & x>b+\beta.\end{cases} \tag{4}$$

The possibilities distribution function is specified [8] for a statement that the value of variable y is the fuzzy element L. The function assumes value $p(y)$ being a possibility of the fact that y is a value of L. The numerical values of the possibilities distribution function and the membership function of a fuzzy set is equal:

$$p(y) = \mu_L(x) \text{ for each } y = x. \tag{5}$$

Possibility measure of the fact that a fuzzy set A contains fuzzy number L equals:

$$MM(A) = \max o \in O \, [\min [p\,(o), \mu_L(o)]]. \tag{6}$$

The notion of necessity measure was introduced in order to specify the absence of possibility of statement A:

$$MK(A) = \min o \in O \, [\max[1 - p\,(o), \mu_L(o)]]. \tag{7}$$

Statement A, the necessity measure of which is $MK(A) = 1$, is a completely true statement. Statement A, the necessity measure of which is $MM(A) = 0$, is a completely false statement. Necessity measure values $MK(A)$ and possibility measure values $MM(A)$ can be considered as limitations of the quantity determining the validity degree (certainty coefficient) of statement A.

As an example, used can be the results of work [11] the aim of which was to develop a system that would support the decision-making process in the inland transport of the over-dimensional freight – selection of a proper vessel for particular cargo.

Membership functions have been attributed to particular regulations of the expertise system. For example, to the question of "cargo length":

- does not exceed 38 meters,
- does not exceed 40 meters,
- does not exceed 50 meters,
- does not exceed 63 meters?

If the answer is:

- 38 meters – the system will attribute such coefficients as:
- 38 meters – 1.0,
- 40 meters – 0.8,
- 50 meters – 0.4,
- 63 meters – 0.0.

For the answer "50 meters" it will be:

- 38 meters – 0.0,
- 40 meters – 0.0,

- 50 meters – 1.0,
- 63 meters – 0.435.

For the answer "63 meters" it will be:

- 38 meters – 0.0,
- 40 meters – 0.0,
- 50 meters – 0.0,
- 63 meters – 1.0.

While applying the uncertainty function, at every moment one can check which certainty coefficients are attributed to particular answers by the system. The expertise system screen corresponding to the question has been presented in Figure 8.

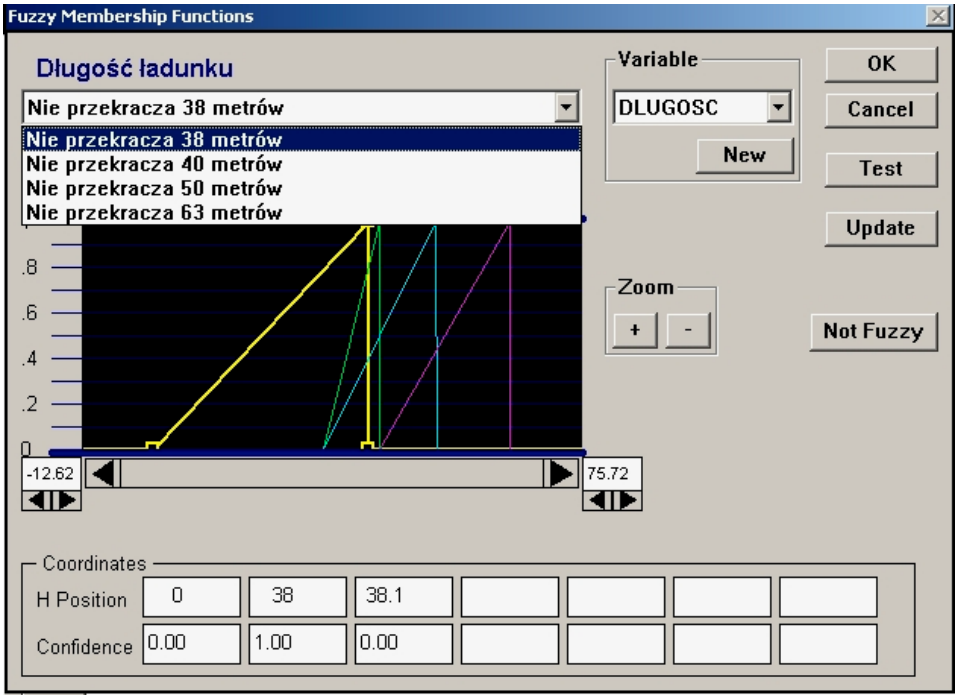

Fig. 8. Fuzzy membership function to the question of "cargo length" [11]

5. Conclusions

Selecting the method of defining uncertainty of the knowledge on technical systems operation still is and will be a crucial problem in creating the knowledge base from the research data. The basic doubts which occur by using the above discussed, relatively simple way of determining the epistemic uncertainty refer to:

- the absence of an unequivocal interpretation of determining the uncertainty measures,
- impossibility of the experimental verification of their correctness,
- one-way processing (concluding): from the symptoms drawn are conclusions about the causes, without the possibility to conclude in the opposite direction,
- application of the same rule in different branches of the same deduction tree.

References

[1] Bolc L., Borodziewicz W., Wójcik M.: *Fundamentals of proceeding of uncertain and unfull information* (in Polish), PWN, Warszawa, 1991.
[2] Bukowski L., Majewska K.: *Evaluation of uncertainty of logistic systems*, (in Polish), Wybrane Zagadnienia Logistyki Stosowanej, Oficyna Wydaw. TEXT, Kraków, No. 3, 2006, pp. 9–22.
[3] Du L., Wang Z., Wang H-Z.: *Cost-type function analysis in dynamic design under uncertainty*, Maintenance and Reliability, Vol. 46, No. 2, 2010, pp. 17–20.
[4] *Evaluation of measurement uncertainty. Guidebook* (in Polish), Główny Urząd Miar, Warszawa, 1999.
[5] Klir G.J.: *Generalized information theory: aims, results and open problems*, Reliability Engineering & System Safety, Vol. 85, 2004, pp. 21–38.
[6] Kornacki A., Sokołowska E.: *The estimation of smooth operation time until failure with application of the AKAIKE information criterion (AIC)*, Maintenance and Reliability, Vol. 45, No. 1, 2010, pp. 69–76.
[7] Nowakowski T.: *Method of foresight of mechanical objects dependability* (in Polish), Oficyna Wydawnicza Politechniki Wrocławskiej, Wrocław, 1999.
[8] Nowakowski T.: *Models of uncertainty of operation and maintenance information*, (in Polish), Zagadnienia Eksploatacji Maszyn, Vol. 35, No. 2, 2000, pp. 143–150.
[9] Nowakowski T.: *Problems of uncertainty of technical systems evaluation* (in Polish), TRANS '09, H. Brdulak, E. Duliniec, T. Gołębiowski (Eds.), Warszawa, Szkoła Główna Handlowa – Oficyna Wydawnicza, 2009, pp. 105–115.
[10] O'Hagen A., Oakley J.E.: *Probability is perfect, but we can't elicit it perfectly*, Reliability Engineering & System Safety, Vol. 85, 2004, pp. 239–248.
[11] Palac M.: *Development of computer expert system for over-dimension loads transportation process aid at waterborne shipping* (in Polish), Master Thesis, Mechanical Engineering Faculty of the Wrocław University of Technology, Wrocław, 2006.
[12] Pate-Cornel M.E.: *Uncertainty in risk analysis: six levels of treatment*, Reliability Engineering & System Safety, Vol. 54, 1996, pp. 95–111.
[13] Rakowski U.K.: *Some notes on probabilities and non-probabilities reliability measures*, Proceedings of ESREL '2005, A.A. Balkema Publishers, London, 2005, pp. 1645–1654.
[14] Seidler J.A.: *Fundamental concepts of intelligent info system theory*, Information Systems Architecture and Technology ISAT '94, Proceedings of 16th Scientific School, Oficyna Wydawnicza Politechniki Wrocławskiej, Wrocław, 1994.
[15] Villemeur A.: *Reliability, availability, maintainability and safety assessment*, Wiley and Sons, 1992.

Problemy analizy niepewności danych eksploatacyjnych

Omówiono wybrane problemy z przeprowadzeniem analizy niepewności danych eksploatacyjnych. Przedstawiono różne sposoby definiowania pojęcia niepewność. Pokazano klasyfikację modeli niepewności bazującą na ogólnej teorii informacji sformułowanej przez G.J. Klira. Przedstawiono przykłady prowadzonych analiz niepewności danych wykorzystując wyniki własnych badań eksploatacyjnych. Pokazano analizę porównawczą oszacowań wskaźników niezawodności na podstawie zgromadzonych danych statystycznych oraz opinii ekspertów. Omówiono możliwości oceny charakterystyka procesu eksploatacji przez ekspertów. Przedstawiono sposób budowy rozmytych miar w procesach decyzyjnych dotyczących użytkowania maszyn.

ARCHIVES OF CIVIL AND MECHANICAL ENGINEERING

Vol. X 2010 No. 3

Diagnostic equivalent for widespread manufacturing system

FRANCISZEK W. PRZYSTUPA
Wrocław University of Technology, Wybrzeże Wyspiańskiego 25, 50-370 Wrocław, Poland.

In the case of diagnosed system with widespread characteristics, the elementary Diagnostic Equivalent Rd, considered as to be a standard object of observation, is an important facilitating factor. When the frequency of diagnoses has been determined for a standard subassembly, this equivalent permits to define the indispensable quantity and quality of simultaneously working diagnosers. Notions of diagnostic potential and diagnosability are proposed, based on systems-based definitions of knowledge and skills. The definition of a diagnostic tandem is introduced. The whole is illustrated by an application example in a MS conveyor.

Keywords: *diagnosability, diagnostic equivalent, widespread manufacturing system, conveyor*

1. Introduction

In substance, technical systems are correlated with various areas of science [1–3]. In technical systems, all the information concerning the Manufacturing System (MS) process is delivered in a computer science based way through different signals [3–7]. If such systems fail, when unrecognizable signals are reaching it, when no signals are reaching it, or when the delivery of information is disappearing – and such situations are unavoidable for different reasons – the possibility exists of utilizing for diagnostic purposes the knowledge about the events that have caused those atypical states. Such type of knowledge is extraordinarily helpful for the SYSTEM in critical states and situations, when a threat or an emergency state of the object, a threat of the process, of system safety and the like appears [8–16].

Technical practice implies a concretization of analyses on the basis of real objects. There exists also an opposed command – an analysis of a technical object should be possible for generalizing and applying in other systems, not only in technical systems. Profits have been repeatedly confirmed, resulting from verifying theoretical considerations in practice before executing the successive theoretical step, and turning back to a generalization after practical verification.

In technology, we agree to use suitable methods that have been applied and verified in other domains. The manufacturing system (MS), for the analysis of which systems principles have been used, is an example of a processing object from the intersystem point of view. The analysis performed on a generalized object (widespread system) has been adapted to an exemplary, real M-system, and the final, concretized conclu-

sions of the analysis have been processed into useful conclusions for a generalized object (widespread system).

When diagnosing widespread M-systems, an attempt is made to use standard diagnosing methods being applied in typical machines. Transferring habits, methods, methods and uses on such systems leads to a reduction of the efficiency of the diagnosing process.

The level of technical differentiation and of innovative saturation of widespread MS is an essential problem during making design decisions when implementing the diagnostic system. Modern assemblies are generally adapted to a diagnostic monitoring of states; older systems do not have such tools. During renewal works that are performed in different time periods, assemblies were introduced that are of a different level of technical advancement, also what concerns diagnosability. The designer of a new working machine, the designer of the renewal of such machine or of the exploitation system for MS, have to make many decisions facilitating the adaptation of the diagnoser.

When making such decisions, particularly in the case of the widespread properties of the working machine being diagnosed, the elementary diagnostic equivalent Rd will be an important facilitating factor.

The diagnostic equivalent is treated as a standard observation object, being diagnostically indivisible. In this paper, I will consider the synthesis of the diagnostic equivalent for widespread working machinery as to be an example of systems analysis. A method of selection of a diagnoser for a MS conveyor is the basic purpose of this scientific work. In the case of widespread characteristics of the machine being diagnosed, a facilitating factor is the diagnostic equivalent Rd, considered to be a standard object of observation and to be indivisible from diagnostic point of view. When the frequency of diagnoses for that standard will be determined then, for a greater quantity of objects of diagnosis, the equivalent permits to determine the necessary quantity and the quality of simultaneously acting diagnosers. Method of synthesis of diagnostic equivalents of diagnosers for widespread MS conveyor will be proposed.

2. Diagnostic equivalent

The diagnostic equivalent for widespread MS is an indicator of the necessity of performing diagnosis, when the object is diagnosed in the form of a multiplied or/and continuous structure.

Main assemblies in the being diagnosed complex systems – for example, in machine systems, a single reduction gear – are proposed as a basis of the standard of the equivalent at a concrete stage of technology development. It can be assumed that a segmentation of the basis of the equivalent standard will occur into elements that are, so far, lower from systems point of view, as a result of an increase of the possibility of application of a set of sensors, without intervening, in arbitrary fragments of the material structure of machines.

In machine the structure of the present standard is composed of two shafts, a pair of toothed wheels, four bearings and auxiliary, negligible from diagnostic point of view elements – all these parts being built in housing. The subassembly consisting of the pair of bearings on the shaft with the toothed wheel is proposed as standard for the equivalent. A characteristic feature of that standard is the fact of existence of bearing elements of the shaft as well as of the kinematic pair of higher order in the pair of toothed wheels.

A simple, complete set of tools and of diagnostic knowledge – the DIAGNOSER – requires always time for executing the process of diagnosis.

If one technical diagnoser set is at the disposal of the decider, and if one standard basic subassembly is observed, then the time of diagnosis must be shorter than the time between potential damages of the diagnostically observed object. This results from the necessity to be in advance of failures or of an exploitation change of state as a result of the diagnostic decision.

When the indispensable frequency of purposeful diagnoses for a standard unitary assembly has been determined then, in the case of a greater quantity of diagnosis objects, the diagnostic equivalent permits to determine the necessary quantity and the quality of simultaneously functioning diagnosers.

The number of diagnosers functioning at the same time results from the necessary frequency of diagnoses being repeated on a concrete subassembly that is compatible with the diagnostic equivalent. For examples of mechanical assemblies and systems, the values of diagnostic equivalents Rd are mentioned in Table 1 [11, 13].

Table 1. Values of diagnostic equivalents Rd for mechanical assemblies

Pair of bearings on a shaft with a toothed wheel	Rd = 1,
Simple-stage gear	Rd = 2,
Two-stage gear	Rd = 3,
Worm gear	Rd = 2,
Runner	Rd = 1,
Assembly of 6 runners	Rd = 6,
Drum of conveyor	Rd = 1,
Electric motor	Rd = 1,
Conveyors (with belt, rollers, runners, etc.)	Rd = from several to several hundred of thousands

A singular object can be diagnosed by laboratory methods even on the working site; that can be performed in extraordinary situations (failures, building a space of diagnostic parameters, etc.) that cannot become, however, a general rule.

Table 2. Diagnosing methods for certain values of diagnostic equivalents [10–16]

Rd < 10	Unitary, laboratory, scientific tools.
10 < Rd < 100	Unitary tools for an object, inspection elements.
100 < Rd < 1000	Locally multi-task tools, unitary for objects with important quantity, testers, inspection elements.
Rd > 1000	Displaceable testers.
Rd >>> 1000	All kinds of tools, testers, diagnostic agents, etc.

It is necessary to apply economically justified methods. The situation is different in the case of widespread working machinery when the user is ready to incur costs in order to assure an appropriate level of safety. Basing on experience, methods of synthesis of diagnosers of such machines are proposed [16]. Values of diagnostic equivalents Rd determine diagnosing methods; see Table 2.

The above example of the shaft with a toothed wheel is useful for typically mechanical objects.

Widespread MS are complex machine systems with different media of power flows. For such systems, it is necessary to build other diagnostic characteristic factors – Rd-type. That concerns, in assemblies of MS, hydraulic, pneumatic, electric systems, etc. A synthesis of diagnostic characteristic factors for a particular system must connect two categories of knowledge – the knowledge about the object and the knowledge about possibilities of diagnosing (diagnostic tandem, see hereinafter). When taking into account the present-day rate of changes of both these categories, synthesizing the characteristic factor must be permanently updated. Thus, the construction of the diagnostic characteristic factor depends upon the knowledge:

- about the object – systems category, process category, widespread property, complexity, teleological feature, and especially "information covering" in time, space aspect as well in the aspect of quality,
- about diagnosing possibilities – costs, timing, and especially "capability to information covering" in time, space aspect as well as in the aspect of quality.

3. A widespread object of diagnosis – manufacturing system conveyor

As an example – MS conveyor was chosen. Construction structure elements, drums with drive, rollers and/or runners are basic groups of being diagnosed assemblies of MS conveyors. There exist an immense number of examination methods, among them diagnostic methods, of assemblies and elements of widespread objects, in the case of roll – runners' conveyors; there is a lack, however, of an evident methodology of selecting a purposefully dedicated diagnoser for a concrete conveyor in a concrete technical situation.

What concerns technical objects of a transportation system, necessary to be diagnosed, two of them require a special consideration: the great quantity of the runners or the rollers and its supports. The other objects are easy diagnosable in the whole range of existence. The special treatment of runners – rollers investigation results from: access difficulties and physical widespread characteristics, high speed, indeterminacy and unpredictability of failures, vulnerability, inaccessibility of visual (thermal) observation of ground run and difficulty of observation in places of transformation of the handled material.

Even in the case of typical supports and bearings of runners, excellent, extended methods of testing and of observation exist, however, in principle, for laboratory conditions or also on the working site but with expensive and unitary tools. Their special

treatment results also from: difficulties what concerns a simultaneous access to all the structures, distribution on hardly accessible sites, inaccessibility of observation of the ground run in places of transformation of the handled material, and important vulnerability.

The above-mentioned innovative saturation of conveyors is an essential problem. When introducing new assemblies – unitary or multiplied assemblies – the necessity of using advanced laboratory methods and tools for the synthesis of characteristics and boundary values is to be taken into consideration.

The evidenced here causes force to leave the conventional treatment of the diagnosing process of widespread objects. Design methods can be proposed that are based on simple table morphologies; these methods do not pretend to be complete and do not assure the selection of the best solution. The presented considerations can only be a basis and starting point for a concretization of the design of diagnosing tools in a known technical situation. The presented examples concerning a roller – runner conveyor can be adapted to other widespread objects. A tester on a mobile element for diagnosing stationary objects is the simplest example.

An inversion of the situation of the tester on a mobile element for diagnosing stationary objects will be a tester on a stationary element for diagnosing mobile elements [11–15]. It is also possible to have the tester on an external object for a remote diagnosis of mobile and stationary elements. Beside a migratory or stationary tester (microphone), the introduction of failure markers can also be considered: labels (of point, line, plane), dyes, adhesive elements, diagnosis agents, etc. Another problem that is not analyzed here concerns the logic of causes and places of damages (failures). Technical methods of diagnosing can be limited to economically acceptable methods.

After failure diagnosis (identification) – counteracting can cover action or prevention. An action consists in reacting in the situation of a developing, being diagnosed failure, but that requires a perfect observation. Prevention not requires such a reconstruction of thinking about designing rollers, bearings or supports so as to assure that they become adapted to a continuous diagnosing or supervising. In the traditional approach to the construction of conveyors, the user does not undertake diagnosing works because of supposing an inefficiency of such activity.

The computation of the diagnostic characteristic factor Rd for a concrete system, which permits to define diagnosing methods, is decisive for the use of two categories of knowledge, about the object and about diagnosing possibilities. These two knowledge categories form the so-called “diagnostic tandem”; this notion will be shortly described further in the article.

4. Diagnostic tandem

The diagnostic tandem is a label of the pair: Object-based knowledge – diagnostic knowledge, evolving in time or, in other words, a notion that determines the indispensability of active coexistence of two categories of knowledge of the diagnoser. The

object-based knowledge determines the necessary area of observation that is a dominant element of all decisions, e.g. concerning the creation of the diagnostic characteristic factor. The diagnostic knowledge concerns tools (from methods up to technical means), e.g. for a unitary characteristic factor. The model of diagnostic tandem can be applied in the synthesis of the Rd index.

Knowledge increases diagnosability and diagnostic potential (see definitions beneath) through an increase of diagnostic information possible to be acquired during the accepted existence of the object. There exists, in the machine (conveyor), a spectrum of signals resulting from energy – existence potential. That is a multidimensional space, being partially observable. During a stabilized exploitation, its image is generally linearly variable for small gradients of changes. In each direction of the vector of signals, conventional values exist (for instance states: good/satisfactory/admissible/failure/...) and their limits that require a reaction of the decider. Beside signals resulting from the potential, other non-typical signals can appear, generally being externally forced by a technical (or not technical) situation. These signals should also be observable in ranges of threats for the process or the object.

In order to perform the diagnosing process, skills are needed, in this case being determined by the capability of executing tasks in a well-known (to the decision maker) and suitable way. The "capability to execute tasks in the well-known way" concerns realization knowledge; and the "capability of executing tasks in the suitable way" concerns decision knowledge.

Two categories of knowledge are always used: the theoretical knowledge – about methodologies, methods, time-based decisions, actions, and the practical knowledge – skills for deciding, selecting a method, the time of execution, the timing, the realization algorithm, etc.

The notions of skills and knowledge are conjointly treated, because, in the interesting observation process, knowledge is necessary that requires skills for using it; skills without the necessary knowledge become useless.

Each observation of the structure of an object or of the quality of the process being realized – in its whole or its components – requires suitable skills – capability of systems intervention, or action-oriented knowledge being used in action (for intervening). For the observer, knowledge can be treated as a feature of his structure.

When summarizing these considerations, it can be stated that knowledge, motivation, time, energy and the technical situation permit to take advantage of skills. That is a certain action potential supported by possibility of distinguishing proper conditions and conditions of the environment (deciding possibility). The skills themselves are valueless, or have only a potential value; their real value is manifested during the action-based realization of the purpose. Designing with regard to diagnosability is carried out in the criterial space of diagnoser, object – process, decider and realizer – actioner.

The realization triad: knowledge $\rightarrow$ skills $\rightarrow$ (process) realizing, is ordered by the principle: action through knowledge creates skills. That is against the logic of algo-

rithm creating, but it is a process of the type: trials → errors → correction. Skills are a synthesis of knowledge and action. Action without knowledge creates habits, generally with a low efficiency. Realization – action must not always result in realization – effect.

5. Purposes of diagnosing MS conveyors

The goals of the diagnosing process have to be defined first of all, according to its morphology, in the form of fundamental problems that are not developed in a detailed way in the morphological table.

A path in the morphological table determines the kinds of diagnoses. A concrete, defined, generally unitary diagnoser transmits the necessary information for supporting the action of the diagnostically observed object. The other side of the diagnostic tandem – object-based knowledge – is the knowledge about the roller-runner conveyor.

When diagnosing the object, i.e. the MS conveyor system, its whole structure, components, their cooperation, etc. (elements, properties, systems relations) are diagnosed. The determination of the state for defining process capability is the purpose of diagnosing. In the conveyor of MS, that concerns construction elements (supports), drives and rollers-runners.

During diagnosing the MS transportation system-process (on conveyor), the course, algorithms, dynamics, total and partial results are diagnosed. The purpose consists generally in forecasting for controlling the developing process, in order to avoid undesirable states or to assure functioning within optimal limits.

What concerns conveyor diagnosing processes, the following considerations should be taken into account:

- transformation of the conveyor (structures, supports, drives, controllers, regulators, diagnoser, auxiliary equipment).
- transformation of information in controllers, regulators, diagnosers.

Diagnostic evaluation of the process or object can take place in different situations (before functioning, during functioning and after functioning), with possible combinations according to the phase of existence of the object and the time position of the diagnoser (phase reference point). Each situation requires separate diagnostic methods resulting from the diagnostic potential of the object.

The diagnostic potential is a sum of diagnostic information being consciously received by the diagnostician, and being possible to be acquired during the accepted existence of the object. The diagnostic potential determines the possibility of diagnosing the object trough all channels. This potential should be defined and estimated; then the possibility of use of that potential should be evaluated. After the evaluation, it should be adapted to information needs of the decider.

This potential is controllable because, beside information resulting from diagnostic signals of existence and functioning (process and accompanying signals), it is possible

also to acquire forced signals. The use of the potential is controllable by a regulation of the diagnosability. In the case of information resulting from signals of existence and functioning (process and accompanying signals), the potential can be subject to exhaustion [16] – the functioning potential of the object is subject to an irreversible exhaustion. In the case of information resulting from forced signals, the information diagnostic potential is not subject to exhaustion because it does not depends upon an irreversible exhaustion of the functioning potential of the object.

Diagnosability is a part of the diagnostic potential that is possible to be used in a determined situation (time, means, knowledge, media, etc.). Diagnosability is based on diagnostic potential. Diagnosability determines the possibility (for instance, by probability) of a positive end of the diagnosing process. Measures of diagnosability can be similar to measures of information capability or systems controllability.

Then – the diagnostic tandem is always necessary. The use thereof for a synthesis of the diagnostic equivalent must concern problems that are indicated in the morphology of diagnosis of conveyors.

The differential method is a typical example of a system-based application of the generalized method of state evaluation. This method, well known in medicine is transferred into other domains. The most advantageous feature of the method is the possibility of diagnosing without knowledge about the object of observation. Apparently, that is contradictory with regard to the idea of the diagnostic tandem, the lack of a concretized knowledge results, however, from the necessity to possess knowledge about the generalized object of diagnosis.

The use of the differential method reduces the Rd equivalent at least to half the value.

In a conveyors, special tools can be proposed to compare images, learning with an incorporation of dedicated media, as magnets, gravimeters, balances, measuring instruments, cameras, microphones. For roller-runners conveyors, conditions of application of the method exist, namely:

- the following kinds of assemblies and elements appear: similar, generally identical or identical from a multi-criterion point of view, among them from construction point of view – assemblies and elements being driven by the same power flux,
- there exists a potential of: creation of standards, their interchange and replacement, rejection, redundancy for uncertain situations, confirmation of inferring logics, overloads, changes of trends and their creation, degradation characteristics, failures and catastrophes.

Return to systems generalization from the differential method:

- for machines, by use of well-known observation techniques (identity of processes),
- for technical systems with similar space structure (linear widespread characteristics of object distribution), by application of methods of signal acquisition,
- for generalized systems with multiplied structure (train of structurally identical objects), by transfer of the differential algorithm.

6. Example

A conveyor is composed of (without determining the quantity of objects): a driving rollers – runners with drive, passive rollers – runners, coupling elements; stabilizing runners; limit stops; elastic supports and others (reducers, motors, controllers).

Recommendations that concern an application of the Rd equivalent result from the presented table. As the conveyor is composed of systems with heterogeneous history and thus with corresponding different degradation characteristics, it is necessary, in the preliminary phase of exploitation and up to acquaintance with and stabilization of dynamics of degradation, to select differentiated tools of diagnostic observation for following kinds of objects:

- well-known, new, unitary objects (e.g. motoreducers), well-known, degraded, unitary objects (e.g. reducers),
- well-known, new, multiple objects, being known on the basis of exploitation experience (e.g. supports with rollers–runners, of modern type), well-known, degraded, multiple objects (supports with runners, of traditional type),
- new, unitary objects, which the users learn to know (e.g. reducers),
- degraded, multiple objects, which the users learn to know (e.g. auxiliary motors),

Let us consider, as examples, two categories of objects:

- well-known, degraded, multiple objects (e.g. supports with runners, of traditional type) – in the situation being analysed:

200 supports, 240 runners with two rolling bearings in each support,

then $Rd = 200 \times 240 = 48\,000$,

for the supports, the equivalent $Rd = 48\,000$ (according to table 1, $Rd > 1000$ – displaceable testers), it determines the necessity of an intensive use of advanced displaceable diagnostic tools with possibilities of real time observing and diagnosing an important quantity of objects.

- new, unitary objects, which the users learn to know (e.g. new type reduction spur gears) – in the situation being analyzed:

10 three-stage reduction spur gears,

then $Rd = 10 \times 4 = 40$,

for the three-stage reduction spur gears the equivalent $Rd = 40$ (according to table 1, $10 < Rd < 100$ – unitary tools for an object, inspection elements), it determines the necessity of advanced unitary diagnostic tools with possibilities of real time observing and diagnosing few of objects.

The traditional approach indicates the necessity of a more precise observation of reducers, although the value of Rd is not high. It can appear that arguments concerning high costs of their purchase, renewal, etc., justify such reasoning. However, exploitation experience shows that there is a systems equivalence of simple bearings of reducers and of runners of supports. Their failure causes comparable exploitation costs – in the case of a degradation of a reducer bearing, that signifies a high cost of renewal of an unitary reducer; but in the case of a failure of

a support – that causes the costs of renewal (replacement, reconstruction) of a greater section of supports and, also, of other expensive assemblies, even the purchase of a new conveyor.

An intensive application of advanced diagnostic tools with possibilities of observing and real time diagnosing in the case of a great quantity of objects will permit to create knowledge about degradation of support elements. An analogical reasoning indicates a necessity of précising diagnosing methods in the case of reducers, in the aspect of diagnostic tools being technically coherent with testers of supports, for creating knowledge about characteristics of degradation of reducers.

It is possible to propose displaceable testers in the form of thermovision cameras, as well as WBA methods for a diagnostic localization of failures of bearings or for the evaluation of degradation; the same tools can be used for diagnosing reducers. Suggestions concerning a technical concretization of diagnostic activity through morphological methods can be found in works [13–15].

In the phase of exploitation, after a stabilization of the dynamic characteristic of degradation, and after the acquaintance thereof, a trial of unification and simplification of diagnosing methods for all objects of a conveyor can be undertaken (of both above discussed, and the other objects being neglected here); however, the necessity of their differentiation is to be taken into account.

7. Summary

A method of selection of a dedicated diagnoser for a MS conveyor in a technical situation was the basic purpose of this scientific work. A trial is made of the use, for diagnosing widespread MS, of standard diagnosing methods being applied in typical machines. The transfer of habits onto widespread systems leads to a reduction of the efficiency of the diagnosing process. In the case of widespread characteristics of the machine being diagnosed, a facilitating factor is the diagnostic equivalent Rd, considered to be a standard object of observation and to be indivisible from diagnostic point of view (e.g. a shaft with a toothed wheel, the shaft being equipped with bearings). When the frequency of diagnoses for that standard has been determined then, for a greater quantity of objects of diagnosis, the equivalent permits to determine the necessary quantity and the quality of simultaneously acting diagnosers. Methods of synthesis of diagnostic equivalents of diagnosers for widespread manufacturing system conveyor have been proposed.

The whole of considerations in this work has been realized according to systems principles of following type: generalization – concretization, concrete – generalization on example. The following notions have been proposed: diagnostic potential (it is the sum of diagnostic information of which the diagnostician is aware, information that is possible to be acquired during the accepted existence of the object, and that determines the possibility of diagnosing the object through all channels), and diagnosability (part of the diagnostic potential that is possible to be used in a determined situation,

that appears on the basis of the diagnostic potential and that determines the possibility of a positive termination of the diagnosing process in the case of a multi-criterion evaluation) – based upon systems definitions of knowledge and skills.

The definition of the diagnostic tandem has been introduced – as an evolving in time pair: object-oriented knowledge – diagnostic knowledge; this pair determines the indispensability of action-based coexistence of categories of knowledge of the diagnoser. The whole has been illustrated by an application example in rollers – runners' conveyor.

References

[1] Młyńczak M.: *Structures of a technical object – basis of its exploitation evaluation*, Systems, Vol. 6, No. 1–2, 2001, pp. 170–176.
[2] Nowakowski T.: *Problems of safety & reliability analysis of transportation system*, Systems, Vol. 6, No. 1–2, 2001, pp. 158–169.
[3] Radkowski S.: *WBA diagnostyka uszkodzeń niskoenergetycznych* (Vibroacoustical diagnosis of the low-energy failures), WiZP ITE, Warsaw–Radom, 2002.
[4] Ho D., Randall R.B.: *Optimization of bearing diagnostic techniques using simulated and actual bearing fault signals*, Mechanical Systems and Signal Processing, Vol. 14, No. 5, 2000, pp. 763–788.
[5] Lee G.J. A.: *Scalable architecture for network fault diagnosis in the knowledge plane*, MIT Computer Science and AI Laboratory, 32 Vassar Street, Cambridge MA, 2006.
[6] Zhou W.: Stator current-based bearing fault detection techniques: A general review, Proceedings of IEEE, SDEMPED 2007, IEEE, Poland, 2007, pp. 7–10.
[7] Żółtowski, B.: *Technical diagnostics of folded objects. Directions of development*, Diagnostyka, No. 3, Vol. 47, 2008, pp. 101–110.
[8] Collacott R. A.: *Mechanical fault diagnosis and condition monitoring*, Chapman and Hall, 1987.
[9] Collacott R.A.: *Structural integrity monitoring*, Chapman & Hall, London, 1985.
[10] Przystupa F.W.: *Diagnosing – fundamental questions*, Systems, Vol. 13, No. 1–2, 2008, pp. 74–85.
[11] Przystupa F.W.: *Diagnostic equivalent for widespread working machinery*, Systems, Vol. 8, No. 2, 2003, pp. 115–131.
[12] Przystupa F.W.: *Diagnostics of "UUUU..." type situations in systems*, Systems, Vol. 12, No. 3, pp. 36–48.
[13] Przystupa F.W.: *Diagnostics of a wide area object; case of a system of belt conveyors*, Systems, Vol. 6, No. 1–2, 2001, pp. 135–157.
[14] Przystupa F.W.: *Monitoring of inform. disturbances in logistic systems*, Systems, Vol. 10, No. 2, 2005, pp. 32–43.
[15] Przystupa F.W.: *Proces diagnozowania w ewoluującym systemie technicznym* (Diagnosis process in the evolving technical system), Oficyna Wydawnicza Politechniki Wrocławskiej, Monografie W10/29, Wrocław, 1999.
[16] Przystupa F.W.: *Variability of structures of diagnosis objects*, Systems, Vol. 3, No. 2, 1998, pp. 35–48.

Ekwiwalent diagnostyczny rozległego systemu produkcyjnego

W przypadku rozległego systemu produkcyjnego, niezbędne jest wykorzystanie współczynnika Rd – ekwiwalentu diagnostycznego, określającego konieczność wykorzystania większej ilości systemów diagnostycznych. Gdy określi się częstotliwość obserwacji jednostkowego zespołu w systemie, określenie jakości i ilości niezbędnych diagnozerów staje się proste. Wprowadzono definicje kilku istotnych czynników procesu diagnozowania – potencjału diagnostycznego, tandemu diagnostycznego, itp. Całość zilustrowano przykładem diagnozowania przenośnika w systemie produkcji.

ARCHIVES OF CIVIL AND MECHANICAL ENGINEERING

Vol. X 2010 No. 3

Multiple criteria analysis of foundation instalment alternatives by applying Additive Ratio Assessment (ARAS) method

E.K. ZAVADSKAS, Z. TURSKIS, T. VILUTIENE
Vilnius Gediminas Technical University, Sauletekio al. 11, LT-10223 Vilnius, Lithuania.

The paper presents the process of selection the foundation instalment alternative, which have to be the most appropriate and safe for building which stands on the aquiferous soil. The selection is based on a set of criteria: costs of instalment, instalment duration, the complexity of decisions, advantages and disadvantages of decisions, transferability and maintainability of installed foundation system, past experience implementing the approved decisions, etc. The criteria for evaluation and their importance are selected by taking into consideration the interests and goals of the client as well as factors that influence the efficiency of construction process and safety of future building. The solution of problem was made by applying Additive Ratio ASsessment (ARAS) method. The proposed technique could further be applied to substantiate the selection of effective alternative of structures, technologies, investments and etc.

Keywords: *foundation, selection, evaluation, decision making, alternative, weights, operation research, multiple criteria, MCDM, Additive Ratio ASsessment, ARAS*

1. Introduction

Technological progress and innovation in civil engineering, management, and conditions of life level yields an enormous influence over economic activity, employment and growth rates. There is an increasing complexity and interplay between all issues associated with property management decisions [1].

Existing buildings are a “mine” of raw materials for new buildings [2]. However, refurbishment projects generate enormous risks of works, are complicated processes, and are a set of processes in which is dominated uncertainty and heuristics. There is hardly to obtain accurate and exact information. Furthermore, refurbishment project is intrinsically unique and subject to its environment. In this way refurbishment differs from new buildings projects.

The Roman philosopher Seneca said “Nothing is certain except the past”. It is necessary to learn about criteria determining both development and downfall of feasible alternatives [3]. In a mono-criterion approach, the analyst builds a unique criterion capturing all the relevant aspects of the problem. Such a one-dimensional approach is an oversimplification of the actual nature of the problem. All new ideas and possible variants of decisions in real world must be compared according to a set of multiple

conflicting criteria [4]. MCDM is one of the most widely used decision methodologies in the sciences, business, and government worlds, which are based on the assumption of a complex world, and can help to improve the quality of decisions by making the decision making process more explicit, rational, and efficient.

In practical construction projects are complex systems are usually quite difficult to be designed, because large amount of multidisciplinary knowledge and needs multidisciplinary operations research techniques. Operations research is based on four main assumptions:

- the problem situations exist as realities and not depend on decision maker and aims of problem solution [5];
- the analysis o problem is objective (not related with different viewpoints of stakeholders, contractors, final user and impact on environment) and described only by quantitative data [6–7];
- all participants of decision making seeks optimal solution [6];
- the solutions are clearly optimal and can be implemented without complications [8].

The multiple criteria decision making is a model that allows the analysis of several preference criteria simultaneously. As the economic, environmental, social and technological actors must be considered further development needs to be given attention to sustainability [9–11]. Life cycle assessment approach seeks to determine and measure impact of all actors, applied materials, constructions, technologies, and maintenance "from cradle to grave". However, prices do not incorporate all information about materials and products. There is some agreement that criteria describing feasible alternatives are dimensions, which are important in determining preferences. Their studies aim at choosing appropriate solution between possible actions, strategies and feasible alternatives.

The construction process is influenced by many factors [12]. The analysis of structures with different parameters plays an important role in structural design and optimization modelling [13]. The relation between architects and human being and the role of places in creation of human architecture are needed to find the proper solution. Problems can only be solved if people have some basis for comparison [14]. This applies to all the stages and parameters (e.g. development, infrastructure, execution time, the resources required, etc.) of the investment construction project being implemented. Collaboration of the project's participants is the main condition ensuring the effective management of a construction project [15].

MCDM researches in civil engineering and management is dominated in the Lithuanian-German-Polish triangle (Vilnius Gediminas Technical University, Poznan University of Technology, and Leipzig University of Applied Science) [16–18]. There are lot of even sophisticated issues in collaboration with specialists representing other domains of science (e.g. mathematicians) [19]. Techniques and planning methods and decision making methods develop dynamically [3, 20–34].

2. Multiple criteria methods for problem solution

The problem of decision-maker consists of evaluating a finite set of alternatives in order to find the best one, to rank them from the best to the worst, to group them into predefined homogeneous classes, or to describe how well each alternative meets all the criteria simultaneously.

Classical methods of multiple criteria optimization and determination of priority and utility function were first applied by Pareto in 1896 [35]. Methods of multiple criteria analysis were developed to meet the increasing requirements of human society and the environment. Keeney and Raiffa [36] offered the representation theorems for determining multiple criteria utility functions under preferential and utility independence assumptions. Seo [37] suggested a multiple criteria decision making method that was concerned with balancing some conflicting objectives in a hierarchical structure. Saaty [38] showed the global importance of solving problems with conflicting goals by using multiple criteria models and presented decision making models with incomplete information.

Meuthe and Scanella [39] pointed that there are many different methods of multiple criteria analysis which can be recommended depending upon the circumstances of decision making. In an MCDM approach, first it is necessary to define the problem clearly, and then identify realistic alternatives. It is important to define the actors involved in the decision making, select the evaluation criteria, and evaluate each alternative according to the set of criteria. Next, an MCDM method is selected to aggregate the performance of each alternative. The need of comparing MCDM methods and the importance of the selection problem were first recognized by MacCrimmon [40] who suggested taxonomy of MCDM methods. There are many comparative studies presented in scientific research works. Guitoni and Martel [41] proposed a methodological approach to select an appropriate MCDM method to a specific decision-making situation. Computations of different examples reveal the fact that evaluation outcome depends on both choice of utility function and its parameters [42].

There are many ways to classify MCDM methods. The classification of MCDM methods according to the type of information based on the Larichev's [43] proposal is given bellow:

- methods based on quantitative measurements. The methods based on multiple criteria utility theory may be referred to this group (TOPSIS – Technique for Order Preference by Similarity to Ideal Solution [44], SAW – Simple Additive Weighting [40], LINMAP – Linear Programming Techniques for Multidimensional Analysis of Preference [45], COPRAS – Complex Proportional ASsessment [46–47], its modification COPRAS-G (Complex Proportional ASsessment method with Grey interval numbers) [48–50], and ARAS (Additive Ratio Assessment) method [27].
- methods based on qualitative initial measurements. These include two widely known groups of methods, i.e. Analytic Hierarchy Methods (AHP) [38] and fuzzy set theory methods [51].

• comparative preference methods based on pair-wise comparison of alternatives. This group comprises the modifications of the ELECTRE [52], PROMETHEE [53], UTA [54], MUSA [55], AKUTA [56], TACTIC [57], ORESTE [58] and other methods.

• methods based on qualitative measurements not converted to quantitative variables. This group includes methods of verbal decision-making analysis [59, 43] and uses qualitative data for decision environments involving high levels of uncertainty.

An alternative in multiple criteria evaluation is usually described by quantitative and qualitative criteria [60]. The criteria have different units of measurement. Normalization aims at obtaining comparable scales of the criteria values. Different techniques of criteria value normalization are used. The impact of the decision-matrix normalization methods on the decision results has been investigated by many authors [61–68].

3. A new Additive Ratio Assessment (ARAS) method in multiple criteria decision-making [27]

Sustainable development and environment can be influenced by major accidents [69–70]. Many constructional processes are carried out by machines working together and forming technological systems. For process design purposes most important are the effectiveness ratios relating to the profits and losses stemming from system use [71]. In order to rank alternatives and select the best alternative a new ARAS method will be used. The typical MCDM problem is concerned with the task of ranking a finite number of decision alternatives, each of which is explicitly described in terms of different decision criteria which have to be taken into account simultaneously [72–73]. According to the ARAS method, a utility function value determining the complex relative efficiency of a feasible alternative is directly proportional to the relative effect of values and weights of the main criteria considered in a project.

The first stage is decision-making matrix (DMM) forming. In the MCDM of the discrete optimization problem any problem to be solved is represented by the following DMM of preferences for m feasible alternatives (rows) rated on n signfull criteria (columns):

$$X = \begin{bmatrix} x_{01} & \cdots & x_{0j} & \cdots & x_{0n} \\ \vdots & \ddots & \vdots & \ddots & \vdots \\ x_{i1} & \cdots & x_{ij} & \cdots & x_{in} \\ \vdots & \ddots & \vdots & \ddots & \vdots \\ x_{m1} & \cdots & x_{mj} & \cdots & x_{mn} \end{bmatrix}; \qquad i = \overline{0,\, m}; \qquad j = \overline{1,\, n}, \tag{1}$$

where:

m – number of alternatives,

n – number of criteria describing each alternative,

x_{ij} – value representing the performance value of the i alternative in terms of the j criterion,

x_{0j} – optimal value of j criterion.

If optimal value of j criterion is unknown, then

$$x_{0j} = \max_i x_{ij}, \text{ if } \max_i x_{ij} \text{ is preferable and } x_{0j} = \min_i x_{ij}^*, \text{ if } \min_i x_{ij}^* \text{ is preferable.} \quad (2)$$

Usually, the performance values x_{ij} and the criteria weights w_j are viewed as the entries of a DMM. The system of criteria as well as the values and initial weights of criteria are determined by experts. The information can be corrected by the interested parties by taking into account their goals and opportunities.

Then the determination of the priorities of alternatives is carried out in several stages.

Usually, the criteria have different dimensions. The purpose of the next stage is to receive dimensionless weighted values from the comparative criteria. In order to avoid the difficulties caused by different dimensions of the criteria, the ratio to the optimal value is used. There are various theories describing the ratio to the optimal value. However, the values are mapped either on the interval [0; 1] or the interval $[0; \infty]$ by applying the normalization of a DMM.

In the second stage the initial values of all the criteria are normalized – defining values $\bar{x}_{ij}$ of normalised decision-making matrix $\bar{X}$:

$$\bar{X} = \begin{bmatrix} \bar{x}_{01} & \cdots & \bar{x}_{0j} & \cdots & \bar{x}_{0n} \\ \vdots & \ddots & \vdots & \ddots & \vdots \\ \bar{x}_{i1} & \cdots & \bar{x}_{ij} & \cdots & \bar{x}_{in} \\ \vdots & \ddots & \vdots & \ddots & \vdots \\ \bar{x}_{m1} & \cdots & \bar{x}_{mj} & \cdots & \bar{x}_{mn} \end{bmatrix}; \quad i = \overline{0,\ m}; \quad j = \overline{1,\ n}. \quad (3)$$

The criteria, whose preferable values are maxima, are normalized as follows:

$$\bar{x}_{ij} = \frac{x_{ij}}{\sum_{i=0}^{m} x_{ij}}. \quad (4)$$

The criteria, whose preferable values are minima, are normalized by applying two-stage procedure:

$$x_{ij} = \frac{1}{x_{ij}^*};$$

$$\overline{x}_{ij} = \frac{x_{ij}}{\sum_{i=0}^{m} x_{ij}}. \tag{5}$$

When the dimensionless values of the criteria are known, all the criteria, originally having different dimensions, can be compared.

The third stage is defining normalized-weighted matrix – $\hat{X}$. It is possible to evaluate the criteria with weights $0 < w_j < 1$. Only well-founded weights should be used because weights are always subjective and influence the solution. The values of weight w_j are usually determined by the expert evaluation method. The sum of weights w_j would be limited as follows:

$$\sum_{j=1}^{n} w_j = 1 . \tag{6}$$

$$\hat{X} = \begin{bmatrix} \hat{x}_{01} & \cdots & \hat{x}_{0j} & \cdots & \hat{x}_{0n} \\ \vdots & \ddots & \vdots & \ddots & \vdots \\ \hat{x}_{i1} & \cdots & \hat{x}_{ij} & \cdots & \hat{x}_{in} \\ \vdots & \ddots & \vdots & \ddots & \vdots \\ \hat{x}_{m1} & \cdots & \hat{x}_{mj} & \cdots & \hat{x}_{mn} \end{bmatrix}; \qquad i = \overline{0,\ m}; \qquad j = \overline{1,\ n} . \tag{7}$$

Normalized-weighted values of all the criteria are calculated as follows:

$$\hat{x}_{ij} = \overline{x}_{ij} w_j ; \qquad i = \overline{0,\ m} , \tag{8}$$

where:

w_j – the weight (importance) of the j criterion,

$\overline{x}_{ij}$ – the normalized rating of the j criterion.

The following task is determining values of optimality function:

$$S_i = \sum_{j=1}^{n} \hat{x}_{ij} ; \qquad i = \overline{0,\ m} , \tag{9}$$

where S_i is the value of optimality function of i alternative.

The biggest value is the best, and the least one is the worst. Taking into account the calculation process, the optimality function S_i has a direct and proportional relationship with the values x_{ij} and weights w_j of the investigated criteria and their relative

influence on the final result. Therefore, the greater the value of the optimality function S_i, the more effective the alternative. The priorities of alternatives can be determined according to the value S_i. Consequently, it is convenient to evaluate and rank decision alternatives when this method is used.

The degree of the alternative utility is determined by a comparison of the variant, which is analysed, with the ideally best one S_0. The equation used for the calculation of the utility degree K_i of an alternative a_i is given below:

$$K_i = \frac{S_i}{S_0}, \qquad i = \overline{0, m},$$

where S_i and S_0 are the optimality criterion values, obtained from Equation (9).

It is clear, that the calculated values K_i are in the interval [0, 1] and can be ordered in an increasing sequence, which is the wanted order of precedence. The complex relative efficiency of the feasible alternative can be determined according to the utility function values.

4. Case study

Case study presents the process of selection the foundation alternative in redeveloping building, which have to be the most appropriate and safe for building which stands on the aquiferous soil (Figure 1). The aim of problem is to design and install the foundation and cellar floor structures in the way that will be ensured the reliable barrier for moisture infiltration in cellar. Some aspects of these problems are presented in this study. Here was made the assumption that proposed alternatives are thoroughly investigated, estimated and could be really implemented. The aim of this study is to show how decision-maker can find the most reasonable alternative having the set of certain data.

In real life, a decision-maker first of all must to understand and describe the situation. This stage includes the determination and the assessment of the stakeholders, the different alternatives of feasible actions, the large number of different and important decision criteria, the type and the quality of the information, etc. It appears to be the key point defining MCDM as a formal approach.

The results of the site investigation are presented in a detailed report, which provides a step-by-step account of the processes undertaken.

The building, which is analysing in this case study, stands on the aquiferous soil. The area of cellar is 1500 m^2. The results of hydro geological analysis had shown that the lowest altitude of soil moisture is 91.20 m in the middle of the building; highest is 91.95 m in the courtyard of the building. The altitude of floor level of building downstairs is 90.82 m. It means that the soil moisture will cover the cellar walls from the height of 0.38 m till the height of 1.13 m. Consequently, the level of soil water above the top of cellar floor will be 0.38–1.13 m and above the level of mining founda

tion pit will be 1.33–1.63 m. Therefore, the foreseen highest level of soil moisture is 3.13 m above the mining level (and 2.63 m above the floor level). Besides, building cellar will have two different levels – one of them is 0.30 m below. Determined water flow yield is 10–40 m^3 per hour. Direction of water flow is from south to north.

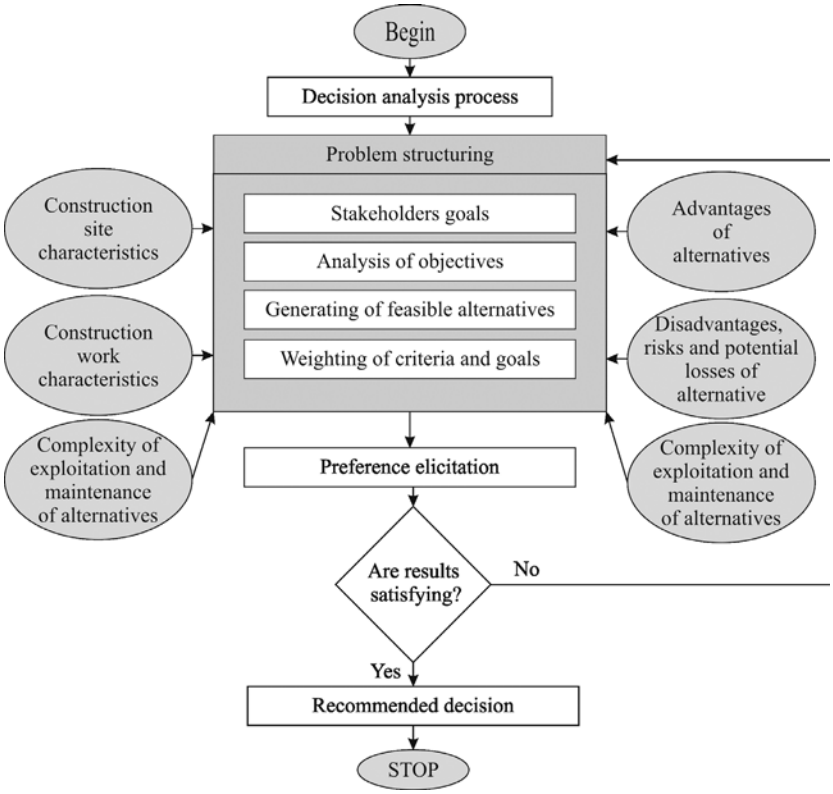

Fig. 1. Structure of the decision support system, based on the ARAS method and SWOT analysis

Experts stated the opinion that the double levelled floor structure of cellar will be the most expedient and will have a less risk during exploitation. Experts also stated that due to the complicated conditions in the beginning of the works, technical decisions have to be as simple as possible and unlade by complex details. Experts suggested the following means:

- Excavation should be environed by protective wall in order to make the side fence for water flow.
- During construction it was recommended to reduce the level of soil water by installing the additional drainage.
- In existing internal walls beneath the level of finished floor the moisture fences have to be installed.

- The double cellar floor plates with drainage layer were suggested to install.
- The junctions of the different zones of double cellar floor plates have to be moisture protected.
- Recommended to install the drainage well for collection of water, which flows from drainage layer of floor structure.
- Recommended thickness of double floor plate is about 300 mm, plate have to be strengthened enough in order to ensure the minimising of cracking and resistance to water pressure.

Taking into account the aforementioned suggestions and references of experts and the aim to install the safest variant of foundation and cellar floor structure, the three following alternatives were considered:

A_1) Floor structure of cellar is installing with internal drainage system for moisture collection from internal floor layers. This drainage system is intended to be constant. Isolation of capillary moisture ensured by installed protection wall (rabbet) around the building. The additional drainage system, which works only during construction, is not installing. External walls are not strengthening and foundation anchors are not installing.

A_2) Moisture protection of cellar structures ensuring by installing additional floor plate aggregated it in double floor construction. The additional floor plate was intended be anchored. Foundation and internal floor structure installing with internal drainage system for accidental moisture collection. Cellar external walls are strengthening to ensure the protection from water pressure in case of flooding. Isolation of capillary moisture ensured by installed protection wall (rabbet) around the building. The additional floor layers and better moisture isolation are installing. The additional drainage system, which works only during construction, is installing.

A_3) Foundation and cellar are installing without internal drainage system. Drainage system works only during construction. Ensuring moisture resistance of cellar structures by installed of additional ribbed reinforced TT cross-section panels. Foundation anchors are not installing. Flooring additional layers and better moisture isolation are installing. Therefore the deepening of foundation is necessary. To ensure the better resistance of installed structures to pressure of soil moisture the cellar external wall are strengthening. Ensuring isolation of capillary moisture by installed protection wall (rabbet).

The brief description of foundation and cellar floor structures instalment is shown in Table 1.

The advantages and disadvantages of alternatives are presented in Tables 2 and 3.

The courses of action are called alternatives in the model, and they are represented by consequence sets in the decision problem. The description of possible consequences of implementation of alternatives (disadvantages, risks and potential losses) is presented in Table 4.

When all characteristics of alternatives were analysed, the set of criteria for evaluation was formed.

The criteria are described below:

- Cost of instalment – criterion covers all costs which appear during installation of each foundation alternative: costs of internal foundation instalment, costs of strengthening of external walls, costs of elevator shaft and pool shell instalment, costs of isolation of capillary moisture and soil moisture, costs of foundation anchors instalment, costs of instalment of constant drainage system, costs of instalment of additional structures and layers, costs of deepening structures, unexpected costs.
- Instalment duration – criterion shows the duration of foundation installation work and is measuring in month.
- Index of advantages – generalized criterion, which meanings were calculated by adding the comparative weights of advantages described in Table 2.
- Index of loses (risk) – generalized criterion, which meanings were calculated by adding the comparative weights of disadvantages described in Table 4.
- Complexity of maintenance – generalized criterion, which meanings were calculated by adding the comparative weights of additional means needed for proper usage and maintenance of foundation, cellar spaces and equipment inside.
- Transferability of decisions – criterion shows the level on which the means minimizing the risk of alternative decisions could be applied to each alternative. Its meanings were calculated by adding the comparative weights of different transferable decisions.

Table 1. Characteristics of foundation instalment alternatives

No.	Foundation instalment works	Foundation instalment alternatives		
		A_1	A_2	A_3
1	Instalment of additional substructures	+	+	+
2	Strengthening of external walls	+	+	+
3	Instalment of elevator shaft and pool shell	+	+	+
4	Isolation of capillary moisture by installed protection wall (rabbet)	+	+	+
5	Foundation anchors instalment	–	+	–
6	Instalment of constant drainage system for accidental moisture collection	+	+	–
7	Instalment of drainage system which works only during construction	–	+	+
8	Instalment of soil moisture isolation system	+	+	+
9	Strengthening of external walls by concreting by perimeter	–	+	+
10	Instalment of additional ribbed reinforced TT cross section panel	–	–	+
11	Flooring additional layers	–	+	+
12	Foundation deepening	–	+	+
13	Unexpected costs concerning complexity of decisions	–	+	+
Remark: here and in following tables 2–4 "+" means work, which is included in the alternative, and "–" means work, which is not included.				

Table 2. The advantages of alternatives

No.	Advantages	Foundation instalment alternatives		
		A_1	A_2	A_3
1	Practically implemented and examined	+	–	–
2	Shortest duration of instalment	+	–	–
3	Minimal instalment costs	+	–	–
4	Not complicated instalment	+	–	–
5	The exploitation of cellar not depend on run of drainage system	–	+	+
6	Better protection from soil moisture	–	+	–
7	Better resistance of installed structures to pressure of soil moisture	–	+	–

Table 3. Complexity of exploitation and maintenance of foundation alternatives

No.	Additional necessary means enlarging the expensiveness of exploitation	Foundation instalment alternatives		
		A_1	A_2	A_3
1	The additional source of energy is necessary	+	–	–
2	The additional drainage pomp is necessary	+	–	–
3	The additional space (rooms) is necessary	+	–	–
4	The additional facility is necessary	+	–	–
5	Building insurance is necessary	+	+	+

Table 4. Consequences of alternatives (disadvantages, risks and potential losses)

No.	Consequences	Notation	Foundation instalment alternatives		
			A_1	A_2	A_3
1	Forced drainage could break if energy source is missing	C_{11}	+	–	–
2	The failure of drainage pomp could appear	C_{12}	+	–	–
3	The failure of drainage channel between building and well could appear	C_{13}	+	–	–
4	Drainage water well overflows and disallow inflowing water	C_{14}	+	–	–
5	The river overflows, territory floods, water gets in building over the upper level of soil	$C_{15}(C_{21}, C_{31})$	+	+	+
6	Foundation and cellar could be installed improperly or even not installed	$C_{16}(C_{22}, C_{32})$	+	+	+
7	41–62 m2 of space will be lost if external walls protected from moisture be installed	$C_{23}(C_{33})$	–	+	+
8	The bottom layer of cellar floor will be installing 0.5 m below	$C_{24}(C_{34})$	–	+	+
9	Longer instalment duration	$C_{25}(C_{35})$	–	+	+
10	The additional drainage eliminating the water between panels is necessary	$C_{26}(C_{36})$	–	+	+
11	Foundation, floor and cellar instalment is complex and therefore the error occurrence probability is high	$C_{27}(C_{37})$	–	+	+
12	Decisions unforeseen all means for protection of structures from soil moisture and water	C_{17}	+	–	–

Criteria, their level of optimality (the maximum or minimum value is preferable), criteria measuring units and their weights w_j are presented in Table 5. The criteria significance indexes q_j are converted to the criteria weights w_j as follows:

$$w_j = \frac{q_j}{\sum_{j=1}^{n} q_j}; \qquad j = \overline{1, n}, \tag{11}$$

where $n = 6$ is criteria number.

Table 5. Set of criteria for evaluation

Set of criteria		Optimal	Units of measure	q	w
1. Cost of instalment	x_1	minimum	10^6 €	7.18	0.171
2. Instalment duration	x_2	minimum	month	7.77	0.185
3. Index of advantages	x_3	maximum	–	7.43	0.177
4. Index of loses (risk)	x_4	minimum	–	9.45	0.225
5. Complexity of maintenance	x_5	minimum	–	6.59	0.157
6. Transferability of decisions	x_6	maximum	–	3.57	0.085

After the calculating the values of criteria the initial decision making matrix was formed (Table 6). The values of criteria – index of advantages, index of loses, complexity of maintenance, transferability of decisions were determined using expert method.

Table 6. Initial decision-making matrix X*

Alternative	Criteria					
	x_1^*	x_2^*	x_3	x_4^*	x_5^*	x_6
Optimisation direction	min	min	max	min	min	max
Weights of criteria – w	0.171	0.185	0.177	0.225	0.157	0.085
A_o – Optimal value	0.71	4.1	1	0.31	0.42	1
A_1	0.71	4.1	0.18	0.72	0.99	0.25
A_2	1.33	5.9	0.74	0.31	0.42	0.83
A_3	1.45	4.9	0.27	0.65	0.42	0.44

5. The results of multiple criteria analysis

The criteria, whose preferable values are minima, are changed (formula (5), Table 7). The initial values of criteria were recalculated by applying normalization (formulae (4) and (5)). That way the discrepancy between the different dimensions of the optimal values was eliminated. Normalized decision-making matrix (Table 8) was processed applying the ARAS method (formulae (5)–(10)).

The calculation results are also presented in Table 9. The most reasonable alternative according to calculation results is second (A_2). The priority order of the investigated foundation instalment alternatives can be represented as (Figure 1):

$$A_2 \succ A_3 \succ A_1 \tag{12}$$

Table 7. Initial decision-making matrix X with values, which must be minimised, changed to maximised values

Alternative	Criteria					
	x_1	x_2	x_3	x_4	x_5	x_6
Weights of criteria – w	0.171	0.185	0.177	0.225	0.157	0.085
A_o	1.408	0.244	1.000	3.226	2.381	1.000
A_1	1.408	0.244	0.180	1.389	1.010	0.250
A_2	0.752	0.169	0.740	3.226	2.381	0.830
A_3	0.690	0.204	0.270	1.538	2.381	0.440
$\sum$	4.258	0.861	2.190	9.379	8.153	2.520

Table 8. **N**ormalised decision-making matrix $\overline{X}$

	$\overline{x}_1$	$\overline{x}_2$	$\overline{x}_3$	$\overline{x}_4$	$\overline{x}_5$	$\overline{x}_6$
w	0.171	0.185	0.177	0.225	0.157	0.085
A_o	0.331	0.283	0.457	0.344	0.292	0.397
A_1	0.331	0.283	0.082	0.148	0.124	0.099
A_2	0.177	0.197	0.338	0.344	0.292	0.329
A_3	0.162	0.237	0.123	0.164	0.292	0.175

Table 9. Weighted-normalised criteria values of foundation instalment alternatives (Weighted-normalised decision-making matrix $\hat{X}$) and solution results

	$\hat{x}_1$	$\hat{x}_2$	$\hat{x}_3$	$\hat{x}_4$	$\hat{x}_5$	$\hat{x}_6$	S	K	Rank
A_o	0.057	0.052	0.081	0.077	0.046	0.034	0.057	1.000	
A_1	0.057	0.052	0.015	0.033	0.019	0.008	0.057	0.533	3
A_2	0.030	0.036	0.060	0.077	0.046	0.028	0.030	0.801	1
A_3	0.028	0.044	0.022	0.037	0.046	0.015	0.028	0.551	2

It means that the best alternative is second, and the worst alternative is the first. It can be stated that the alternative 2 is only 80 percent of optimal alternative performance level, and the performance of the worst alternative 1 is only 53 percent.

Although the second alternative has fewer advantages than other alternatives (Table 2), the same number of disadvantages, potential losses and risks as them has other alternatives (Table 4), longer duration of instalment and not the minimum cost of instalment (Table 6), the implementation of this alternative will ensure the less exploitation complexity and minimise the possible risks.

The reason of such results is the difference of importance of possible consequences (Table 4) and the number of means and solutions (Table 1 and 2) intended to implement for minimising the negative consequences. The influence of importance of possible conse-

quences and the additional incorporated solutions was evaluated during the calculation of the values of alternatives. Hereby, the additional incorporated solutions make this variant of foundation more reliable than others and influence the results of calculation.

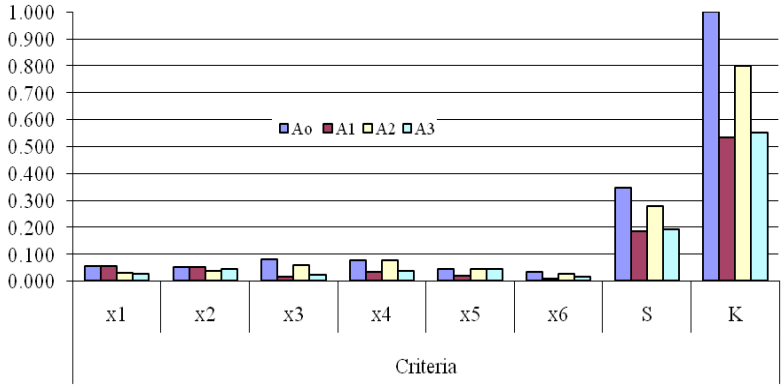

Fig. 2. Comparison of foundation instalment alternatives performance level

According to the given data on the criteria describing the foundation instalment alternatives, rational solutions about its construction improvement and maintenance cost reduction can be made. The studies performed help to identify effective parameters of foundation instalment alternatives, which do not meet stakeholders' goals and specifications. The data obtained can also be used for developing and implementing measures aimed at construction process.

6. Conclusions

Traditional optimization, statistical and econometric analysis approaches used within the engineering context are often based on the assumption that the considered problem is well formulated and decision-makers usually consider the existence of a single objective, evaluation criterion or point of view that underlies the conducted analysis. In such a case the solution of engineering problems is easy to obtain.

But in reality, the modelling of engineering problems is based on a different kind of logic taking into consideration the existence of multiple criteria, the conflicting aims of decision maker, the complex, subjective and different nature of the evaluation process, and the participation of several decision makers. Recently operation researchers have started to embrace the complexity of decision making process and foresee the innovative perspective, which overcomes the restrictive nature of optimization.

Therefore, MCDM contributes in engineering context through the identification of the best alternatives according to the problematic chosen, the satisfactory solution of the conflicts between the criteria, the determination of the relative importance of the criteria in the decision making process, and the revealing of the preferences and system of values.

Overall, the main advantages that the MCDM provides in decision making, could be summarized in the following aspects: the possibility to analyze complex problems; the possibility to aggregate both quantitative and qualitative criteria in the evaluation process; the possibility of good evidence of decisions; the possibility for decision-maker to participate actively in the decision-making process; and the application of flexible scientific methods in the decision making process.

According to the newly proposed ARAS method, the utility function value determining the complex efficiency of a feasible alternative is directly proportional to the relative effect of values and weights of the main criteria considered in a project.

The priorities of alternatives can be determined according to the utility function value. Consequently, it is convenient to evaluate and rank decision alternatives when this method is used.

The degree of the alternative utility is determined by a comparison of the variant, which is analysed, with the ideally best one.

It can be stated that the ratio with an optimal alternative may be used in cases when it is seeking to rank alternatives and find ways of improving alternative projects.

In conclusion, ARAS method has a promising future in the construction engineering field, because he offers a highly methodological basis for decision support. Nevertheless, his success in practice depends heavily on the development of computerized multiple criteria decision support systems.

References

[1] Langston C., Wong F.K.W., Hui E.C.M., Shen L.-Y.: *Strategic assessment of building adaptive reuse opportunities in Hong Kong*, Building and Environment, Vol. 43, No. 10, 2008, pp. 1709–1718.

[2] Chusid M.: *Once is never enough*, Building Renovation, Mar.–Apr., 1993, pp. 17–20.

[3] Kapliński O.: *Usefulness and credibility of scoring methods in construction industry*, Journal of Civil Engineering and Management, Vol. 14, No. 1, 2008, pp. 21–28.

[4] Turskis Z., Zavadskas E.K., Peldschus F.: *Multi-criteria optimization system for decision making in construction design and management*, Inzinerine Ekonomika – Engineering Economics, No. 1, 2009, pp. 7–17.

[5] Roy B.: *Decision science or decision-aid science*, European Journal of Operational Research, Vol. 66, No. 2, 1993, pp. 184–203.

[6] Ackoff R.: *The future of operational research is past*, Journal of Operational Research Society, Vol. 30, No. 2, 1979, pp. 93–104.

[7] Brauers W.K., Zavadskas E.K.: *Robustness of the multi-objective MOORA method with a test for the facilities sector*, Technological and Economic Development of Economy, Vol. 15, No. 2, 2009, pp. 352–375.

[8] Eden C., Sims D.: *On the nature of problems in consulting practice*, OMEGA: The International Journal of Management Science, Vol. 7, No. 2, 1979, pp. 119–127.

[9] Lombera J.-T. S.-J., Rojo J.C.: *Industrial building design stage based on a system approach to their environmental sustainability*, Construction and Building Materials, Vol. 24, No. 4, 2010, pp. 438–447.

[10] Lombera J.-T. S.-J., Aprea I.G.: *A system approach to the environmental analysis of industrial buildings*, Building and Environment, Vol. 45, No. 3, 2009, pp. 673–683.
[11] Juan Y.-K., Gao P., Wang J.: *A hybrid decision support system for sustainable office building renovation and energy performance improvement*, Energy and Buildings, Vol. 42, No. 3, 2010, pp. 290–297.
[12] Popov V., Juocevicius V., Migilinskas D., Ustinovichius L., Mikalauskas S.: *The use of a virtual building design and construction model for developing an effective project concept in 5D environment*, Automation in Construction, Vol. 19, No. 3, 2010, pp. 357–367.
[13] Kaminski M.M., Szafran J.: *Random eigenvibrations of elastic structures by the response function method and the generalized stochastic perturbation technique*, Archives of Civil and Mechanical Engineering, Vol. 9, No. 4, 2009, pp. 5–32.
[14] Gronostajska B.: *The affect of human feelings on creation of housing*, Archives of Civil and Mechanical Engineering, Vol. 8, No. 1, 2008, pp. 109–119.
[15] Shevchenko G., Ustinovichius L., Andruškevičius A.: *Multi-attribute analysis of investments risk alternatives in construction*, Technological and Economic Development of Economy, Vol. 14, No. 3, 2008, pp. 428–443.
[16] Kapliński O., Tamošaitienė J.: *Game theory applications in construction engineering and management*, Technological and Economic Development of Economy, Vol. 16, No. 2, 2010, pp. 348–363.
[17] Zavadskas E.K.: *History and evolving trends of construction colloquia on sustainability and operational research*, Technological and Economic Development of Economy, Vol. 14, No. 4, 2008, pp. 578–592.
[18] Kapliński O.: *Planning instruments in construction management*, Technological and Economic Development of Economy, Vol. 14, No. 4, 2008, pp. 449–451.
[19] Kapliński O.: *Development and usefulness of planning techniques and decision-making foundations on the example of construction enterprises in Poland*, Technological and Economic Development of Economy, Vol. 14, No. 4, 2008, pp. 492–502.
[20] Peldschus F.: *Experience of the game theory application in construction management*, Technological and Economic Development of Economy, Vol. 14, No. 4, 2008, pp. 531–545.
[21] Ginevičius R., Podvezko V.: *Multicriteria graphical-analytical evaluation of the financial state of construction enterprises*, Technological and Economic Development of Economy, Vol. 14, No. 4, 2008, pp. 452–461.
[22] Zavadskas E.K., Turskis Z., Tamosaitiene J.: *Contractor selection of construction in a competitive environment*, Journal of Business Economics and Management, Vol. 9, No. 3, 2008, pp. 181–187.
[23] Kalibatas D., Turskis Z.: *Multicriteria evaluation of inner climate by using MOORA method*, Information Technology and Control, Vol. 37, No. 1, 2008, pp. 79–83.
[24] Ustinovichius L., Zavadskas E.K., Podvezko V.: *Application of a quantitative multiple criteria decision making (MCDM-1) approach to the analysis of investment in construction*, Control and Cybernetics, Vol. 36, No. 1, 2007, pp. 251–268.
[25] Ustinovichius L., Barvidas A., Vishnevskaja A., Ashikhmin I.V.: *Multicriteria verbal analysis for the decision of construction problems*, Technological and Economic Development of Economy, Vol. 15, No. 2, 2009, pp. 326–340.
[26] Zavadskas E.K., Turskis Z.: *A new additive ratio assessment (ARAS) method in multicriteria decision-making*, Technological and Economic Development of Economy, Vol. 16, No. 2, 2010, pp. 159–172.

[27] Liaudanskiene R., Ustinovicius L., Bogdanovicius A.: *Evaluation of construction process safety solutions using the TOPSIS method*, Inzinerine Ekonomika – Engineering Economics, No. 4, 2009, pp. 32–40.
[28] Sobotka A., Rolak Z.: *Multi-attribute analysis for the eco-energetic assessment of the building life cycle*, Technological and Economic Development of Economy, Vol. 15, No. 4, 2009, pp. 593–611.
[29] Błaszczyk T., Nowak M.: *The time-cost trade-off analysis in construction project using computer simulation and interactive procedure*, Technological and Economic Development of Economy, Vol. 15, No. 4, 2009, pp. 523–539.
[30] Turskis Z.: *Multi-attribute contractors ranking method by applying ordering of feasible alternatives of solutions in terms of preferability technique*, Technological and Economic Development of Economy, Vol. 14, No. 2, 2008, pp. 224–239.
[31] Zavadskas E.K., Kaklauskas A., Turskis Z., Kalibatas D.: *An approach to multi-attribute assessment of indoor environment before and after refurbishment of dwellings*, Journal of Environmental Engineering and Landscape Management, Vol. 17, No. 1, 2009, pp. 5–11.
[32] Sivilevičius H., Zavadskas E.K., Turskis Z.: *Quality attributes and complex assessment methodology of the asphalt mixing plant*, The Baltic Journal of Road and Bridge Engineering, Vol. 3, No. 3, 2008, pp. 161–166.
[33] Ginevicius R., Podvezko V., Raslanas S.: *Evaluating the alternative solutions of wall insulation by multicriteria methods*, Journal of Civil Engineering and Management, Vol. 14, No. 4, 2008, pp. 217–226.
[34] Keeney R.L., Raiffa H.: *Decision with multiple objectives: preferences and value trade-offs*, New York, John Wiley & Sons, 1976.
[35] Seo F.: *Organizational aspects of multicriteria decision making*, in: Lecture Notes in Economics and Mathematical System, Berlin, Heidelberg, New York, 1981, pp. 363–379.
[36] Saaty T.L.: *A scaling method for priorities in hierarchical structures*, Journal of Mathematical Psychology, Vol. 15, 1977, pp. 234–281.
[37] Meuthe M., Scanella G.: *Comparative analysis of UTA multicriteria methods*, European Journal of Operational Research, Vol. 130, No. 2, 2001, pp. 246–262.
[38] MacCrimon K.R.: *Decision marking among multiple–attribute alternatives: a survey and consolidated approach, RAND Memorandum, RM-4823-ARPA*, The Rand Corporation, Santa Monica, Calif., 1968.
[39] Guitoni A., Martel J.M.: *Tentative guidelines to help choosing an appropriate MCDA method*, European Journal of Operational Research, No. 109, 1998, pp. 501–521.
[40] Podvezko V., Podviezko A.: *Dependence of multi-criteria evaluation result on choice of preference functions and their parameters*, Technological and Economic Development of Economy, Vol. 16, No. 1, 2010, pp. 143–158.
[41] Larichev O.: *Decision-making theory and methods*, Moscow: Logos (in Russian), 2000.
[42] Hwang C.L., Yoon K.: *Multiple attribute decision making*, [in:] Lecture Notes in Economics and Mathematical Systems 186, Springer-Verlag, Berlin, 1981.
[43] Srinivasan V., Shocker A.D.: *Linear programming techniques for multidimensional analysis of privileged*, Psychometrika, Vol. 38, 1973, pp. 337–369.
[44] Zavadskas E.K., Kaklauskas A.: *Determination of an efficient contractor by using the new method of multicriteria assessment*, [in:] D.A. Langford, A. Retik (Eds.) International Symposium for "The Organisation and Management of Construction". Shaping Theory and Practice, Vol. 2: Managing the Construction Project and Managing Risk, CIB W 65;

London, Weinheim, New York, Tokyo, Melbourne, Madras, London: E and FN SPON, 1996, pp. 94–104.

[45] Zavadskas E.K., Kaklauskas A., Vlutienė T.: *Multicriteria evaluation of apartment blocks maintenance contractors: lithuanian case study*, International Journal of Strategic Property Management, Vol. 13, No. 4, 2009, pp. 319–338.

[46] Zavadskas E.K., Kaklauskas A., Turskis Z., Tamošaitienė J.: *Selection of the effective dwelling house walls by applying attributes values determined at intervals*, Journal of Civil Engineering and Management, Vol. 14, No. 2, 2008, pp. 85–93.

[47] Zavadskas E.K., Kaklauskas A., Turskis Z., Tamosaitiene J.: *Multi-attribute decision-making model by applying grey numbers*, Informatica, Vol. 20, No. 2, 2009, pp. 305–320.

[48] Zavadskas, E.K., Turskis Z., Tamošaitienė K., Marina V.: *Multicriteria selection of project managers by applying grey criteria*, Technological and Economic Development of Economy, Vol. 14, No. 4, 2008, pp. 462–477.

[49] Zimmermann H.-J.: *An application-oriented view of modelling uncertainty*, European Journal of Operational Research, Vol. 122, No. 2, 2000, pp. 190–198.

[50] Roy B.: *Decision-aid and decision-making*, European Journal of Operational Research, Vol. 45, 1990, pp. 324–331.

[51] Brans J.P., Mareschal B., Vincke P.: PROMETHEE: *A new family of outranking methods in multicriteria analysis*, [in:] J.P. Brans, (Ed.), *IFORS 84*, North Holland, Amsterdam, 1984, pp. 477–490.

[52] Jacquet-Lagreze E., Siskos J.: *Assessing a set of additive utility functions for multicriteria decision-making, the UTA method*, European Journal of Operational Research, Vol. 10, No. 2, 1982, pp. 151–164.

[53] Grigoroudis E., Siskos Y.: *Preference disaggregation for measuring and analysing customer satisfaction: The MUSA method*, European Journal of Operational Research, Vol. 143, No. 1, 2002, pp. 148–170.

[54] Bous G., Fortemps P., Glineur F., Pirlot M.: *ACUTA: A novel method for eliciting additive value functions on the basis of holistic preference statements*, European Journal of Operational Research, No. 206, 2010, pp. 435–444.

[55] Vansnick J.C.: *On the problem of weights in multiple criteria decision making (the moncompensatory approach)*, European Journal of Operational Research, Vol. 24, 1986, pp. 288–294.

[56] Roubens M.: *Preference relations on actions and criteria in multi-criteria decision making*, European Journal of Operational Research, Vol. 10, No. 1, 1982, pp. 51–55.

[57] Berkeley D., Humphreys P., Larichev O., Moshkovich H.: *Aiding strategic decision making: Derivation and development of ASTRIDA*, [in:] Y. Vecsenyi, H. Sol (Eds.), Environment for Supporting Decision Processes, North-Holland, Amsterdam, 1991.

[58] Zavadskas E.K., Liias R., Turskis Z.: *Multi-attribute decision-making methods for assessment of quality in bridges and road construction: state-of-the-art surveys*, The Baltic Journal of Road and Bridge Engineering, Vol. 3, No. 3, 2008, pp. 152–160.

[59] Zavadskas E.K.: *Multiple criteria evaluation of technological decisions of construction* (in Russian), Dissertation of Dr. Sc. Moscow Civil Engineering Institute, Moscow, 1987.

[60] Hovanov N.: *Analysis and synthesis of parameters under information deficiency*, St. Petersburg: St. Petersburg University Press, 1996, pp. 11–22.

[61] Peldschus F.: *The analysis of the quality of the results obtained with the methods of multicriteria decisions*, Technological and Economic Development of Economy, Vol. 15, No. 4, 2009, pp. 580–592.

[62] Peldschus F.: *The effectiveness of assessment in multiple criteria decisions*, International Journal of Management and Decision Making, Vol. 8, No. 5–6, 2007, pp. 519–526.
[63] Ginevičius R., Podvezko V.: *Multicriteria evaluation of lithuanian banks from the perspective of their reliability for clients*, Journal of Business Economics and Management, Vol. 9, No. 4, 2008, pp. 257–267.
[64] Ginevičius R.: *Normalization of quantities of various dimensions*, Journal of Business Economics and Management, Vol. 9, No. 1, 2008, pp. 79–86.
[65] Noarul Haq A., Kannan G.A.: *Hybrid normalised multi criteria decision making for the vendor selection in a supply chain model*, International Journal of Management and Decision Making, Vol. 8, No. 5–6, 2007, pp. 601–622.
[66] Thiel T.: *Determination of the relative importance of criteria when the number of people judging is a small sample*, Technological and Economic Development of Economy, Vol. 14, No. 4, 2008, pp. 566–577.
[67] Vaidogas E.R., Juocevicius V.: *Sustainable development and major industrial accidents: the beneficial role of risk-oriented structural engineering*, Technological and Economic Development of Economy, Vol. 14, No. 4, 2008, pp. 612–627.
[68] Vaidogas E.R., Juocevicius V.: *Reliability of a timber structure exposed to fire: estimation using fragility function*, Mechanika, No. 5, 2008, pp. 35–42.
[69] Schabowicz K., Hola B.: *Application of artificial neural networks in predicting earthmoving machinery effectiveness ratios*, Archives of Civil and Mechanical Engineering, Vol. 8, No. 4, 2008, pp. 73–84.
[70] Zavadskas E.K., Vaidogas E.R.: *Multiattribute selection from alternative designs of infrastructure components for accidental situations*, Computer-Aided Civil and Infrastructure Engineering, Vol. 24, No. 5, 2009, pp. 346–358.
[71] Vaidogas E.R., Juocevicius V.: *Assessment of structures subjected to accidental actions using crisp and uncertain fragility functions*, Journal of Civil Engineering and Management, Vol. 15, No. 1, 2009, pp. 95–104.

Analiza wielowymiarowa alternatywnego usadowienia fundamentu przy użyciu metody oszacowania współczynnika addytywności (ARAS)

Artykuł prezentuje proces wyboru alternatywnego usadowienia fundamentu najbardziej odpowiedniego i bezpiecznego dla budynku stojącego na gruncie wodonośnym. Wybór bazuje na zestawie kryteriów: koszt usadowienia, okres usadowienia, stopień skomplikowania decyzji, zalety i wady decyzji, możliwość przenoszenia i konserwacji usadowionego systemu fundamentu, doświadczenie z wdrożenie przyjętych decyzji, itd. Kryteria oceny i ich znaczenie są wybierane z uwzględnieniem interesów i celów klienta oraz czynników wpływających na efektywność procesu budowlanego i bezpieczeństwa budynku. Rozwiązania problemu dokonano przy zastosowaniu metody ARAS. Proponowana metoda może w przyszłości być zastosowana do uzasadnienia wyboru struktury, technologii, inwestycji itd.